Synthesis of internal amide bond short interfering RNAs (siRNAs) and investigation of their gene silencing properties

Wei Gong
Faulty of Science, *University of Ontario Institute of Technology*
Oshawa, ON, Canada
October, 2012
A thesis submitted to University of Ontario Institute of Technology in partial fulfillment of the requirements of the degree of Master of Science in Applied Bioscience

Abstract

Cancer is a leading cause of death worldwide, accounting for around 13% of all death [1]. Traditional cancer therapeutics usually require careful selection of one or more intervention, such as surgery, radiotherapy, and chemotherapy, which have made momentous progress, but have ample limitations [2]. The next generation of cancer therapeutics will specifically target processes responsible for the growth and survival of cancer cells. Among the most promising of these molecularly-targeted therapeutics are short interfering RNAs (siRNAs). These siRNAs serve as the effectors of RNA interference, a naturally occurring and highly specific mechanism for regulating gene expression through sequence-specific degradation of messenger RNA. However, the native structure of RNA is plagued with undesirable chemical properties. For example, the sugar-phosphate backbone contains a negative charge which hinders its ability to cross the negatively charged lipid bilayer. Furthermore, the phosphodiester backbone is a substrate for nucleases, which catalytically cleaves the phosphate-oxygen bond, thus degrading the native RNA [3]. As such, there is widespread interest in chemically modifying the backbone of siRNAs in order to overcome some of the inherent problems with its native structure.

There have been only two reports that have employed amide-bond linkages as phosphate replacements within siRNAs [4, 5]. In both of these studies, the amide bond containing monomer units were placed at the 3'-overhangs and not within the internal Watson-Crick region of the double stranded siRNA due to the limitation of standard solid-phase oligonucleotide synthesis. In this thesis, we proposed to utilize phosphoramidite chemistry to localize internal amide-bond modifications [6]. A practical synthesis of a peptide nucleic acid unit combined with an RNA nucleoside (PNA-RNA dimer, U_aU) is reported [7]. Using this PNA-RNA dimer phosphoramidite allows us to control the site-specific location of the internal amide-bond

modification throughout the desired RNA strand. Polyacrylamide gel (PAGE) and mass spectrometry analysis were performed to ensure the formation of full-length modified siRNA molecules.

The effects of these modifications were explored with respect to the biophysical and biological properties of the modified siRNAs. The techniques used in this work included hybridization affinity assays (melting temperature), secondary structure determination (circular dichroism), cell-based luciferase assays, and nuclease stability assays. Melting temperature experiment reveals that localizing a U_aU dimer unit within the RNA oligonucleotides has an overall destabilizing effect, whereas U_aU modifications at the 3'-overhang positions show little change in thermal stability. Circular dichroism experimental results illustrate that all chemically modified siRNAs exhibit the standard A-form helix. In cell-based luciferase assays, we utilized two different target sequences and our results highlight the compatibility of utilizing a neutral amide-bond backbone within siRNAs. Specifically, the internal amide-bond modification is compatible within the RNAi machinery when placed at 3'-overhang position in the sense strand of the double-stranded siRNA. However, poor efficacy is observed when this unit is placed adjacent the Ago 2 cleavage site on the antisense strand. The nuclease stability assays reveal that the introduction of a PNA-RNA dimer at the 3'-end of the siRNA where the exonuclease cleaves the terminal nucleotide, increased markedly the resistance to serum-derived nucleases. To the best of our knowledge, this is the first report that involves amide-bonds as phosphate backbone replacements within the internal regions of siRNAs and thus opens the future possibility for examining and utilizing this modification in studying new structure-function relationships.

Acknowledgements

I would like to express my sincere appreciation of my advisor, Dr. Jean-Paul Desaulniers for inviting me to join his group and providing such a stimulating learning environment. He expresses a great deal of confidence in his students. It has been a real encouragement throughout my studies. He has given me many opportunities for development, in research, and publishing.

The Desaulniers group has been a very open place to conduct research, and I have been very lucky to have wonderful co-workers. I thank Tim Efthymiou for being a good friend and a big brother, for conversations that will stay with me for years to come and for his admirable patience with all the training process which led to the eventual success of my project and possibly saved the instruments from destruction at my hands. All other folks, including Brandon Peel and Jaymie Oentoro have inspired me in research through our interactions during the long hours in the lab.

I would also like to thank Dr. Holly Jones Taggart for allowing me to use her lab space and equipment to perform all the cell work. Thanks are due to Dr. Julia Green-Johnson for letting me use their luminometer. I am also thankful for all the folks in Dr. Ayush Kumar's lab for the assistance with the bacteria work.

I am grateful to Dr. Liliana Trevani, Dr. Holly Jones Taggart and Dr. Yuri Bolshan for participating as my committee members.

My special thanks are reserved for NSERC and CFI for funding that has allowed me to conduct research at UOIT.

Finally, I express my very deep appreciation for my parents. I am incredibly grateful for their ongoing support and encouragement**.**

Table of Contents

List of Figures

List of Schemes

List of Tables

List of Abbreviations

Ago Argonaute

BCL2 B-cell lymphoma protein 2

CD circular dichroism

EDTA ethylenediaminetetraacetic acid

COSY correlation spectroscopy

CPG controlled pore glass

DCC dicyclohexylcarbodiimide

DCM dichloromethane

DIPEA *N*,*N*-diisopropylethylamine

DMAP 4-(dimethylamino)pyridine

DMEM Dulbecco's modified Eagle medium

DMF *N*,*N*-dimethylformamide

DMSO dimethylsulfoxide

DMT 4,4'-dimethoxytrityl

DNA 2'-deoxyribonucleic acid

ds double-stranded

dt doublet of triplets

dT 2'-deoxythymidine

EDC·HCl 1-ethyl-3-(3-diethylaminopropyl)carbodiimide hydrochloride

EMAN methylamine 40 % wt. in H_2O and methylamine 33 % wt. in ethanol, 1:1

ESI-MS electrospray ionization mass spectrometry

Et ethyl

EtOAc ethyl acetate

EtOH ethanol

2'F-ANA 2'-deoxy-2'-fluoroarabinonucleic acid

FBS fetal bovine serum

G guanosine

HOBt 1-hydroxy-1*H*-benzotriazole

HBTU O-Benzotriazole-*N*,*N*,*N*′,*N*′-tetramethyl-uronium- hexafluoro-phosphate

J scalar coupling contstant (in Hz)

LNA locked nucleic acid

MALDI matrix-assisted laser desorption/ionization (mass spectrometry)

Me methyl

MeCN acetonitrile

MOE methoxyethyl

MeOH methanol

miRNA micro RNA

mRNA messenger RNA

nt nucleotide

NOESY nuclear Overhauser effect spectroscopy

NMI N-methylimidazole

NMR Nuclear magnetic resonance

ONs oligonucleotides

Oligo oligonucleotides

PAGE polyacrylamide gel electrophoresis

PCR polymerase chain reaction

PET positron emission tomography

Pf *Pyrococcus furiosus*

PKC protein kinase C

PNA Peptide nucleic acids

PS phosphorothioate

PTDs peptide-transduction domains

PTGS post-transcriptional gene silencing

RSV respiratory syncitial virus

RISC RNA-induced silencing complex

RNA ribonucleic acid

RNAi RNA interference

rt. room temperature

shRNA short hairpin RNA

siRNA small interfering RNA

SNALP stable nucleic acid–lipid particles

t triplet

T thymidine

TBE tris-boric acid EDTA

TBS *tert*-butyldimethylsilyl

TCA trichloroacetic acid

TEA triethylamine

THF tetrahydrofuran

TIPS triisopropylsilyl

TLC thin-layer chromatography

T_m melting temperature

U uridine

UV ultraviolet

wt wild-type

Chapter 1: Introduction

1.1. Structure and Conformation of Nucleic Acids

DNA and RNA consist of heterocyclic bases built on a sugar–phosphate backbone polymer (**Figure 1-1**). At neutral pH, the phosphates are constitutively negatively charged. DNA and RNA differ in two important structural aspects. In DNA, the four nitrogenous bases are adenine (A), guanine (G), cytosine (C), and thymine (T), while in RNA, the thymine is substituted by uracil (U). Secondly, the main difference between DNA and RNA is the presence of the 2' hydroxyl group attached to the pentose ring in RNA. This small difference leads to very different conformational properties through stereoelectronic and steric effects.

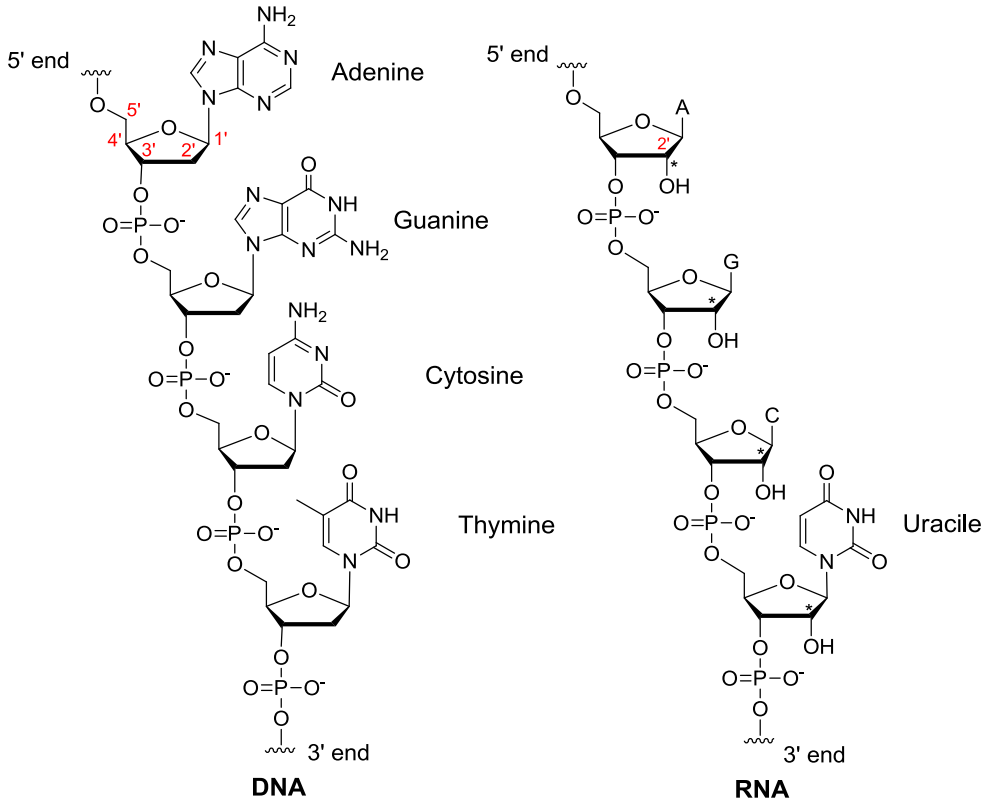

Figure 1-1: Primary structure of DNA and RNA. Note that RNA contains uracil instead of thymine. Sugar numbering is shown at top left.

The bases of DNA and RNA are capable of hydrogen bonding to each other via canonical (i.e. Watson-Crick) base pairs, A-U/T and G-C to form a double helix. The phosphate moiety and the sugar form the backbone of the helix. Each nucleic acid strand has polarity, or sense, and pairing occurs with one strand lies in the 5' to 3' orientation and the other strand in the 3' to 5' orientation to form a double stranded duplex.

As described in the central dogma of molecular biology, the genetic information is transferred from DNA to RNA to proteins (**Figure 1-2**). During replication, the double helical DNA unwinds and creates a copy of itself. The genetic information stored in double helical DNA is faithfully transmitted to the progeny of any cell or organism. The information contained in a section of DNA is transferred to messenger RNA (mRNA) by a process called transcription, and RNA binds to ribosomes to assemble proteins by a process called translation. In the case of retroviruses, such as HIV, as well as in eukaryotes, reverse transcription occurs, creating single-stranded DNA from an RNA template. Since the 1970s, tremendous interest has been generated in the development of technologies that employ synthetic oligonucleotides (ONs) as therapeutics for manipulating gene expression in living cells. For instance, synthetic ONs can be used to modify gene expression and inhibit the replications of certain virus in the cells [8]. ONs therapeutics has been considered as a potential treatment for viral diseases and also for cancer which is caused by aberrant gene expression [9].

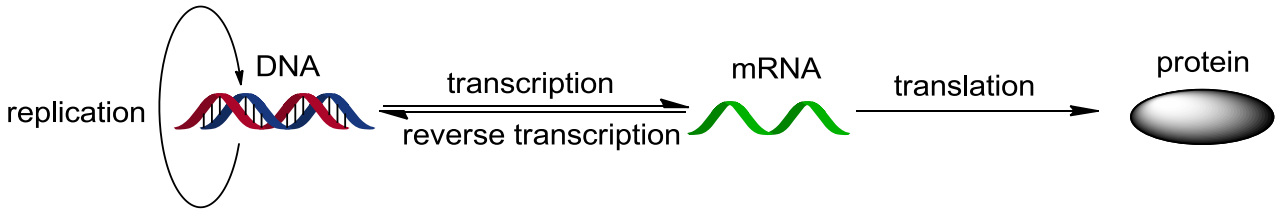

Figure 1-2: The central dogma of molecular biology.

1.2. RNA Interference (RNAi)

ONs are chemically synthesized short nucleic acid sequences (DNA or RNA). They can selectively inhibit the gene expression by interfering with the flow of genetic information in biological systems, resulting from their binding to the target sequence by a variety of mechanisms. One of the most investigated mechanisms is the antisense pathway, in which complementary ONs (antisense ONs) hybridize to the mRNA strand of the targeted gene based on complementarity [10]. After hybridization, the gene expression of the target mRNA is blocked either sterically by obstructing the ribosomes, or by forming an RNA-DNA hybrid, which is a substrate for RNase H enzyme, thereby causing the cleavage of desired target mRNA. Besides antisense, there are other mechanisms that are available for selective inhibition of gene expression. For instance, the antigene mechanism where a single-stranded ON, also called triplex-forming oligonucleotides (TFOs), hybridizes to the purine or pyrimidine-rich region in the major groove of double-helical DNA through Hoogsteen base pairing and prevents the unwinding of double helical DNA necessary for transcription of the targeted region or blocks the binding of transcription factor complexes [11].

The focus of this thesis will involve using the RNA interference (RNAi) pathway, which has generated the most interest in recent years as a therapeutic potential. Another name for RNAi is post-transcriptional gene silencing (PTGS), which is a natural process in eukaryotic cells, by which double-stranded short interfering RNA (siRNAs) targets mRNA for cleavage in a sequence-specific manner [12]. It provides an innate defense mechanism against invading viruses and transposable elements. If siRNA is delivered to the cell, it will utilize the endogenous RNA-induced silencing complex (RISC) and this results in potent and specific silencing of the targeted mRNA at the post-transcriptional level. The basic premise underlying the broad utility of RNAi

is that, in theory, we can design siRNAs to target virtually any gene of interest. Because of the potency and selectivity of RNAi, it has become the method of choice for silencing specific gene expression in mammalian cells. Specially, control of disease-associated genes makes RNAi an attractive choice for future therapeutics.

The discovery of the RNAi mechanism occurred in a successive way. The RNAi phenomenon was first reported by Napoli and Jorgensen in 1990 [13]. The suppression of the endogenous gene by the introduction of homologous RNA sequence was later reported by Romano and Macino in *Neurospora crassa* in 1992 [14]. In 1995, Guo and Kemphues demonstrated the capacity of single-stranded RNAs (ssRNAs) to induce PTGS in the nematode *Caenorhabditis elegans* [15]. However, the role of double-stranded RNA (dsRNA) in gene silencing was not evident in the effects discovered in plants and *C. elegans*. Clear evidence for the participation of dsRNA in post transcriptional gene silencing was revealed in 1998 by Fire, Mello, and coworkers, who reported that an externally introduced long dsRNA could decrease the expression of a complementary mRNA in *C. elegans* [16]. Research into the therapeutic applications of RNAi gained momentum after the seminal discovery in 2001 by Tuschl and co-workers that synthetic 21-nucleotide (nt) siRNAs could trigger an RNAi response in mammalian cells [17].

1.2.1. Mechanism of siRNA-Initiated RNAi in Humans

Since the discovery and characterization of RNAi in *C elegans* [15], the broad mechanistic details for the pathway have been largely characterized. Unlike *C. elegans*, longer double-stranded RNAs cannot be used to initiate RNAi in mammalian cells because of the innate immune response [18]. Therefore, siRNAs are used to initiate RNAi [17, 19], although these still

have potential immunogenicity [20]. Nonetheless, siRNAs remain the most viable candidates for application of RNAi as a human therapeutic approach. The development of RNAi for therapy is based on our understanding of small RNA biogenesis pathways. The two main types of small RNAs involved in gene silencing are siRNAs and microRNAs (miRNAs).

SiRNAs are small double-stranded RNAs (dsRNAs), 20–24nt (nucleotide) in length, that are processed from longer dsRNAs. One strand is the 'guide' strand and directs silencing, with the other strand - the 'passenger' - is degraded after the 'guide' strand is loaded within the RISC complex [21, 22]. SiRNAs generally show full complementarity to their target mRNA, and cleavage occurs 10–12 bases from the 5'-end of the guide strand binding site [17, 23]. The most common method to harness the RNAi pathway for targeted gene silencing is to transfect 21-22nt siRNAs into cells. Another way is to use longer, 25-27nt duplexes that can be later processed by Dicer which is a member of the RNase III family of ribonucleases that cleaves dsRNA into siRNA in the cytoplasm [24]. The complex of double-stranded siRNA and Dicer is then loaded into the RNA-induced silencing complex (RISC) [25] which is a group of proteins, including one of the Argonaute (Ago) proteins, that induces target mRNA cleavage based on loaded siRNA [26]. Ago proteins are a highly conserved family that have been implicated in RNAi across several species [27]. Family members have two characteristic domains: PAZ and PIWI [28]. A group led by Joshua-Tor crystallized an Ago protein from the archebacterium *Pyrococcus furiosus* (PfAgo) [29]. The PIWI domain of PfAgo showed a remarkable similarity to the conserved secondary structure of RNase H enzymes [29]. Using the structure of PfAgo, Joshua-Tor and colleagues modeled the structure of human Argonautes. Accordingly, the N-terminal, PIWI, and middle domains of Argonaute lie in a crescent to support the fourth domain, PAZ. The 3'-end of the single-stranded siRNA sits in the groove of the PAZ domain, which allows the rest

of the siRNA to bind to target mRNA. The target mRNA then sits on top of the PIWI domain, which causes cleavage of target mRNA. Immunoprecipitation results show that among the Argonaute family (Ago 1-4), Ago 2 is the enzyme responsible for cleaving the passenger strand siRNA as well as the target mRNA.

The siRNA-Dicer complex recruits Ago 2 to form the RISC-loading complex (RLC) [30]. The RLC initiates siRNA unwinding and determines which strand is assembled into the RISC by preferentially binding the strand with lower thermodynamic stability at the 5'-end, which becomes the guide strand [31-34]. The passenger strand is cleaved by Ago 2 and departs the complex, facilitating assembly of RISC [21]. RISC mediates sequence-specific binding of the guide strand RNA to the corresponding target mRNA mainly with the 5' seed region [35] (nucleotides 2–8 which is essential for the initial binding of the siRNA to most targets) of the siRNA [36]. The mRNA is then cleaved by Ago 2 at the centre of the oligonucleotide. RISC remains bound to the single-stranded siRNA and can execute several rounds of cleavage [37].

Like siRNA, single-stranded RNA molecules, known as microRNAs, regulate gene expression as well as nucleic acids (ribozymes and DNAzymes) with catalytic activity against the target sequences are also being investigated as therapeutics.

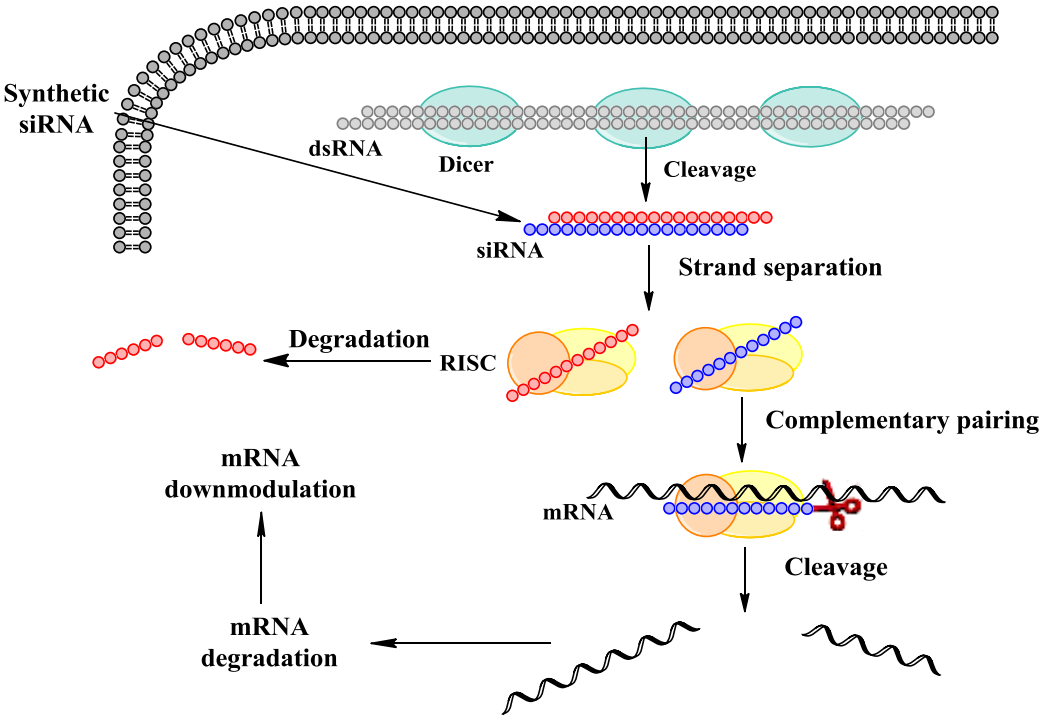

Figure 1-3: Diagrammatic Representation of Mechanism of siRNA-initiated RNA interference [38].

Today, RNAi has become a promising technique in the field of life sciences as well as in the biomedical science to characterize and knock-down a single gene or a collection of genes that are associated with the disease development. Cancer, AIDS, and hepatitis are diseases in which the effectiveness of RNAi has been already tested by scientists [39, 40].

Rules for Selecting siRNA Sequences

The initial selection of candidate siRNA sequences was based on complementarity of one strand of the double-stranded RNA to the target mRNA. Moreover, the structure of the siRNA, with the internal 19 nucleotides hybridized and 2-nucleotide overhangs at each 3'-end (typically TT), was also important for recognition by the pathway proteins. Another critical feature that

subsequently came to light was that siRNAs must possess a 5'-PO_3 rather than a 5'-OH [41], which is the typical terminal group for chemically synthesized siRNAs. This 5'-PO_3 group is important for recognition of the siRNA by Dicer, because 5'-OCH_3 and modified strands are bound far more weakly than phosphorylated strands [42, 43]. As such, modifying the passenger strand with a 5'-OCH_3 can prevent its phosphorylation and therefore prevent incorporation into RISC [44].

1.2.2. Terminal Asymmetry Prediction

Because siRNAs are double-stranded, either strand is capable of serving as the guide for active RISC. Thus, to maximize the activity of siRNAs, it is advantageous for one of the two strands of the siRNA to be loaded preferentially into RISC. The preference for loading one strand over the other is referred to as siRNA asymmetry. Based on early studies in *Drosophila*, it was proposed that siRNAs were asymmetric because of the difference in the hybridization free energy for the terminal four nucleotides on each end of the siRNA [31, 45]. The strand whose 5'-end was located at the less stably hybridized end of the siRNA would preferentially be loaded into active RISC. This was confirmed using sequences with terminal mismatches to induce significant instability at one end of the siRNA. Subsequently, thermodynamic asymmetry was confirmed to be a useful predictor of siRNA function [46]. Theoretically placing a destabilizing unit at the 5'-end of the guide strand will improve the efficacy of siRNAs.

In a recent study reported by a collaboration amongst various European research groups, several pairs of guide and passenger siRNA strands modified with 21 different modifications were used to generate a total of 2160 siRNA duplexes, which were studied for silencing activity and cell viability [47]. It was observed that the thermodynamic asymmetry of the duplex and the

3’-overhangs are the major factors that affect silencing activity [47]. Stabilizing the 3’-end of the guide strand or the 5’-end of the passenger strand by the use of chemical modification and destabilizing the 5’-end of the guide strand or the 3’-end of the passenger strand resulted in improved RNAi activity due to improved strand selection [48]. However, if the seed region is strongly destabilized, the corresponding weakening of the interaction between the guide strand and the target mRNA results in decreased silencing activity [47]. The highly stabilized duplexes were also shown to have decreased silencing activity [47]. It was thus suggested that destabilizing the 3’-end of the passenger strand is an optimal way of designing the desired efficient siRNAs. Certain favored 3’-overhangs in the guide strand and disfavoured 3’-overhangs in the passenger strand have been identified, which affect strand selection irrespective of the thermodynamic asymmetry of the duplex [47]. The passenger strand was found to be more tolerant to modifications than the guide strand.

1.2.3. Challenges Involved in siRNA Therapeutics and Opportunities for Using Chemical Modifications

Despite the promise shown, the clinical success has been disappointing. After several decades of research and development, so far very few nucleic acid therapeutics have been approved for human use. The limited success of ONs in clinics is attributed to the fact that unmodified ONs show unfavourable pharmacokinetic and pharmacodynamic properties. For instance, the natural siRNAs have a phosphodiester backbone, which is rapidly degraded by the nucleases in biological fluids. Moreover, they show extremely poor penetration (diffusion) across the cell membrane owing to their size and negative charge. Currently, the most mature therapeutic approach using RNAi is the use of chemically modified siRNAs, which can address

some of the problems discussed above. Broadly speaking, chemical modifications used in siRNAs fall into three specific areas: backbone, sugar, and base.

Improving Nuclease Resistance

Unmodified siRNAs have a half-life of less than 15 min in serum, which makes them impractical for use in RNAi-based therapeutics. This is because the phosphodiester backbone is a substrate for nucleases, which catalytically cleaves the phosphate-oxygen bond, thus degrading the native RNA [3]. The most viable method to address the nuclease vulnerability of siRNAs is to use various chemical modifications. The backbone modifications involve alterations to the phosphate ester linkages in the nucleic acid (**Figure 1-4. a**). One of the more common modifications of this type is the phosphorothioate (PS) modification (**Figure 1-4. b**), in which one of the nonbridging phosphate oxygen atoms is replaced by sulfur to give a PS group [49]. This modification is widely used in antisense oligonucleotide therapeutics and is now being employed in siRNAs, as it provides improved nuclease resistance and favourable pharmacokinetic properties [50]. However, the PS modification has a tendency to bind nonspecifically to cellular membrane proteins, which can lead to toxicity [51].

Another backbone modification used in siRNA is the boranophosphate modification (**Figure 1-4. c**), in which one of the non-bridging oxygen atoms of the phosphate moiety is replaced with a borane (BH_3) group [52]. This modification is known to improve nuclease resistance by >300-fold relative to native siRNAs. A major drawback to the boranophosphate modification is that chemical methods for introducing the boron modification have not been optimized. Instead of using more convenient phosphoramidite reagents to site-specifically incorporate this modification into a RNA strand (reviewed in Chapter 2), they can only be

enzymatically produced from the nucleoside boranotriphosphates using T7 RNA Polymerase [52], which lacks the site-specific control of the boron modification.

The most widely used sugar modifications in siRNAs are the 2’ modifications of the sugar ring, namely 2’-OMe (**Figure 1-4. d**) [53], 2’-fluoro (**Figure 1-4. e**) [53, 54], and 2’-*O*-methoxyethyl (2’-MOE) **(Figure 1-4. f**) [54]. Due to their ability to favor the 3’-endo sugar conformation, all these modifications are expected to form thermally stable A-type helical siRNA duplexes once they are introduced into siRNAs. Even though, conformational features alone do not decide the interfering activity, a RNA-like A type conformation is required for effective gene silencing.

Another important 2’-modification employed in siRNAs is the 2’-fluoro-β-D-arabinonucleotide (2’-*O*-FANA) (**Figure 1-4. g**) [55]. An siRNA duplex with a 3’-overhang in the guide strand and the entire passenger strand modified with FANA showed a 24-fold increase in serum half-life over unmodified siRNAs [55]. FANA differs from the other 2’ modifications because it is based on an arabinose sugar; the stereochemistry is opposite to that of a ribose 2’-fluoro group (**Figure 1-4, e**).

The locked nucleic acid (LNA) modification (**Figure 1-4. h**) is a specialized modification in which the 2’ and 4’ positions of the ribose ring are linked through a methylene bridge [56, 57]. This linkage constrains the ribose ring, “locking” it into a conformation close to that formed by RNA after hybridization. The rigidity of the conformation of this modification also leads to better organization of the phosphodiester backbone, which enhances base stacking interactions as a result of stronger hybridization of the guide strand with the target strand. The LNA modification increases the thermal stability of RNA duplexes and prevent them from digestion by nucleases [58]. LNA-containing RNA duplexes are active silencing agents inside cells [58,

59]. Gene silencing is sensitive to the position of the LNA nucleotides within the duplex, but well-placed LNA modification within the sense strand can enhance potency [59].

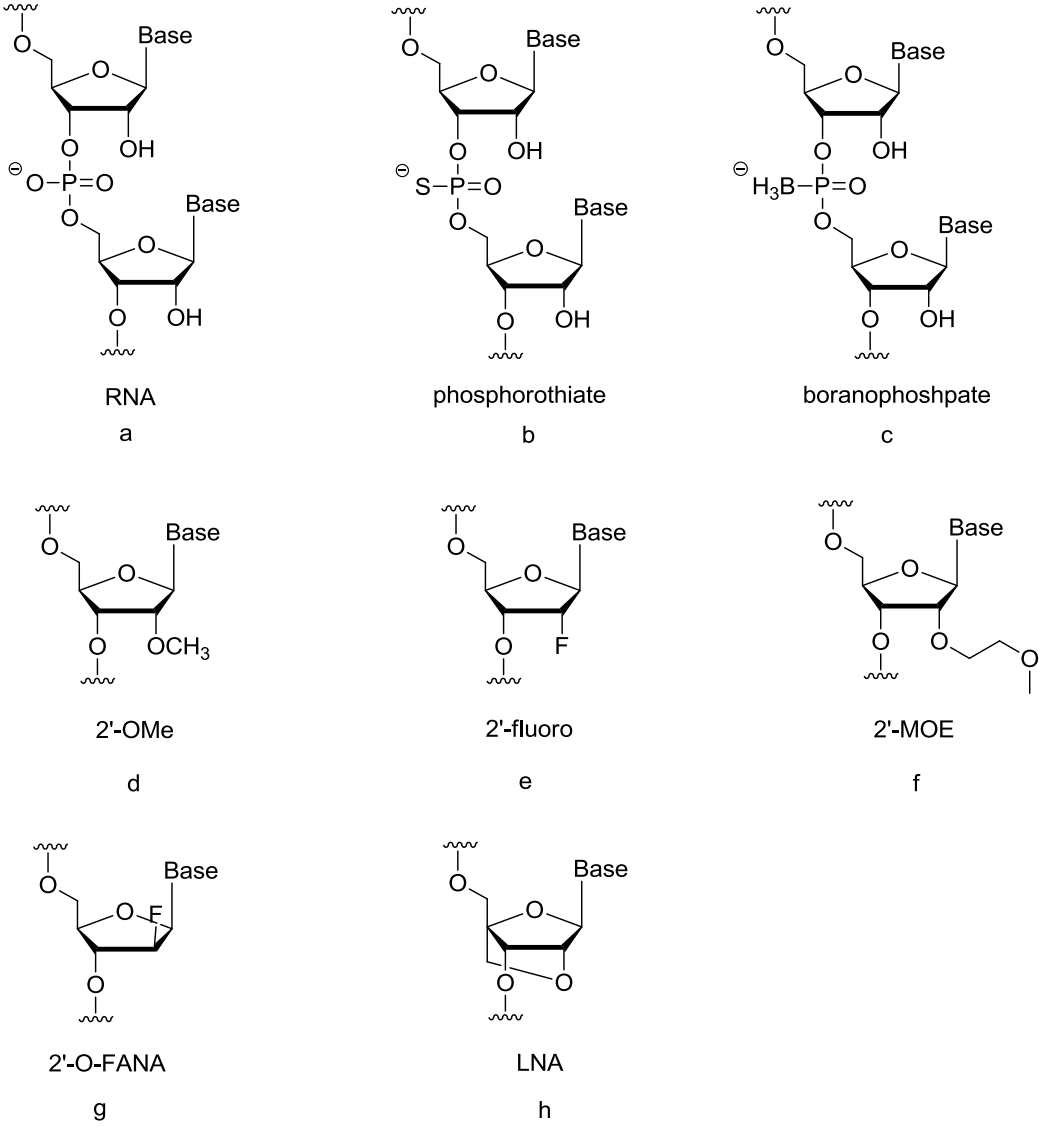

Figure 1-4: Chemical modifications used with siRNA in therapeutic approaches.

Addressing siRNA Delivery

Along with the rapid progress made in the design of efficient siRNAs, much effort is being directed at finding an appropriate delivery vehicle for siRNAs [60]. Unmodified siRNAs are much larger than small-molecule drugs, can be easily degraded in the blood stream by

endogenous enzymes, and are unable to cross the cellular membrane due to their negative charge [61, 62]. However, unmodified siRNAs have been delivered *in vivo* using what is known as 'local delivery', in which the siRNAs are administered through an injection or passed through the respiratory tract directly to the affected tissues [63-65]. Clearly, this approach is only appropriate for organs such as lungs and eyes. Localized injection of unmodified siRNAs to the vitreal cavity in the eye has been shown to be beneficial in wet AMD-related complications; the drug has entered phase III clinical trials [66]. A similar approach is being taken in which the epithelial cells in the lung are targeted for the treatment of respiratory syncitial virus (RSV); the drug is currently in phase II clinical trials (ALN-RSV01, Alnylam Pharmaceuticals). Not all cells of the human body, however, can be accessed through localized delivery, owing to the problem of the negative charge on siRNAs. In most cases, systemic delivery of siRNAs is essential. Systemic delivery involves intravenous injection of the siRNAs along with a delivery agent, which should be able to travel in the bloodstream to the desired organ or tissue without being degraded or taken up by non-target tissues in the process [12]. A systemically injected siRNA has to undergo a series of processes before it can enter the cell and produce the desired result.

Two known approaches for systemic delivery are 'complexation' and 'conjugation' [62]. The complexation method involves formation of complexes of siRNAs with motifs that bind to their negative charges. The techniques used for this include lipids and liposomes such as stable nucleic acid–lipid particles (SNALP), antibody complexes, polycationic peptides known as peptide transduction domains (PTDs), and polycationic polymers. The conjugation approach involves attaching the siRNA to the delivery vehicle and has shown success in targeting cell types that are specific to the siRNAs [67, 68]. The conjugation approach is also useful, as the passenger strand can be conjugated to the delivery vehicle, leaving the guide strand to perform

its desired function once the delivery vehicle is cleaved away [69]. Conjugates currently in use include lipophilic species such as cholesterol, as well as peptides and aptamers, which were reported to exhibit high biocompatibility and efficient gene silencing *in vitro*, but toxicity studies revealed problems *in vivo*. The field of siRNA delivery has undergone major improvements in recent years. New delivery methods are being tested, and some of the results are indeed very encouraging for addressing the issues associated with siRNA delivery. However, a perfect delivery vehicle that can overcome all associated hurdles has yet to be developed. Moreover, the viability of the existing delivery vehicles and strategies in clinical settings have yet to be evaluated.

The research in RNA interference has made a lot of progress and improvement since its ground-breaking discovery in 1998. The improved design of siRNAs will be crucial, as the ideal drug should address such challenges as nuclease stability, immunostimulation, off-target effects, and delivery. Clearly these designs are in their nascent stage of development, and more *in vivo* studies are required to ascertain their full potential. Importantly, a majority of chemical modifications employed in siRNAs so far were originally devised for antisense technology. Although these modifications have proven useful to a certain extent, efforts to explore novel modifications for siRNAs are warranted, as their structural and functional requirements are different from those of antisense oligonucleotides.

1.3. Peptide Nucleic Acids (PNAs)

Peptide nucleic acids (PNAs or aegPNAs) (**Figure 1-5**) are oligonucleotide mimics, in which the pyrimidine and purine bases are connected through a methylene carbonyl linker to an amino ethyl glycine backbone. The polyamide backbone was designed by Nielsen in 1991 to recognise DNA strands through Hoogsteen-like base pairing [70]. It was demonstrated that PNA oligomers form duplexes with complementary DNA, RNA and PNA strands following the Watson–Crick base pairing rules, whose structure differs from that of natural nucleic acids. The following properties make PNA so unique among other backbone modifications. They have the resistance to enzymatic degradation, and, they bind target gene with high affinity and high specificity [71]. Despite the fact that many synthetic oligonucleotides have been identified, very few of them, like PNA, can meet all of these key requirements simultaneously. It is for these reasons that scientists including us invest time and resources on this type of backbone modification.

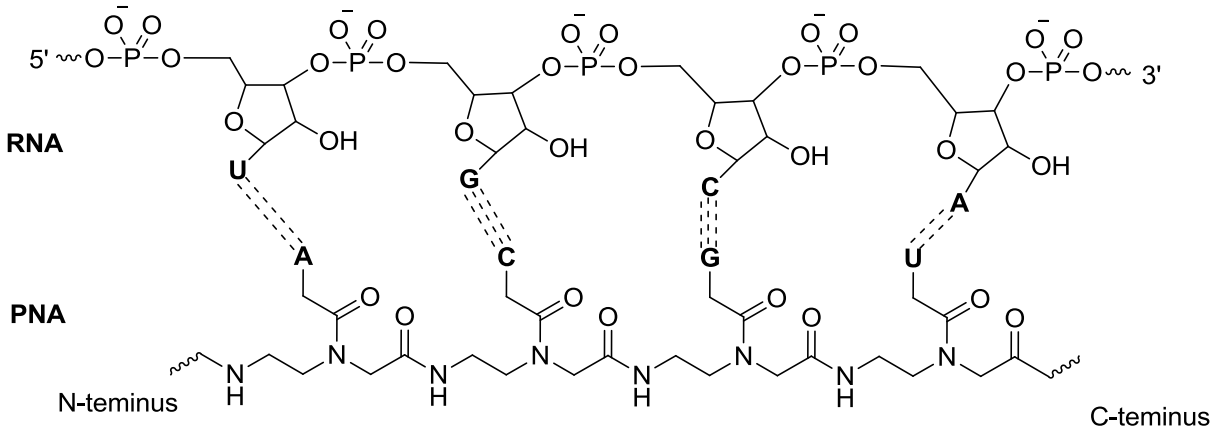

Figure 1-5: Chemical structures of RNA and PNA oligomers

1.3.1. Important Properties of PNAs

Resistance to nucleases and proteases

Unlike DNA or other DNA analogues, PNAs do not contain any pentose sugar moieties or phosphate groups. They are not molecular species that are easily recognizable by either nucleases or proteases. Therefore the lifetime of these compounds is extended both *in vivo* and *in vitro* [72].

Thermal stability of PNA and its hybrid complexes

PNAs are capable of hybridizing to complementary DNA as well as RNA obeying the Watson-Crick hydrogen bonding rules with an affinity greater than that of native nucleic acids [70, 73-76], which makes the discovery of PNAs invaluable. This reason can be attributed to the intramolecular distances and the configurations of the nucleobases that are similar to those in natural nucleic acids. The properties of various duplexes of PNA, both pure and hybrid have been investigated extensively by absorption spectroscopy. Its hybrids complexes exhibit extraordinary thermal stability and display unique ionic strength properties. Typically, the T_m of a 15-mer PNA/DNA duplex is ~70 ˚C, whereas the corresponding DNA/DNA duplex exhibits a T_m of ~55 ˚C (pH 7, 100 mmol dm^{-3} NaCl). The thermal stability of a PNA–RNA duplex is even higher than that of a PNA–DNA duplex [77, 78]. The increased stability of PNA-DNA and PNA-RNA hybrids in comparison to DNA-DNA (RNA) hybrids is mainly attributed to the lack of inter-strand electrostatic repulsion [79].

Stronger binding independent of salt concentration

Another important consequence of the neutral backbone is that the change in ionic strength has little effect on the stability of PNA-DNA duplexes. This is in sharp contrast to the T_m values of DNA/DNA duplexes, which are highly dependent on ionic strength [72]. The neutral amide backbone also enables PNAs to hybridize to DNA molecules under low salt conditions where DNA hybridization is strongly inhibited, because no positive ions are necessary for counteracting the inter-strand repulsion that hampers duplex formation between two negatively charged nucleic acids. Consequently, the abundance and stability of intramolecular folding structures in the DNA or RNA molecules are significantly reduced, which makes the molecules more accessible to complementary PNAs. Furthermore, PNAs are stable across a wide range of temperature and pH values [80], unlike DNA which depurinates under acidic conditions. However, under basic conditions degradation of PNA may occur.

Greater specificity of interaction

PNA also shows greater specificity in binding to complementary DNA [72]. A PNA/DNA mismatch is more destabilizing than a mismatch in a DNA/DNA duplex. A single mismatch in mixed PNA/DNA 15-mers lowers T_m by 8–20 ˚C (15˚C on average). In the corresponding DNA/DNA duplexes a single mismatch lowers T_m by 4–16 ˚C (11˚C on average) [81].

Insolubility of PNA

There are however a few drawbacks of PNA which complicate its direct use of PNA in many applications. Since PNAs do not carry any charges, they have poor water solubility compared to DNA. The degree of how PNA solubilize in aqueous environments is related to the length of the oligomer and to the purine/pyrimidine ratio [78]. To address this solubility issue,

some recent modifications have been reported, including the incorporation of positively charged lysine residues (carboxyl-terminal or backbone modification in place of glycine) and the introduction of negatively charged residues such as PNA/DNA chimeras [82]. These modifications of PNAs have shown improvements in solubility. PNAs have low cellular permeability, thus limiting its applications for antigene or antisense therapies.

Cellular effects and delivery of PNA

It is very important to understand the effect of PNA on intact cells and problems related to its delivery into the cell. The cellular uptake of PNA is very slow due to the presence of neutral backbone, which is still considered to be the major challenge than must overcome before it can be used as a therapeutic agent [83, 84]. So far, there are hardly any reports of the antisense activity of PNA in cell culture with the use of brute techniques to help bypass the membrane barrier. PNA–nucleic acid chimeras are reported to be taken up by Vero or NIH3T3 cells even at a relatively lower extracellular concentration (1 μM), which leaves us with the idea that a PNA–DNA chimera may be a better antisense agent. The kinetics of uptake is similar to that observed for an oligonucleotide of the same sequence [85].

Flexibility of PNA

Neutral PNA molecules have a tendency to self-aggregate to a degree that is dependent on the sequence of the oligomer [86]. This self-aggregation is due to the flexible natural of achiral polyamide backbone. Rigidification of the PNA backbone via conformational constrain to pre-organize the PNA structure will influence the orientational selectivity in complementary DNA/RNA binding [87].

1.3.2. Application of PNAs

Today there are four major groups of applications for this novel compound. First, it can be used a molecule tool in molecular biology and biotechnology [88-92]. Secondly, its role as a lead compound for the development of gene-targeted drugs applying antigene or antisense strategy [93, 94]. Third is the use of PNAs for diagnostic purposes and development of biosensors [95-98]. Forth, the study of basic chemistry related to PNAs [77, 99, 100] for the improvement of basic architecture, e.g., for supramolecular constructs and to possibly generate a subsequent generation of PNA molecules [86].

Antisense properties of PNA

Although it is not the intention to give an elaborate account of the ongoing development gene therapeutic drugs based on PNA oligomers, it is fair to say that PNA does possess many of the properties desired from an antisense reagent. It binds strongly and with excellent sequence specificity to complementary mRNA, it has very high biological stability, and targeting of specific mRNAs with PNA has been shown to inhibit translation of this mRNA. This has been demonstrated in several biological systems *in vitro*, and the introduction of various novel methods for improved delivery of PNA to eukaryotic cells has recently also shown good efficacy in cell culture *ex vivo* as well in a few cases *in vivo* [100-104].

1.3.3. Chemical Modification of PNAs

The limitations of PNA as described above include: low aqueous solubility, ambiguity in DNA binding orientation and poor membrane permeability. In order to obtain improved properties for various applications with medicine, diagnostics, and molecular biology, the classic structure of PNA has been subjected to a variety of modifications. The strategic rationale behind

the modifications are (i) introduction of chirality into the achiral PNA backbone to influence the orientational selectivity in complementary binding, (ii) rigidification of PNA backbone via conformational constrain to pre-organize the PNA structure and entropically drive the duplex formation, (iii) introduction of cationic functional groups directly in the PNA backbone, in a side chain substitution or at the N or C terminus of the PNA, (iv) modulate nucleobase pairing either by modification of the linker or the nucleobase itself and (v) conjugation with 'transfer' molecules for effective penetration into cells [104].

1.4. Project Definition

The success of PNA as a DNA backbone mimic has inspired scientists to further utilize its improved properties in nucleic acid therapeutics. One strategy is to use the PNA monomers as a single unit and incorporate them into a DNA/RNA single strand. The resultant chimeric oligomers, in which both type of monomeric unit are present in a single chain, might combine the favourable hybridisation characteristics of PNA with the high water solubility of DNA/RNA.

Early in 1996, the Brown group has synthesized adenine, thymine and cytosine PNA monomers and used these monomers to assemble DNA chimeric oligomers [105]. PNA monomers have been placed at the 5'-end of the chimeric oligomers. The resultant chimeras hybridised specifically to complementary DNA. The chimeric oligomers formed more stable complexes with complementary DNA than do the equivalent DNA sequences. Uhlmann *et al*. also did one study on PNA-DNA chimeras [85]. In their study, the PNA monomer was placed not only at each end but also in the middle of the DNA single strand. They found that an insertion of a single PNA unit into a DNA single strand results in a significant drop of T_m especially when it is placed in the middle of the sequence. This indicates that a degree of thermal

destabilization was displayed, which is mostly due to a strong structural perturbation occurring at the PNA-DNA junction. However, they found these DNA chimeras were more stable in human serum compared to the unmodified wild type. At the same time they showed improved aqueous solubility due to their partially negatively charged structure. Furthermore, because of their DNA component, they are more easily taken up by the cells. More importantly, DNA-PNA chimeras are recognized as substrates by various nucleic acid processing enzymes, which makes them capable of stimulating RNase H activity. Messere *et al.* have further examined the biological ability of the DNA-PNA chimeras in (a) interfering with reverse transcription reaction of eukaryotic mRNA and (b) inhibiting DNA-protein interactions [106]. They found that these chimeric molecules are efficient in interfering with real-time reaction and can inhibit DNA-protein interactions, which makes them useful tool in the transcription factor decoy approach to alter gene expression.

Compared to DNA, RNA is less stable due the presence of the 2'-OH attached to the pentose ring (**Figure 1-6**). These functional groups can chemically attack the adjacent phosphodiester bond to cleave the backbone (an intermolecular nucleophilic attack). Thus, there is widespread interest in chemically modifying the backbone of RNA in order to overcome some of the inherent problems with its native structure of RNA [107-109]. The success of DNA-PNA chimeras has encouraged us to go one step further into the RNA field by synthesizing RNA-PNA chimeras.

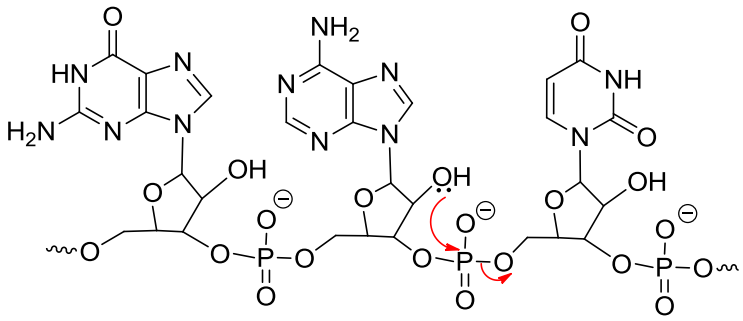

Figure 1-6: The phosphate backbone can be cleaved from an intermolecular nucleophilic attack.

There have been only two reports that have employed amide-bond linkages as phosphate replacements within siRNAs [4, 5]. In both studies (**Figure 1-7, A and B**), the PNA monomer unit were placed at 3'-overhang regions of siRNAs due to the limitation of standard solid-phase oligonucleotide synthesis (reviewed in Chapter **2**). In both studies, all amide-bond modified siRNAs showed enhanced nuclease resistance. In Messere's study, the PNAs were conjugated to thymine dimers at the 3'-overhang of one or both strands of the siRNA (**Figure 1-7, A**). The siRNAs having PNA monomers at the passenger strand overhangs showed efficient gene silencing and also showed persistent silencing activity relative to other siRNAs tested. Similarly, Iwase *et al*. synthesized siRNAs modified with amide-linked oligonucleotides (**Figure 1-7, B**) at their 3'-overhangs. These modified siRNAs reduced the target gene expression in a similar manner to the unmodified siRNA in mammalian cells. Chimeras consisting of siRNA-PNA can therefore be used as potent RNAi tools with the passenger strand preferably modified as outlined in these studies.

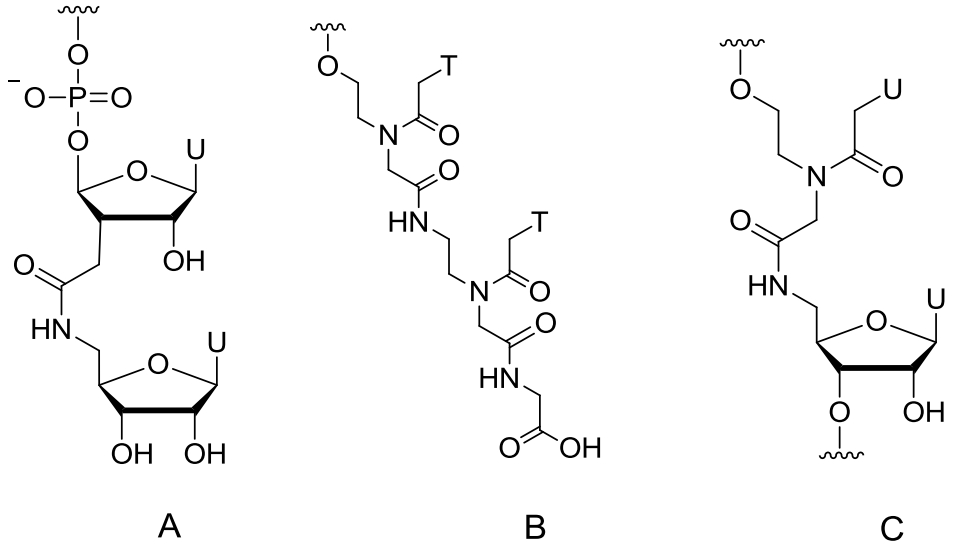

Figure 1-7: Structures of different amide-bond derivatives used within siRNAs.

In our study, through solid-phase RNA phosphoramidite chemistry, we were able to control the site-specific location of the PNA monomer by controlling its location within the desired RNA strand (**Figure 1-7, C**) [7]. We want to explore the scope of the PNA monomer in multiple positions especially within the internal Watson-Crick region of the double stranded siRNA. The effects of this modification were explored with respect to the biophysical and biological properties of the modified siRNAs by studying the thermodynamic stability, overall conformation, enzymatic stability, and biocompatibility of these backbone modified oligomers within the RNAi machinery.

Chapter 2: Synthesis and Purification of Modified Nucleotides and Oligonucleotides

2.1. Introduction

In this chapter, the synthesis of PNA-RNA dimer unit and the synthesis of chemically modified oligonucleotides will be explored. The dimer unit was placed within various RNA oligonucleotides via phosphoramidite chemistry [7].

2.1.1. Synthesis of PNA-RNA Dimer Unit

There is widespread interest in chemically modifying the backbone of RNA to improve its therapeutic properties, due to the presence of the 2'-hydroxy group which makes RNA more susceptible to the nuclease-assisted hydrolysis compared to DNA. Replacing an amide-bond with a phosphodiester via an amide-bond dimer unit could potentially offer favourable properties for siRNA or other nucleic-acid based applications. **Figure 2-1** illustrates the structure of a uracil-based PNA-RNA dimer unit that contains an aminoethyl glycine unit (U_aU).

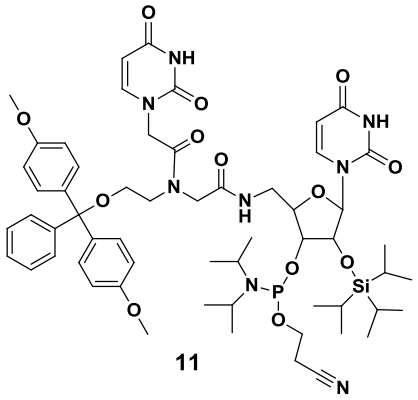

Figure 2-1: Structure of uracil-based PNA-RNA dimer (U_aU)

The synthesis of this PNA-RNA dimer unit was conceived based on the amide bond formation which is formed between two molecules when the carboxyl group (-COOH) of one molecule reacts with the amino group (-NH_2) of the other molecule. As one half of the dimer unit, a PNA monomer (**Figure 2-2**) carrying the carboxyl group was coupled with a RNA monomer (**Figure 2-2**) which has the amino group, via amide synthesis with the assistance of coupling reagent EDC·HCl.

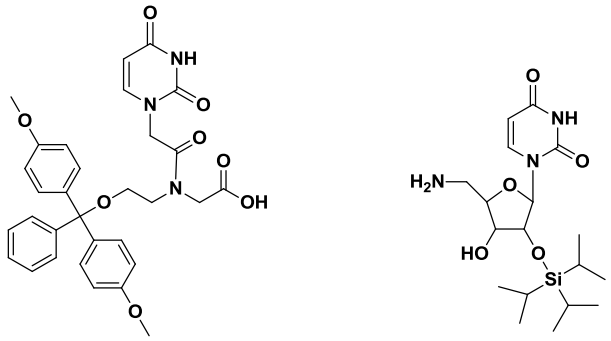

Figure 2-2: Structure of PNA and RNA monomer

2.1.2. Synthesis of Modified Oligonucleotides

The synthetic oligonucleotides can be considered as the fuel which drives the engine of molecular biology. They can be found in nearly every technique in use today in molecular biology, such as DNA sequencing, PCR, real-time PCR, microarrays and site directed mutagenesis. In recent years, advances in oligonucleotide synthesis chemistry as well as in purification and quality control technologies have led to substantial increases in both quality and yield and to substantial decreases in cost. In addition, high throughput manufacturing of the full range of possible syntheses has largely expanded the range of the applications of modified oligonucleotide. This section will focus on the fundamentals of chemical synthesis of

oligonucleotides as it is practiced today with a focus on the phosphoramidite approach and the solid- phase approach.

In nature, DNA or RNA is synthesized by the use of DNA/RNA polymerase for gene replication and transcription in the presence of suitable primers. The formation of the phosphate linkages in DNA/RNA is catalyzed enzymatically in a reversible reaction. That is, a deoxynucleotide triphosphate is added to a growing deoxynucleotide monophosphate polymer by a polymerase in the presence of Mg^{2+} and that the forward reaction resulted in the n+1 polymer and a pyrophosphate. In late 1950's, Professor H. Gobind Khorana and his group at the University of Wisconsin accomplished this synthetically, which helped Khorana receive the 1968 Nobel Prize in Physiology and Medicine [110]. By employing this technique, DNA/RNA can be synthesized chemically and enzymatically in several hundred base pairs in length. The deficiencies of this strategy which made this technique no longer popular and dominant are its inefficiency and high expenses. The coupling yields decreased markedly as the oligonucleotide length increased and complicated mixtures of by-products resulted. Each oligonucleotide required several months to a year or more to synthesize. They were considered so valuable at that time that they were kept under lock and key in the Khorana laboratory [110]. Moreover, modified oligonucleotides cannot be synthesized by using this technique.

2.1.3. Phosphoramidite Chemistry

In 1983 a breakthrough was achieved in oligonucleotide chemistry that made it possible to make synthetic modified oligonucleotides with high efficiency [111]. The new synthesis process was based upon the use of phosphoramidite monomers and the use of tetrazole catalyst (**Figure 2-3. a & c**). Phosphoramidite reagents are stable and can be easily prepared in the

laboratory, which make it feasible to produce these reagents commercially. To synthesize a standard phosphoramidite monomer (**Figure 2-3, a**), a dimethoxytrityl (DMT) protecting group (**Figure 2-3, d**) was attached to the 5' position before reacting with 2-cyanoethyl *N*,*N*-diisopropyl-chloro-phosphoramidite **(Figure 2-3, b)** which is later added onto the 3' position, to avoid both 3' and 5'-OH groups reacting with 2-cyanoethyl *N*,*N*-diisopropyl-chloro-phosphoramidite. All subsequent internucleotide phosphate linkages are formed by coupling a 5'-OH to 3'-OH nucleotides. DMT is chosen as a protecting group due to several factors. First, due to its bulky nature, DMT chloride selectively reacts with the primary 5'-hydroxyl group over more hindered secondary 3'-hydroxyl group. Secondly, the DMT group can be easily quantified and removed using a mild acid, such as trichloroacetic acid. Finally, when the detritylation happens, the intensity of orange colored trityl cations released from the solid-phase support can provide an easy way to rapidly and quantitatively monitor the solid-phase coupling reactions.

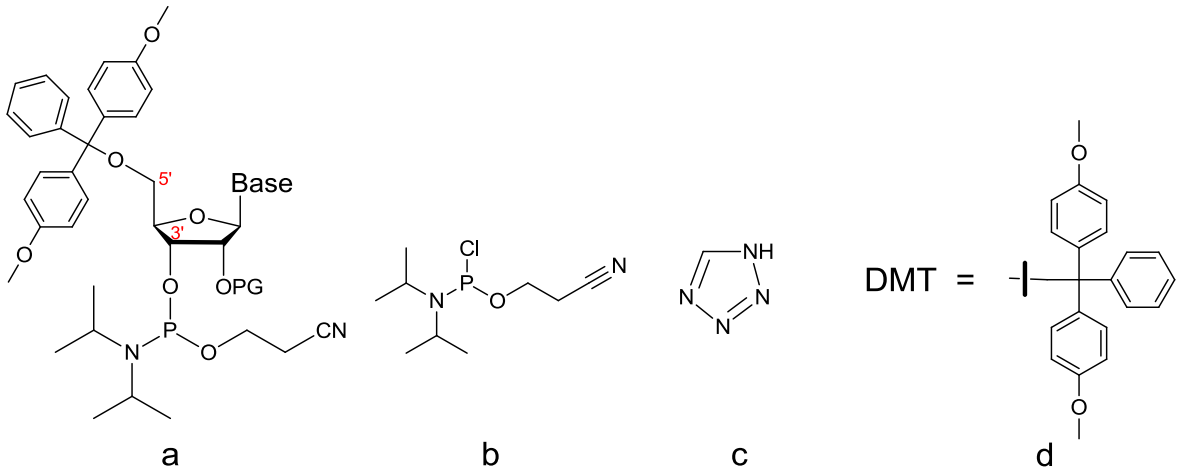

Figure 2-3: 2-cyanoethyl protected phosphoramidite reagent (a), 2-cyanoethyl N,N-diisopropyl-chloro-phosphoramidite (b), tetrazole (c) and dimethoxytrityl (d)

2.1.4. Solid-Phase Synthesis

All phosphoramidite coupling cycle reactions are performed on the base of the solid-phase support which is a controlled pore glass bead (CPG). This bead has a surface with holes and channels. It is in these that the protected nucleotide is attached covalently. The solid support is the highlight in genetic engineering. In 1962, Robert B. Merrifield at the Rockefeller Institute devised a scheme for the solid-phase synthesis of peptides [112]. The big advantage of it is the ease with which immobilized products can be separated from other reactants and by-products. The emergence of this approach elegantly reduced the tedious and time-consuming isolation of the product for the coupling reaction to a simple filtration step by covalently attaching one end of the product to an insoluble support. It is very important to select an optimum solid-phase support in oligonucleotides synthesis. The ideal support should act as an inert carrier without hindering coupling reactions and provide sufficient surface functionality to yield synthesis capacities of between 10 and 50 μmol/g (for small-scale) or 100 to 20 μmol/g (for large scale). In our lab, we use CPG which is widely used in small-scale synthesis and use succinic acid as the linker arm which is the compound used to join the surface of the support to the first nucleoside. The support is first succinylated and then coupled to a nucleoside. The solid-phase synthesis is performed automatically by using DNA synthesizers. It only requires delivery of reagents to a reservoir containing the insoluble support and the subsequent elution of the unreacted reagents from the support using solvent washes. With appropriate computer control, many dozens of even hundreds of individual, repetitive steps can be programmed to run automatically, and such automation held the promise of making synthetic oligonucleotides readily available.

2.1.5. Phosphoramidite Coupling Cycle Chemistry

The link to the solid support is made through the 3’ carbon and synthesis precedes 3’ to 5’ rather than the 5’ to 3’ synthesis used previously in enzymatic approach. Phosphoramidite synthesis begins with the 3’-most nucleotide and proceeds through a series of cycles composed of fours steps that are repeated until the 5’-most nucleotide is attached. These steps are deprotection, coupling, capping, and oxidation (**Figure 2-4**).

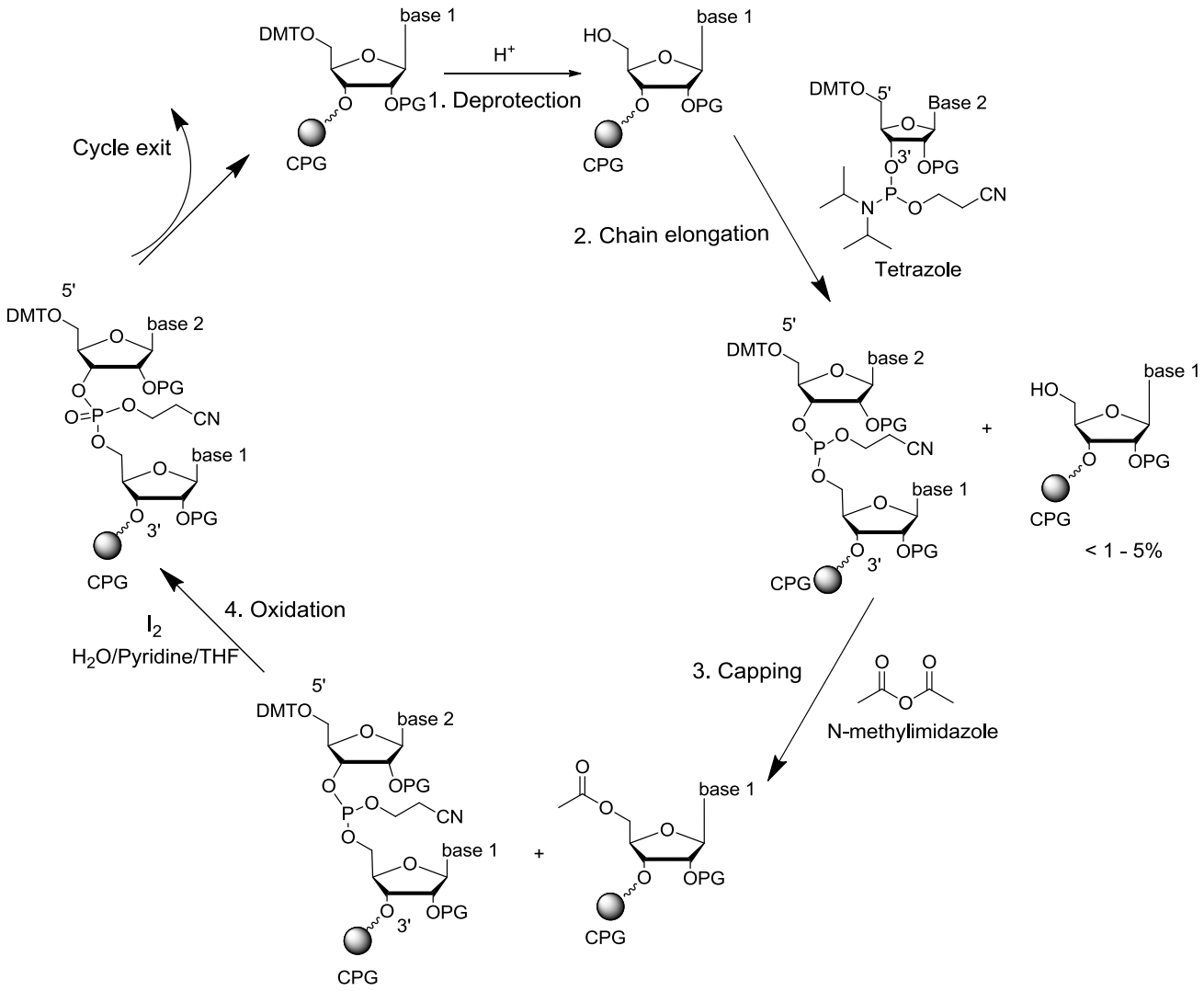

Figure 2-4: The phosphoramidite coupling cycle. (1) deprotection with acid. (2) Chain extension using a nucleoside-3′-O-phosphoramidite activated with tetrazole. (3) Capping (acetylation) of unreacted residues. (4) Oxidation of phosphite linkages into phosphate linkages with iodine and water.

Step 1: Deprotection

The first base, which is attached to the solid support, is at first inactive because all the active sites have been protected by DMT group. To couple the next base on, the DMT group protecting the 5'-hydroxyl group must be removed. This is done by adding an acid, trichloroacetic acid in dichloromethane (DCM), to the synthesis column. The 5'-OH is now the only reactive group on the base monomer. This ensures that the addition of the next base will only bind to that site. The reaction column is then washed to remove any extra acid and by-products. The amount of the trityl cation flowing out of the synthesis column is quantified which indicates the coupling efficiency. This feature is built in many automated DNA synthesizers.

Step 2: Activation and Coupling of Next Phosphoramidite

After the detritylation reagent has been washed from the support, the next step is the activation of the next nucleoside-3'-phosphormaidite and coupling of the activated base to the growing oligonucleotide. The activation is achieved by adding tetrazole (**Figure 2-3, c**) to the base. Tetrazole cleaves off one of the groups protecting the phosphorus linkage. This base is then added to the reaction column. The active 5'-OH of the preceding base and the newly activated phosphorus bind to loosely join the two bases together. This forms an unstable phosphite linkage.

The reaction column is then washed to remove any extra tetrazole, unbound base and by-products.

Step 3: Capping

Although the efficiency of the coupling reaction is quite high (95-99% in yield), there are still some unreacted molecules left. In order to prevent these unreacted molecules to further participate in chain growing to form a mixture of oligonucleotide impurities, the unbound, active 5'-OH is capped with a protective group which subsequently prohibits that strand from growing again. This is done by adding acetic anhydride and N-methylimidazole (NMI) to the reaction column. These compounds only react with the 5'-hydroxyl group. The base is capped by undergoing acetylation. The reaction column is then washed to remove any extra acetic anhydride or NMI.

Step 4: Oxidation

In step 2 the next desired base was added to the previous base, which resulted in an unstable phosphite linkage. To stabilize this linkage a solution of dilute iodine in water, pyridine, and tetrahydrofuran (THF) is added to the reaction column. The unstable phosphite linkage is oxidized to form a much more stable phosphate linkage. The progress of this step can be observed by the instantaneous disappearance of the dark iodine color on contact with phosphite compounds.

At this point, if the oligonucleotide sequence is incomplete then the cycle can be repeated as many times as necessary until the full-length sequence has been assembled. Once the sequence is complete, it must be cleaved from the solid support and deprotected before it can be

effectively used. This is done by incubating the chain in concentrated ammonium hydroxide solution at 55 ºC for overnight. All the protecting groups are now cleaved, including the cyanoethyl group, the heterocyclic protection groups, and the DMT group on the very last base. For RNA synthesis, The left 2'-*O* protecting groups on the ribose sugar can be later removed through a variety of different approaches.

2.2. Experimental Procedures

Synthesis of PNA-RNA Dimer Unit

Unless otherwise noted, all starting materials were obtained from commercial sources and were used without any additional purification. Anhydrous CH_2Cl_2, THF and DMF were purchased from Sigma-Aldrich and degassed by stirring under a dry N_2 atmosphere. Purification by flash column chromatography was carried out with Silicycle Siliaflash 60 (230-400 mesh) according to the procedure of Still, Kahn, and Mitra [113]. ^{1}H NMR, ^{13}C NMR, and ^{31}P NMR spectra were recorded at 400, 100, and 167 MHz, respectively, in either DMSO-d_6, $CDCl_3$ or CD_3OD. ESI-MS spectra were recorded on a Waters Quattro Micro MS. Both HRMS and ESI Q-TOF spectra were recorded on an Agilent Q-TOF.

2-(*tert*-Butyldimethylsilyloxy)ethanamine (1):

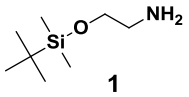

1

To a solution of ethanolamine (9.6 mL, 159 mmol) in 100 mL of dichloromethane was dissolved imidazole (10.8 g, 159 mmol) and this solution was cooled in an ice-water bath. To this solution

was added *tert*-butyldimethylsilyl chloride (24 g, 159 mmol) and the reaction mixure was stirred overnight at rt. Saturated $NaHCO_3$ was added and the resulting mixture was partitioned. The organic fractions were concentrated *in vacuo* to afford the title compound as a clear light yellow oil (26.8 g, 96%) [114].

Ethyl 2-((2-((tert-butyldimethylsilyl)oxy)ethyl)amino)acetate (2):

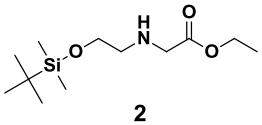

2

To a solution of **1** (6.5 g, 37 mmol) in 100 mL of dichloromethane was added triethylamine (3.7 g, 37 mmol), and this solution was cooled in an ice-water bath. To this solution was added ethyl 2-bromoacetate (3.1 g, 18.5 mmol) dropwise over 30 min. This reaction mixture was stirred at rt. until TLC analysis indicated the complete consumption of starting material (3 h). Saturated $NaHCO_3$ was added and the reaction mixture was partitioned. The organic fraction was concentrated *in vacuo*, to afford an oil which was purified by silica gel chromatography eluting with a gradient of hexanes/EtOAc (7:3 to 3:7) to afford the title compound as a clear yellow oil (2.9 g, 71%); ^{1}H NMR (500 MHz, $CDCl_3$) δ 0.00 (s, 6H), 0.84 (s, 9H), 1.19-1.23 (t, 3H, J = 8.0 Hz), 1.87(s, 1H), 2.65-2.68 (m, 2H), 3.37 (s, 2H), 3.64-3.68 (m, 2H), 4.10-4.15 (q, 2H, J = 8.0 Hz); ^{13}C NMR (100 MHz, $CDCl_3$) δ -5.39, 14.2, 18.2, 18.3, 25.9, 51.0, 51.3, 60.6, 62.6, 172.2; ESI-HRMS (ES^+) *m/z* calcd for $[C_{12}H_{27}NO_3Si + H]^+$: 262.1833, found 262.1839 $[M + H]^+$.

Ethyl-2-(N-(2-((tert-butyldimethylsilyl)oxy)ethyl)-2-(2,4-dioxo-3,4-dihydropyrimidin-1(2H)-yl)acetamido)acetate (3):

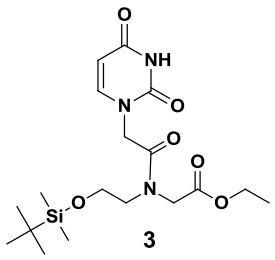

3

To a solution of uracil-1-yl acetic acid[115](1.79 g, 11.5 mmol) dissolved in 100 mL anhydrous DMF was added compound **2** (3.0 g, 11.5 mmol) and this solution was cooled in an ice-water bath under N_2. The acid was activated with the addition of 1-ethyl-3-(3-diethylaminopropyl)carbodiimide hydrochloride (EDC·HCl) (4.4 g, 22.9 mmol). The reaction mixture was stirred for 24 h at ambient temperature and then extracted with dichloromethane and the organic layer was washed with H_2O and brine (x3). The organic layer was collected and concentrated *in vacuo* to afford the crude product. This crude product was purified by flash chromatography with a gradient of hexanes/EtOAc (7:3) to 100% EtOAc to elute the title compound as a white solid (3.2 g, 68%). Compound **3** is a pair of rotamers; the signals to the major (ma.) and minor (mi.) rotamers are designated; ^{1}H NMR (400 MHz, $CDCl_3$) δ 0.04 (s, 2H, mi.), 0.09 (s, 4H, ma.), 0.88 (s, 3H, mi.), 0.90 (s, 6H, ma.), 1.26 (t, 2H, *J* = 7.0 Hz), 1.31 (t, 1H, *J* = 7.0 Hz), 3.56 (t, 2H, *J* = 4.7 Hz), 3.76 (t, 0.7H, *J* = 5.1 Hz, mi.), 3.81 (t, 1.3H, *J* = 5.1 Hz, ma.), 4.15-4.19 (m, 4H), 4.48 (s, 0.7H, mi.), 4.72 (s, 1.3H, ma.), 5.71-5.74 (m, 1H), 7.15 (d, 0.7H *J* = 7.8 Hz, ma.), 7.21 (d, 0.3H, *J* = 7.8 Hz, mi.), 8.90 (br s, 1H); ^{13}C NMR (100 MHz, $CDCl_3$) δ -5.51, -5.54, 14.1, 18.2, 18.3, 25.8, 25.9, 47.5, 47.7, 48.4, 50.6, 50.7, 50.8, 61.2, 61.4, 62.0, 102.1,

102.2, 145.1, 145.1, 150.8, 158.9, 163.4, 167.0, 167.2, 168.6, 169.2; ESI-HRMS (ES^+) *m/z* calcd for $[C_{18}H_{31}N_3O_6Si + H]^+$: 414.2055, found 414.2057 $[M + H]^+$.

Ethyl 2-(2-(2,4-dioxo-3,4-dihydropyrimidin-1(2H)-yl)-N-(2-hydroxyethyl)acetamido)acetate (4):

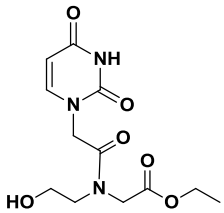

4

To a solution of compound **3** (1.25 g, 3.0 mmol) dissolved in 10 mL of dichloromethane was added TEA/3HF (0.73 g, 4.5 mmol), until TLC analysis showed the consumption of starting material. This reaction mixture was quenched with MeOH and the reaction was evaporated *in vacuo* to afford the crude product. The crude product was dissolved in minimal dichloromethane/MeOH and purified by flash column chromatography eluting with a gradient of 10% NH_4OH in MeOH (5% to 10%) in dichloromethane to afford the title compound as a white solid (0.71 g, 79%). Compound **4** is a mixture of slowly-exchanging rotamers. ^1H NMR (500 MHz, CD_3OD) δ 1.24-1.32 (m, 3H), 3.53 (t, 0.5H, *J* = 5.1Hz, mi.), 3.58 (t, 1.5H, *J* = 5.1Hz, ma.), 3.66 (t, 0.5H, *J* = 5.3 Hz), 3.75 (m, 1.5H), 4.17 (m, 2H), 4.38 (s, 0.5H), 4.64 (s, 0.5H), 4.86 (s, 2H), 5.66 (d, 0.5H, *J* = 8.0 Hz), 5.68 (d, 0.5H, *J* = 8.0 Hz), 7.43-7.48 (m, 1H); ^{13}C NMR (100 MHz, CD_3OD) δ 11.8, 45.7, 45.2, 46.2, 46.6, 46.8, 47.0, 49.2, 57.9, 58.3, 59.9, 99.6, 145.3, 150.2, 164.2, 167.4, 168.5; ESI-HRMS (ES^+) *m/z* calcd for $[C_{12}H_{17}N_3O_6 + H]^+$: 300.1190, found 300.96 $[M + H]^+$.

Ethyl 2-(N-(2-(bis(4-methoxyphenyl)(phenyl)methoxy)ethyl)-2-(2,4-dioxo-3,4-dihydropyrimidin-1(2H)-yl)acetamido)acetate (5):

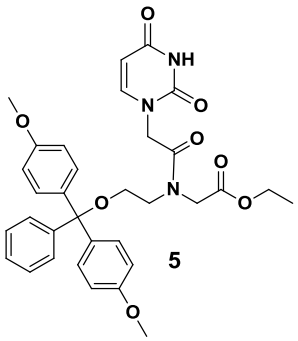

5

To a solution of **4** (1.0 g, 3.3 mmol) dissolved in 10ml of dry pyridine was added 4,4'-dimethoxytrityl chloride (2.3 g, 6.6 mmol) under N_2. The reaction mixture was stirred for 24 h at ambient temperature and then extracted with dichloromethane and the organic layer was washed with H_2O and brine (x3). The organic layer was collected and concentrated *in vacuo* to afford the crude product. The crude product was dissolved in minimal dichloromethane/MeOH and purified by flash column chromatography eluting with a gradient of MeOH (1% to 5%) in dichloromethane to afford the title compound as a white solid (1.3g, 66%). Compound **5** is a pair of rotamers; the signals to the major (ma.) and minor (mi.) rotamers are designated; ^{1}H NMR (500 MHz, $CDCl_3$) δ 1.23-1.27 (m, 3H), 3.31 (m, 0.63H, mi), 3.41 (m, 1.26H, ma), 3.48-3.55 (m, 2H), 3.79 (m, 6H), 4.32 (s, 0.5H, *J* = 8.2Hz), 4.45 (s, 0.5H, *J* = 8.2Hz), 4,72 (s, 1H), 5.62 (t, 0.66H, *J* = 8.2Hz), 5.72(t, 0.33H, *J* = 8.2Hz), 6.85(d, 4.20H, *J* = 7Hz), 7.22-7.39(m, 9H), 8.73(br s, 1H); ^{13}C NMR (100 MHz, $CDCl_3$) δ 14.1, 47.9, 55.3, 61.4, 101.9, 113.3, 127.8, 128.1, 130.1, 144.4, 144.9, 158.7, 163.3, 167.1, 168.5; ESI-HRMS (ES^+) *m/z* calcd for $[C_{33}H_{35}N_3O_8 + Na]^+$: 624.2316, found 624.2315 $[M + Na]^+$.

2-(N-(2-(bis(4-methoxyphenyl)(phenyl)methoxy)ethyl)-2-(2,4-dioxo-3,4-dihydropyrimidin-1(2H)-yl)acetamido)acetic acid (6):

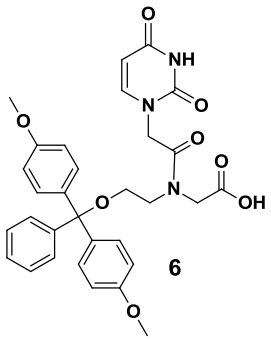

6

To a solution of **5** (550 mg, 0.9 mmol) dissolved in 5 ml of MeOH was added NaOH (146 mg, 3.6 mmol). The reaction mixture was stirred for 4 h at 60˚C. The mixture was cooled in ice-water bath and carefully acidified to pH~5.5 with 2N aq. $NaHSO_4$. The precipitate was filtrated off. The filtrate was collected and concentrated *in vacuo* to afford the crude product (500mg, 96%). Compound **6** is a pair of rotamers; the signals to the major (ma.) and minor (mi.) rotamers are designated; ^{1}H NMR (500 MHz, CD_3OD) δ 3.35-3.36 (m, 2H), 3.51-3.53 (m, 2H), 6.03 (s, 6H), 3.89 (s, 1H), 4.09 (s, 1H), 4.57 (s, 1.5H, ma), 4.66 (s, 0.5H, mi), 6.85-6.88 (m, 4H), 7.25-7.43 (m, 9H); ^{13}C NMR (100 MHz, CD_3OD) δ 50.0, 51.60, 55.9, 60.3, 62.8, 87.8, 102.3, 114.1, 127.9, 128.8, 129.4, 130.6, 137.5, 146.4, 152.9, 160.1, 166.9, 169.4, 169.7; ESI-HRMS (ES^+) *m/z* calcd for $[C_{31}H_{31}N_3O_8 + H]^+$: 572.2038, found 572.2031 $[M + H]^+$.

1-(5-(azidomethyl)-3,4-dihydroxytetrahydrofuran-2-yl)pyrimidine-2,4(1H,3H)-dione (7):

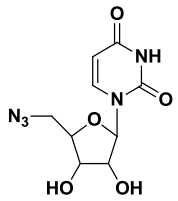

7

To a mixture of uridine (4.0 g, 11.2 mmol), sodium azide(2.2 g, 33.6 mmol) and triphenylphosphine (3.82g, 14.6 mmol) in 100 ml of anhydrous DMF was added carbon tetrabromide(5.57 g, 16.8 mmol). The reaction mixture was stir for 12 h at rt and then concentrated *in vacuo*, to afford crude product which was purified by silica gel chromatography eluting with a gradient of MeOH (3% to 8%) in dichloromethane to afford the title compound as a white solid (2.6 g, 86%). The ^{1}H proton and ^{13}C NMR shifts were confirmed with the report by Winans and Bertozzi.[116]

1-(5-(azidomethyl)-4-hydroxy-3-((triisopropylsilyl)oxy)tetrahydrofuran-2-yl)pyrimidine-2,4(1H,3H)-dione (8):

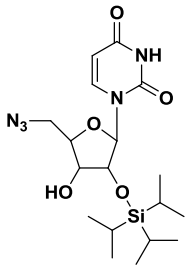

8

To a solution of compound 7 (2.6 g, 9.66 mmol) in 50 ml of dry DMF was added imidazole (1.64 g, 24.15 mmol) and triisopropylsilyl chloride (3.72 g, 19.3 mmol). The reaction mixture was stirred for 12 h at rt and then extracted with EtOAc and the organic layer was washed with H_2O and brine (x3). The organic layer was collected and concentrated in *vacuo* to afford the crude

product. The crude product was dissolved in minimal dichloromethane/MeOH and purified by flash column chromatography eluting with a gradient of a gradient of hexanes/EtOAc (8:2 to 4:6) to afford the title compound as a crystalline solid (2.55 g, 62%). Compound 8 is a pair of rotamers; the signals to the major (ma.) and minor (mi.) rotamers are designated; ^{1}H NMR (500 MHz, $CDCl_3$) δ 1.05-1.08 (m, 18H), 1.09-1.16 (m, 3H), 3.63 (d, 0.33H, J = 3.5Hz, mi), 3.66 (d, 0.66H, *J* = 3.5Hz, ma), 3.75 (d, 0.5H, *J* = 2.7Hz), 3.78 (d, 0.5H, *J* = 2.7Hz), 4.10-4.14 (m, 1H), 4.50 (t, 1H, *J* = 5.1Hz), 5.82 (d, 1H, *J* = 8.2Hz), 5.88 (d, 1H, *J* = 5.1Hz),7.47 (d, 1H, *J* = 8.2Hz); ^{13}C NMR (100 MHz, $CDCl_3$) δ 12.1, 17.8, 52.3, 71.2, 74.7, 82.6, 90.1, 103.3, 140.3, 150.1, 162.7; ESI-HRMS (ES^+) *m/z* calcd for $[C_{18}H_{31}N_5O_5Si + H]^+$: 426.2167, found 426.2166 $[M + H]^+$.

1-(5-(aminomethyl)-4-hydroxy-3-((triisopropylsilyl)oxy)tetrahydrofuran-2-yl)pyrimidine-2,4(1H,3H)-dione (9):

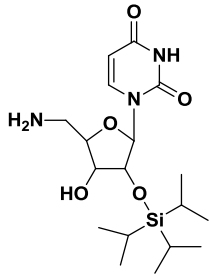

9

To a solution of 8 (2.15 g, 5.06 mmol) in 200 ml of THF was added triphenylphosphine (4.44 g, 15.2 mmol) and H_2O (4.0 g, 0.222 mol). The reaction mixture was stirred for 12 h at rt and then concentrated in *vacuo* to afford the crude product. The crude product was dissolved in minimal dichloromethane/MeOH and purified by flash column chromatography eluting with a gradient of

8% to 10% (10% NH_4OH in MeOH) to afford the title compound as a white solid (1.8 g, 89%). Compound 9 is a pair of rotamers; the signals to the major (ma.) and minor (mi.) rotamers are designated; ^{1}H NMR (400 MHz, DMSO-d_6) δ 0.97-1.14 (m, 21H), 2.50 (p, 1H, J_1 = 3.7Hz, J_2 = 1.7Hz), 2.74-2.76 (m, 2H), 3.79-3.82 (td, 1H, J_1 = 4.8Hz, J_2 = 2.5Hz), 4.13-4.16 (m, 1H), 4.20-4.22 (dd, 1H, J_1 = 5.1Hz, J_2 = 2.3Hz), 5.22 (br, 1H), 5.64 (d, 1H, J = 7.8Hz), 5.80 (d, 1H, J = 6.6Hz), 7.88 (d, 1H, J = 8.2Hz),); ^{13}C NMR (100 MHz, DMSO-d_6) δ 11.7, 17.9, 43.4, 72.4, 72.7, 86.7, 87.3, 102.0, 141.4, 150.9, 163.0; ESI-HRMS (ES^+) *m/z* calcd for $[C_{18}H_{33}N_3O_5Si + H]^+$: 400.2262, found 400.2266 $[M + H]^+$.

N-(2-(bis(4-methoxyphenyl)(phenyl)methoxy)ethyl)-2-(2,4-dioxo-3,4-dihydropyrimidin-1(2H)-yl)-N-(2-(((5-(2,4-dioxo-3,4-dihydropyrimidin-1(2H)-yl)-3-hydroxy-4-((triisopropylsilyl)oxy)tetrahydrofuran-2-yl)methyl)amino)-2-oxoethyl)acetamide (10):

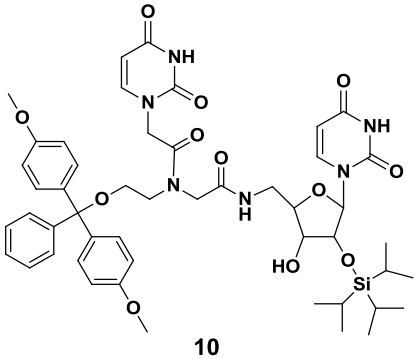

10

To a mixture of compound 6 (100 mg, 0.18 mmol) and 9 (58 mg, 0.15 mmol) in 6 ml of anhydrous DMF under N_2 was added 1-ethyl-3-(3-diethylaminopropyl)carbodiimide hydrochloride (EDC·HCl) (56 mg, 0.29 mmol) in ice-water bath. The reaction mixture was

stirred for 24 h at ambient temperature and then extracted with dichloromethane and the organic layer was washed with H_2O and brine (x3). The organic layer was collected and concentrated *in vacuo* to afford the crude product. This crude product was purified by flash chromatography with a gradient of MeOH (2% to 6%) in dichloromethane to afford the title compound as a white solid (54.7 mg, 40%). ^{1}H NMR (500 MHz, $CDCl_3$) δ 1.00-1.15 (m, 21H), 3.20-3.61 (m, 6H), 3.79-3.85 (m, 8H), 3.98-4.09 (m, 2H), 4.23-4.34 (m, 1H), 4.49 (s, 1H), 4.69-4.99 (m, 2H), 5.21 (d, 1H, *J* = 5.5Hz), 5.51-5.55 (m, 1H), 5.67-5.74 (m, 1H), 6.48-6.55 (m, 1H), 6.82-6.87 (m, 4H), 7.10-7.38 (m, 9H); ^{13}C NMR (100 MHz, CD_3OD) δ 11.0, 13.5, 18.4, 18.7, 42.1, 47.3, 55.9, 62.7, 72.6, 74.3, 75.9, 84.3, 88.7, 92.7, 102.3, 114.5, 128.0, 128.2, 128.7, 129.1, 129.5, 130.6, 131.5, 137.2, 143.9, 144.2, 146.3, 147.8, 160.4, 170.0, 171.3; ESI-HRMS (ES^+) *m/z* calcd for $[C_{49}H_{62}N_6O_{12}Si + Na]^+$: 977.4087, found 977.4106 $[M + Na]^+$.

2-((2-(N-(2-(bis(4-methoxyphenyl)(phenyl)methoxy)ethyl)-2-(2,4-dioxo-3,4-dihydropyrimidin-1(2H)-yl)acetamido)acetamido)methyl)-5-(2,4-dioxo-3,4-dihydropyrimidin-1(2H)-yl)-4-((triisopropylsilyl)oxy)tetrahydrofuran-3-yl (2-cyanoethyl) diisopropylphosphoramidite (11):

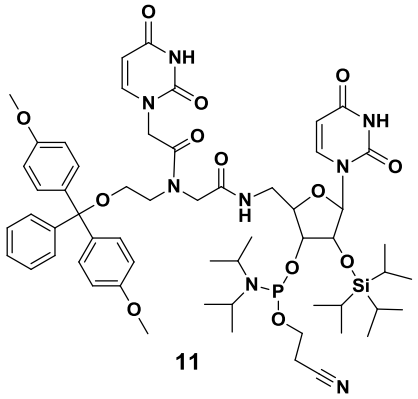

11

To a solution of compound 10 (83 mg, 0.104 mmol) dissolved in 5 mL of anhydrous dichloromethane under N_2 was added N,N-diisopropylethylamine (0.67 mg, 0.52 mmol) and 2-cyanoethyl N,N-diisopropyl-chloro-phosphoramidite (49.2 mg, 0.208 mmol). The reaction mixture was then stirred for 4 h under N_2. This reaction mixture was dried down *in vacuo* to afford the crude product. The crude product was then re-dissolved in minimal dichloromethane with 2% triethylamine and purified by flash column chromatography eluting with a gradient of acetone/hexane (1:1) to (2:1) with 2% triethylamine to afford the title compound as a white solid (62 mg, 59%). ^{1}H NMR (500 MHz, $CDCl_3$) δ 0.97-1.27 (m, 33H), 2.55-2.71 (m, 4H), 3.31-3.68 (m, 6H), 3.81-4.01 (m, 6H), 4.11-4.30 (m, 2H),4.49-4.71 (m, 1H), 4.75-5.03 (m, 1H), 5.49-5.75 (m, 1H), 6.85 (d, 4H, *J* = 9Hz), 7.21-7.36 (m, 9H), 8.26, (d, 2H, *J* = 8.2Hz); ^{13}C NMR (100 MHz, $CDCl_3$) δ 12.4, 18.0, 23.4, 24.6, 26.3, 29.2, 32.1, 43.2, 46.0, 47.9, 48.9, 53.8, 55.3, 57.7, 69.5, 73.0, 84.1, 84.6, 86.5, 87.6, 88.5, 102.4, 113.1, 113.4, 117.7, 127.3, 128.0, 128.1, 130.1, 135.0, 144.0, 144.9, 150.5, 151.5, 158.8, 160.1, 163.3, 167.8, 168.3; ^{31}P NMR (167 MHz, $CDCl_3$) δ

149.7, 150.9; ESI-HRMS (ES^+) *m/z* calcd for $[C_{58}H_{79}N_8O_{13}PSi + Na]^+$: 1177.5166, found 1177.5169 $[M + Na]^+$.

Synthesis of Natural or Modified Oligonucleotides

All standard *β*-cyanoethyl 2'-*O*-TBS protected RNA phosphoramidites, reagents, and solid supports were purchased from Chemgenes Corporation and Glen Research. Sequences such as the wild-type sense and 5'-phosphorylated antisense strands were purchased and purified from Integrated DNA Technologies (IDT). All U_aU-modified oligonucleotides were synthesized on an Applied Biosystems 394 DNA/RNA synthesizer using 1.0 µM or 0.2 µM cycles with 16 min coupling times for standard phosphoramidites. All phosphoramidites were dissolved in anhydrous acetonitrile to a concentration of 0.15 M. We observed an average coupling efficiency of >98% with the use of the U_aU phosphoramidite as monitored by trityl cation absorbance. Sequences containing 3' modifications were synthesized on 1.0 µM Universal III solid supports, while all other sequences were synthesized on 0.2 µM or 1.0 µM dT solid supports (Glen Research). Antisense sequences were chemically phosphorylated on the 5' end using 2-[2-(4,4'-Dimethoxytrityloxy)ethylsulfonyl]ethyl-(2-cyanoethyl)-(N,N-diisopropyl)-phosphoramidite (Glen Research). Cleavage of oligonucleotides from their solid supports were performed through on-column exposure to 1.5 mL of EMAM (methylamine 40 % wt. in H_2O and methylamine 33 % wt. in ethanol, 1:1 (Sigma-Aldrich)) for 1 hr at rt., followed by incubation in EMAM overnight to deprotect the bases. After drying down the EMAM, the samples were resuspended in a solution of 3 HF / TEA (150 µL) and incubated at 65 °C for 48 hr in order to remove the 2'-*O*-TBS and 2'-*O*-TIPS groups. Crude oligonucleotides were precipitated in EtOH and desalted through Millipore Amicon Ultra 3000 MW cellulose centrifugal filters. Oligonucleotides were excised from the 20% denatured gel and were gel purified, followed by

desalting through centrifugal filters. Equimolar amounts of complimentary RNAs were annealed at 90 ^{o}C for 2 min in a binding buffer (75 mM KCl, 50 mM Tris-HCl, 3 mM $MgCl_2$, pH 8.3) and this solution was cooled slowly to rt to generate siRNAs.

ESI Q-TOF Measurements. All single-stranded RNAs were gradient eluted through a Zorbax Extend C18 HPLC column with a MeOH/H_2O (5 : 95) solution containing 200 mM hexafluoroisopropyl alcohol and 8.1 mM triethylamine, and finally with 70% MeOH. The eluted RNAs were subjected to ESI-MS (ES^-), producing raw spectra of multiply-charged anions and through resolved isotope deconvolution, the molecular weights of the resultant neutral oligonucleotides were confirmed for all the RNAs. This service was performed by Dr. Jim Windak at the University of Michigan in Ann Arbor, Michigan.

2.3. Results and Discussion

To synthesize a PNA unit (**Scheme 1**), we started with protecting the hydroxyl group of commercially available ethanolamine with *tert*-butyldimethylsilyl (TBS) chloride to afford TBS-protected ethanolamine in 96% yield. TBS is one of the most common silyl ethers which are usually used as protecting groups for alcohols in organic synthesis. It can be easily removed with acids and fluorides later. The next step is to selectively monoalkylate **1** with the alkylating agent ethylbromoacetate under basic conditions to afford compound **2** in 71% yield. In order to avoid dialkylation of **1**, only 0.5 equivalents of ethylbromoacetate was added dropwise and the reaction progress was closely monitored by TLC analysis. The crude product was immediately purified by silica gel chromatography. With compound **2**, amide-bond formation with uracil-1-yl acetic acid using 1-ethyl-3-(3-diethylaminopropyl)carbodiimide (EDC) (**Figure 2-5, a**) yielded

compound **3** in 68% yield. EDC is a water soluble carbodiimide which is used as a carboxyl activating agent for the coupling of primary amines to yield amide bonds [117]. Compared to other coupling reagents such as dicyclohexylcarbodiimide (DCC) (**Figure 2-5, b**), 1-hydroxy-1H-benzotriazole (HOBt) (**Figure 2-5, c**) and O-Benzotriazole-*N*,*N*,*N'*,*N'*-tetramethyl-uronium-hexafluoro-phosphate (HBTU) (**Figure 2-5, d**), the by-product of EDC assisted amide bond formation is water soluble which can be easily removed in aqueous work-up.

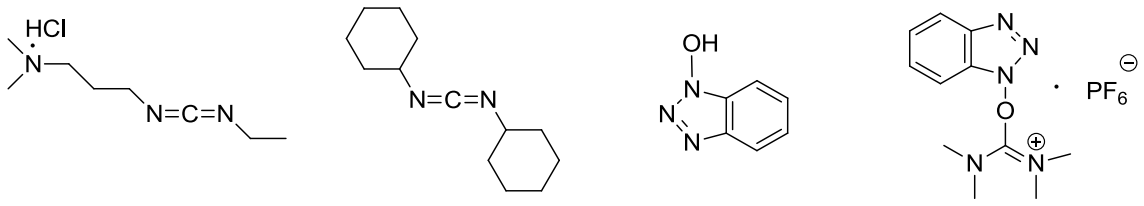

EDC· HCl **a** **DCC** **b** **HOBt** **c** **HBTU** **d**

Figure 2-5: Coupling reagents for amide bond formation

The next step is the removal of TBS protecting group in the presence of 3HF-TEA to yield monoalcohol **4**. This monoalcohol was then protected with 4,4'-dimethoxytrityl (DMT) chloride to afford the DMT-protected **5** in 66% yield. As described in the introduction, the DMT protecting group is needed for the standard solid-phase DNA/RNA synthesis. Compound **5** was readily saponified with NaOH and then acidified with $KHSO_4$ buffer to afford the final acetic acid **6** in 96% yield. Due to the presence of DMT group which is acid labile, during the last step of acidification, the pH value was strictly controlled in the range of 5.5-6 in order to prevent the removal of DMT group. Overall, this PNA building block was synthesized in 30% yield over five steps.

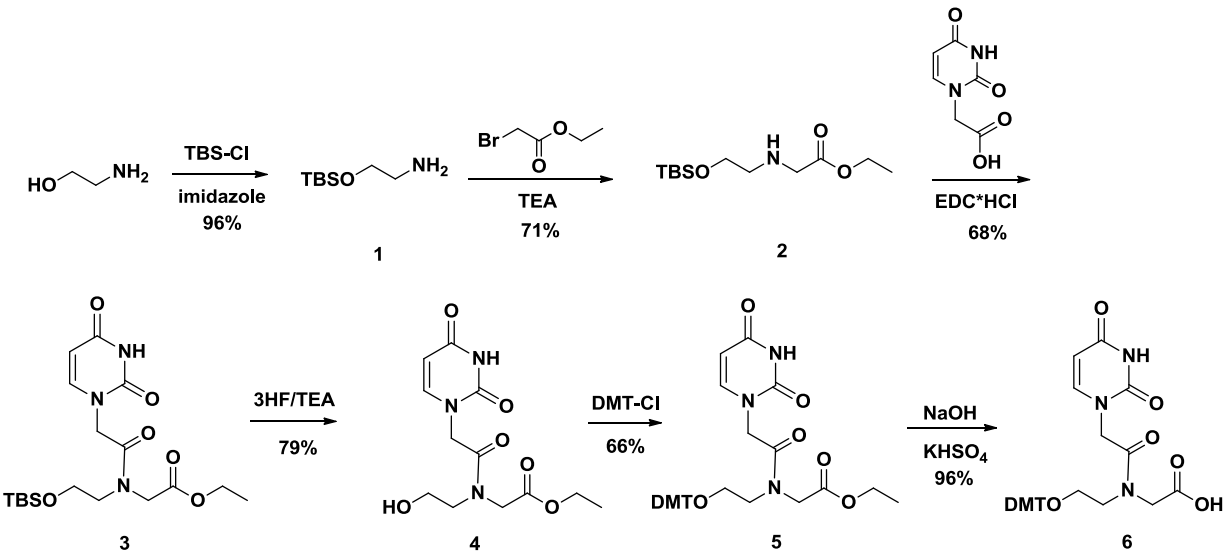

Scheme 1: Synthesis of a 4,4'-dimethoxytrityl-protected uracil acetic acid derivative.

To synthesize the RNA monomer (**Scheme 2**), 5'-azidouridine was synthesized from commercially available uridine in the presence of NaN_3, PPh_3, and CBr_4 [118]. In order to protect 2'-*O* position of compound **7**, triisopropylsilyl (TIPS) chloride was utilized with imidazole to afford compound **8** in 62% yield. In this step, TBS chloride was originally used like the case of the first protection of hydroxyl group in PNA monomer. We later found that TBS group has a tendency to constantly migrate from 2'-*O* and 3'-*O* position, thus resulting in the formation of a mixture of two TBS protected regioisomers. This was confirmed by the results from both TLC and ^{1}HNMR. The isolation of the 2'-*O* TBS protected product was unsuccessful. In order to avoid this problem, TIPS group as another silyl ether was chosen for the 2'-*O* protection of compound **7**. The greater bulkiness of TIPS group makes it more difficult to migrate from 2'-*O* and 3'-*O* position, which resulted in the formation of more stable TIPS protected products (2'-*O* and 3'-*O* protected). Using column chromatography, the isolation the 2'-*O*-TIPS protected isomer was accomplished. The regioselectivity of this isomer was confirmed

by 2D COSY NMR analysis. A characteristic doublet of doublet H2' chemical shift occurred at 4.50 ppm and the H3' and H4' proton shifts were indistinguishable. Reduction of the azido sugar **8** was achieved using standard Staudinger conditions in THF to afford **9** in 89% yield [118]. The characteristic H2' chemical shift of **9** appeared as a doublet of doublet at 4.21 ppm. Overall, this RNA building block was synthesized in 49% yield over three steps.

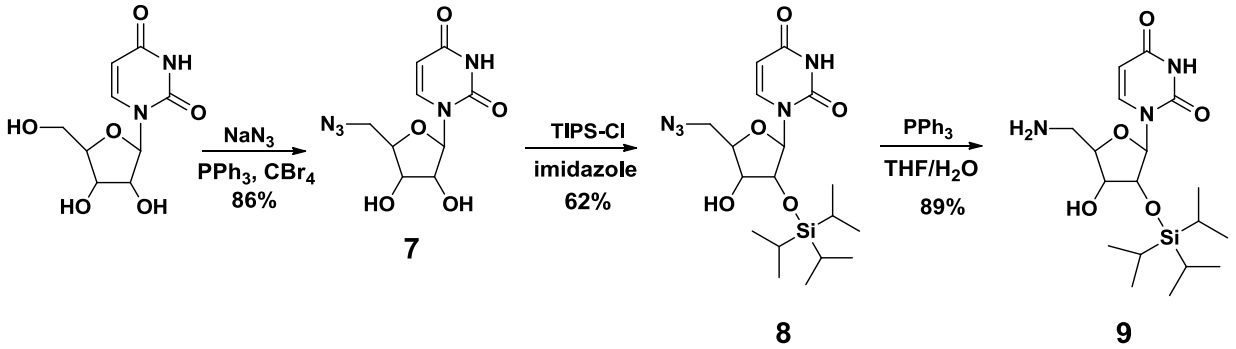

Scheme 2: Synthesis of 5'-amino-2'-*O*-triisopropylsilyluridine

With both compound **6** and **9** available, we amide-bond coupled these two monomers together in the presence of EDC in anhydrous DMF to afford the dimer U_aU **10** in 40% yield. Finally, compound **10** was subsequently phosphorylated with 2-cyano-*N*,*N* - diisopropylchlorophosphoramidite to yield compound **11** in 60% yield (**Scheme 3**). The ^{31}P NMR for this compound showed two phosphorus peak signals due to the diasteromeric nature of the ^{31}P atom for the respective phosphoramidite, thus, indicating a single isomeric form for the phosphoramidite. In this step, due to the fact that water can easily catalyze the conversion of the phosphoramidite to the phosphonate, all glassware was oven-dried; all reagents were either distilled or vacuum dried; anhydrous solvent was used in order to eliminate the presence of moisture. Overall, the final phosphoramidite **11** was synthesized in 27% yield over 12 steps and

stored in the freezer under vacuum until it was ready for the solid-phase DNA/RNA chemistry to synthesize RNA molecules that bear this U_aU dimer modification.

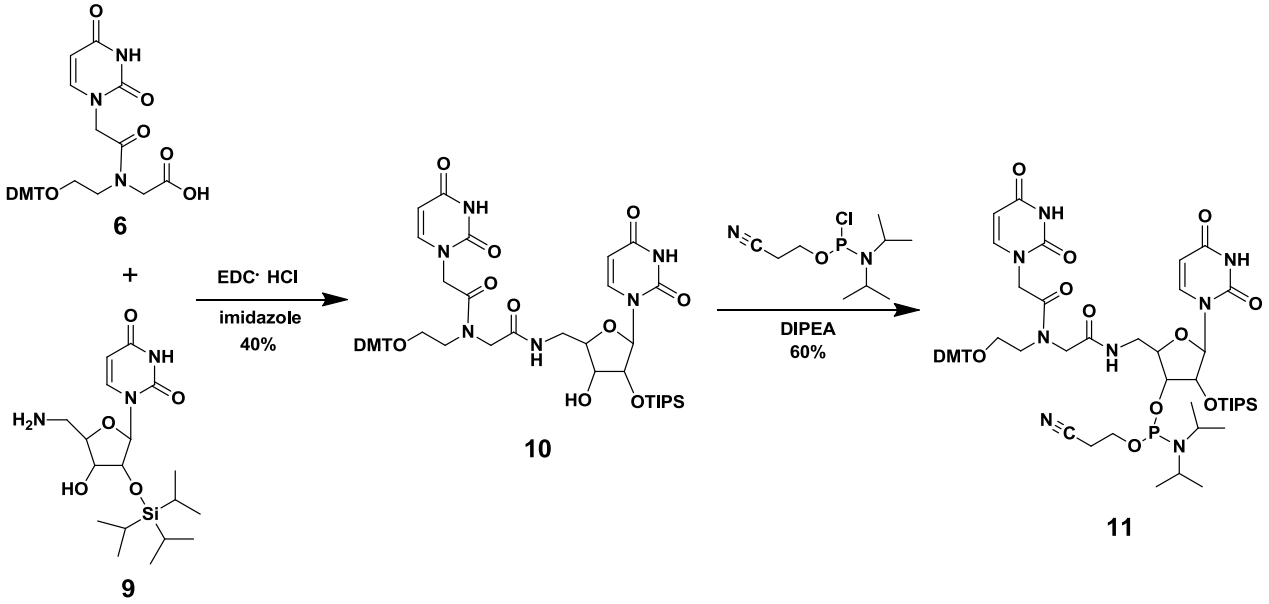

Scheme 3: Synthesis of U_aU phosphoramidite **11**

All natural or unmodified oligonucleotides were synthesized on an Applied Biosystems 394 DNA/RNA synthesizer. All of the DNA synthesis reagents have an impact on good quality DNA synthesis, as are all the steps in the synthesis cycle – coupling, capping, oxidation and detritylation. Fundamental to the successful synthesis of longer oligonucleotides is the need to maintain as high a coupling efficiency as possible. An average coupling efficiency of 98% would theoretically yield 68% full-length product for a 20mer. Therefore, it is imperative to maintain high coupling efficiency throughout the synthesis. One of the main obstacles to this is the presence of moisture. The most simple and effective first measures to increase coupling efficiency are to use anhydrous acetonitrile (ACN) to dissolve all the phosphoramidites, and to use fresh phosphoramidites during synthesis because the lifetime of phosphoramidite solution on

the synthesizer is less than 2 weeks. In addition, the RNA/DNA synthesizer has to be operated under N_2 atmosphere.

With all full length oligonucleotides assembled, the cleavage of oligonucleotides from their solid supports and deprotection of all the bases were performed through the treatment in EMAM (methylamine 40% wt. in H_2O and methylamine 33% wt. in ethanol, 1:1). The silyl protecting groups (TBS and TIPS groups) were deprotected by the treatment in 3HF-TEA. Due to the presence of TIPS groups which is highly stable, extra deprotection time (48 hours incubation) was needed. After the cleavage from the solid supports and the deprotection of all the protecting groups, all oligonucleotides were PAGE gel purified including the following steps: 1) pre-electrophoresis, 2) sample electrophoresis, 3) band excision from the 20% denatured gel, 3) overnight elution from the gel slice into buffer, 4) purification to remove all acrylamide out of the final product, 5) ethanol precipitation, 6) desalting through centrifugal filters, and 7) quantification by UV spectrometer. The overall yield of each oligonucleotide after the gel purification was usually under 20%. The molecular weights of the RNA oligonucleotides were confirmed by ESI Q-TOF analysis recorded on an Agilent Q-TOF. **Table 2-1** illustrated the predicted and recorded masses for U_aU modified RNAs.

Table 2-1: Predicted and recorded masses for U_aU modified sense and antisense RNAs. ESI Q-TOF recorded in negative electrospray mode after HPLC elution using two mobile phases; MeOH/H_2O (5:95) with 200 mM hexafluoroisopropyl alcohol and 8.1 mM triethylamine; and 70% MeOH.

Sample No.	Sense and Antisense RNAs	Predicted Neutral Mass	Observed Neutral Mass
pGL3 RNA 1	5'- CU_aUACGCUGAGUACUUCGAtt -3'	6549.95	6549.99
pGL3 RNA 2	5'- CUUACGCUGAGUACUUCGAU_aU -3'	6553.91	6553.94
pGL3 RNA 3	5'- CUUACGCUGAGUACU_aUCGAtt -3'	6549.95	6549.93
pGL3 RNA 4	5'- CUUACGCUGAGUACU_aUCGAU_aU -3'	6499.97	6500.01
pGL3 RNA 5	5'-ph-UCGAAGUACUCAGCGUAAGU_aU-3'	6719.94	6719.97
pGL2 RNA 6	5'-ph-UCGAAGUAU_aUCCGCGUACGtt-3'	6668.94	6668.94
pGL2 RNA 7	5'-ph-UCGAAGUAUUCCGCGUACGU_aU-3'	6672.90	6672.93
pGL2 RNA 8	5'-CGUACGCGGAAUACUUCGAU_aU-3'	6615.96	6615.96
pGL2 RNA 9	5'-CGUACGCGGAAUACU_aUCGAtt-3'	6612.02	6612.03

2.4. Chapter Summary

The work that has been presented in chapter 2 represents studies on the synthesis of PNA-RNA dimer unit and RNAs that contain such U_aU dimer unit. The use of siRNAs which were made from the RNAs produced in this chapter is presented in the next several chapters in order to elucidate the effect of the modifications on the hybridization affinity, overall conformation, gene-silencing ability, and nuclease stability of modified RNA.

Chapter 3: Biophysical Properties of Modified siRNAs Containing Internal Amide-Bond Linkages

3.1. Background Overview

It has been well established that the structure of nucleic acids plays a significant role in the efficacy of RNA therapeutics [34, 119]. The proper secondary structure is required for the antisense strand of siRNA to be loaded with the RISC complex, which is a programmable endonuclease [120]. Therefore, the secondary structure of siRNA is a major determinant in the success of gene silencing using siRNA.

Two biophysical parameters of modified siRNA were studied in this chapter: melting temperature and circular dichroism. The melting temperature (T_m) of a double stranded nucleic acid can be used to characterize the affinity and the specificity of siRNA for its complementary target. Upon target recognition and binding, the siRNA/mRNA duplex is presumed to form a helix. The most important factors in the formation of a helix are the affinity and specificity that an siRNA has for its complement. Therefore, determination of the T_m of modified duplexes is a good way to determine the effect of the modification upon secondary structure.

It has been shown that for the RISC mechanism to function properly, the siRNA guide strand must form an A-form helix with the target mRNA [121-123]. Therefore, the type of helix that formed between modified siRNAs and their complements were also studied in this chapter in order to determine the effect of the modification on the type of helix that formed. Circular dichroism (CD) can be used to gauge the type of helix formed.

Overall, the work presented in this chapter gives a comprehensive and systemic analysis of the effects of the internal amide bond modification on the secondary structure and duplex stability of siRNA.

3.2. Thermal stability of modified RNA duplexes

3.2.1. Introduction

Two types of base-base interactions occur in the double helix: hydrogen bonding of the bases that occurs within the plane of the bases (**Figure 3-1**), and base stacking that occurs perpendicular to the plane of the bases.

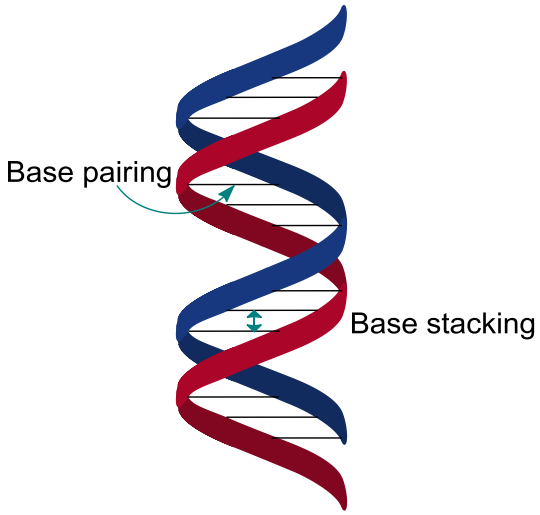

Figure 3-1: Two types of base interactions stabilize the double helix. Base pairing occurs in the plane of the bases and base stacking occurs perpendicular to the plane of the bases.

Helices are stabilized by base stacking and hydrogen bonding. As such, the measurement of the melting temperature (T_m) gives insight to the stability of the duplex [124]. Base stacking that occurs when single strands form the duplex results in decreases in the UV absorption at 260

nm; consequently monitoring the UV spectrum is one way to measure the secondary structure of oligonucleotides. Increasing the temperature of a solution of oligonucleotides will cause a subsequent increase in the UV absorption as the duplex is denatured into separate single strands; this effect is known as hyperchromicity (**Figure 3-2**). The thermal denaturation of double-stranded RNA is progressive and the concerted melting of the whole structure occurs at a well-defined temperature, corresponding to the mid-point of a smooth transition. This temperature is known as the melting temperature (T_m).

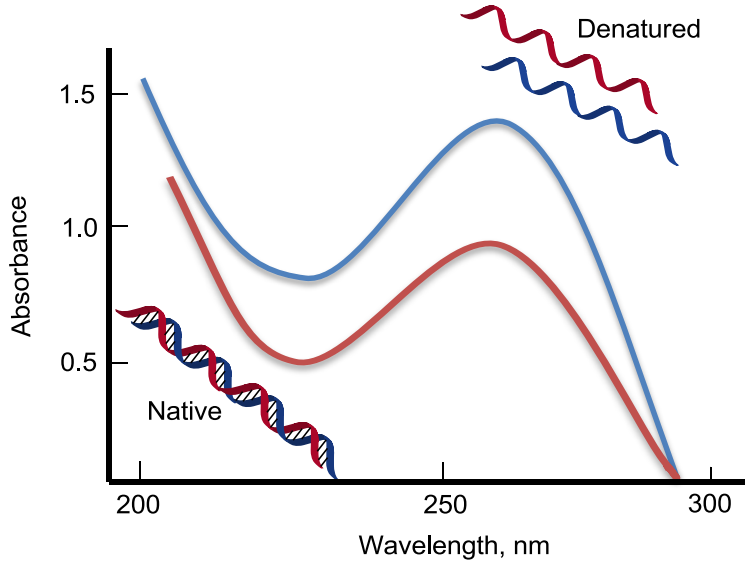

Figure 3-2: Hyperchromicity property of duplex oligonucleotides. Denatured, single stranded oligonucleotides have an increased UV absorbance as opposed to native, double stranded oligonucleotides. Native DNA becomes denatured as temperature is increased, and renatured as the oligonucleotide is slowly cooled [124].

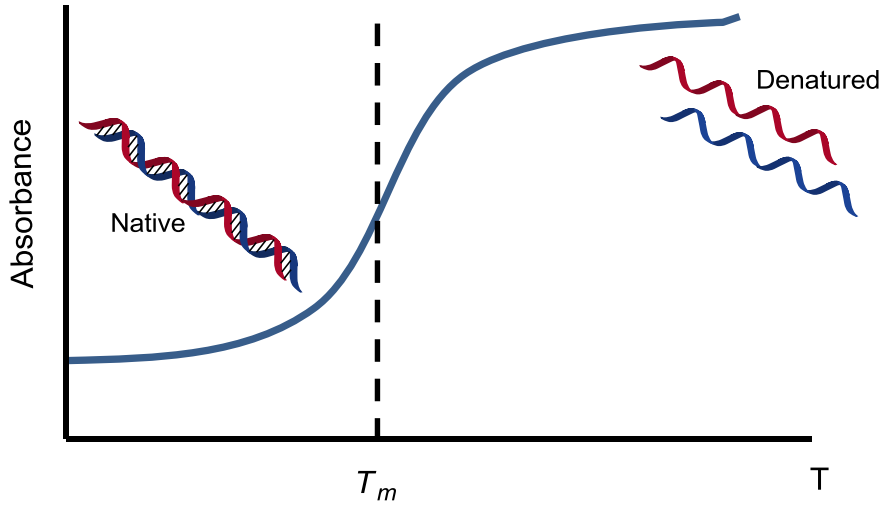

Figure 3-3: A typical UV melting curve

The example in **Figure 3-3** shows a melting curve (UV absorption as a function of temperature). Slow heating of double-stranded RNA causes the unwinding of the ordered helical structure into the two single-stranded constituents. This can be seen as a sigmoidal curve of increasing UV absorption. The mid-point, corresponding to the precise T_{m} of the duplex, is indicated.

The trend of stability of oligonucleotides duplexes has shown that RNA:RNA duplexes are the most stable, then RNA:DNA duplexes, followed by DNA:DNA [125]. This is because the A from helix in RNA stacks neighboring bases in a more stable lattice. In addition, chain length and GC/AT ratio can affect the duplex stability. An increase in either of these variables will increase the T_m [124]. It has been shown that chemical modification can affect the thermal stability of the RNA:RNA duplex that is formed between the siRNA and its complement [126].

Previous work from Iwase *et al*. involved placing dimer or a trimer of an amide-linked oligouridine derivative at the 3'-overhang regions of siRNAs. Their data suggested that the amide-linked RNA segment increase the thermodynamic stability of the siRNA [5]. Messere and coworkers synthesized modified siRNAs in which the 3'-TT overhangs were substituted by an

overhanging tract of PNA. The thermodynamic stability results have shown that the presence of a PNA dimer caused a destabilization effect on the chimeric siRNA [4] due to the fact that this overhang modification disrupted the overall base stacking interactions. On the other hand, work by Uhlmann *et al*. in which the PNA monomer was placed on the 3'-overhangs and the internal region of DNA single strand, has shown that by introducing a single PNA unit into a DNA resulted in a significant drop of T_m [85]. This destabilization effect is mostly due to a strong structural perturbation occurs at the PNA-DNA junction when placed in the internal region of RNA single strand. In this section, the effect of the insertion of our PNA-RNA dimer unit into an RNA duplex on thermal stability will be investigated.

3.2.2. Experimental Procedures

The RNAs that were used in this chapter were all synthesized by solid-phase chemistry and PAGE gel purified. Equimolar amounts of each RNA strand (2.4 nmol) were annealed to their compliment in 400 µL of a sodium phosphate buffer (90 mM NaCl, 10 mM Na_2HPO_4, 1 mM EDTA, pH 7) at 90 °C for 2 min and this solution was cooled slowly to rt. Melting temperatures (T_m) spectroscopy was performed on a Jasco J-815 CD equipped with temperature control. T_ms were measured in the sodium phosphate buffer at 260 nm with a temperature range of 10 to 95 °C. The temperature was increased at a rate of 0.5 °C / min while absorbance was measured at the end of each 0.5 °C increment. Absorbance readings were automatically adjusted against the baseline absorbance of the sodium phosphate buffer. After averaging the range of absorbance values obtained from three independent experiments for each siRNA, T_ms were calculated using Meltwin version 3.5 software assuming the two-state model [127]. To determine

the T_m hyperchromicity method, the software scans the melting curve to determine the temperature at which 50% of the duplex has dissociated.

Analysis of melting profiles

Consider a solution containing equal quantities of complementary single stranded RNA (ssRNA) A and B. Complementary ssRNA associate to form double stranded RNA (dsRNA) A·B. The reaction is governed by the equation:

$$A + B \leftrightarrows A \cdot B$$

The concentration of the reaction products are related by the equilibrium constant: $K_{eq} = \frac{[A \cdot B]}{[A][B]}$, the value of K_{eq} is a function of temperature. We can equate the fundamental definition of the standard free energy change with its relationship to the equilibrium constant in solution.

$$\Delta G° = \Delta H° - T\Delta S°$$

$$= -RT\ln K_{eq}$$

Where $\Delta G°$ is the standard change in free energy

$\Delta H°$ is the standard enthalpy change

$\Delta S°$ is the standard entropy change

T is the temperature

R is the gas constant

Solving for K_{eq}:

$$K_{eq} = \exp(\frac{\Delta S°}{R} - \frac{\Delta H°}{RT})$$

Let C_{ss} be the concentration of single strand RNA (C_{ss} = [A] = [B]) and C_{ds} be the concentration of double strand RNA (C_{ds} = [A·B]). C_T is the total concentration of RNA strands ($C_T = 2C_{ss} + 2C_{ds}$). Let α be the fraction of total RNA is double stranded

$$\alpha = \frac{2C_{ds}}{C_T} = \frac{C_T - 2C_{ss}}{C_T} = 1 - 2\frac{C_{ss}}{C_T}$$

Therefore, $C_{ss} = \frac{(1-\alpha)C_T}{2}$

Solving for K_{eq} in terms of α and C_T:

$$K_{eq} = \frac{C_{ds}}{C_{ss}^2} = \frac{\alpha C_T/2}{[(1-\alpha)C_T/2]^2} = \frac{2\alpha}{(1-\alpha){C_T}^2}$$

Substituting for K_{eq} from $K_{eq} = \exp(\frac{\Delta S^\circ}{R} - \frac{\Delta H^\circ}{RT})$

$$\exp\left(\frac{\Delta S^\circ}{R} - \frac{\Delta H^\circ}{RT}\right) = \frac{2\alpha}{(1-\alpha){C_T}^2}$$

Taking the log of both sides and solving for T:

$$T(\alpha) = \frac{\Delta H^\circ}{\Delta S^\circ - Rln\left(\frac{2\alpha}{C_T(1-\alpha)^2}\right)}$$

From this equation, we know that temperature is a function of dsRNA fraction for a given total RNA strand and RNA identity (ΔH^o and ΔS^o). ΔH^o and ΔS^o values can be estimated from slopes and intercepts of fitted straight lines of $\ln K_{eq}$ versus 1/T plots.

3.2.3. Results and Discussion

In order for gene silencing to occur through the RNAi pathway, the siRNA guide strand must recognize and bind to its target molecule in a sequence-specific manner. Therefore, the thermal stability of the duplex, and the information that it conveys about the structure of the duplex, must be studied for each sequence and modification. The uracil RNA duplexes were formed by the annealing of the uracil and adenine RNA 18mer strands. The two sets of siRNA duplexes (pGL2 & pGL3) were formed by the annealing of the sense and antisense RNA 21mer strands. These two siRNA sequences were chosen because they were both designed to

specifically target reporter genes coding for two variants of *firefly* (*Photinus pyralis*, GL2 and GL3) luciferases which are widely used as reporters for studying gene regulation and function [128, 129]. There are differences in the coding sequence from each reporter gene which allows us to use two different parent siRNAs. **Table 3-1** shows two parent siRNA duplexes that target pGL2 and pGL3.

Table 3-1: The parent siRNA duplexes that target pGL2 and pGL3. These siRNA duplexes only differ by three single-nucleotide substitutions (blue color).

Target plasmid	siRNA duplex
pGL2	5'-C**G**UACGC**G**GA**A**UACUUCGAtt-3' 3'-ttG**C**AUGCG**C**CU**U**AUGAAGCU-5'
pGL3	5'- C**U**UACGC**U**GA**G**UACUUCGAtt -3' 3'-ttG**A**AUGCG**A**CU**C**AUGAAGCU-5’

Analyses of the melting curves were performed as described in the experimental procedures. The melting temperatures and thermodynamic parameters are given in **Table 3-2.**

Table 3-2: Melting temperature (T_m) data of RNAs complemented to rA_{18}.

RNA	RNA duplex	T_m (^{0}C)	ΔT_m (^{0}C)
wt RNA	5'-UUUUUUUUUUUUUUUUU-3' 3'-AAAAAAAAAAAAAAAAA-5'	31.4	0
a	5'-U_aUUUUUUUUUUUUUUUUU-3' 3'-AAAAAAAAAAAAAAAAA-5'	25.7	-5.7
b	5'-UUUUUUUUUUUUUUUUU_aU-3' 3'-AAAAAAAAAAAAAAAAA-5'	25.9	-5.5
c	5'-UUUUUUUUU_aUUUUUUUUU-3' 3'-AAAAAAAAAAAAAAAAA-5'	22.9	-8.5

As illustrated in **Table 3-2**, localizing a U_aU dimer unit within the RNA oligonucleotide has a destabilizing effect when complemented to rA_{18}. When the U_aU dimer unit is located on either the 3'-end or the 5'-end, a decrease of approximately 5.5 °C is observed. When the U_aU dimer is located internally, a larger loss in melting temperature of 8.5 °C is observed. These observed drops in melting temperature are consistent with other studies involving PNA-DNA chimeras [130].

Table 3-3: Sequences of anti-luciferase siRNAs that target pGL2 and T_m Data.

RNA	siRNA duplex	T_m (^{0}C)	ΔT_m (^{0}C)
wt pGL2	5'-CGUACGCGGAAUACUUCGAtt-3' 3'-ttGCAUGCGCCUUAUGAAGCU-5'	73.1	--
1	5'-CGUACGCGGAAUAC**U$_a$U**CGAtt-3' 3'-ttGCAUGCGCCUUAUGAAGCU-5'	66.6	-6.5
2	5'-CGUACGCGGAAUAC**U$_a$U**CGAtt-3' 3'-**U$_a$U**GCAUGCGCCUUAUGAAGCU-5'	66.2	-6.9
3	5'-CGUACGCGGAAUAC**U$_a$U**CGAtt-3' 3'-ttGCAUGCGCC**U$_a$U**AUGAAGCU-5'	62.9	-10.2
4	5'-CGUACGCGGAAUACUUCGA**U$_a$U**-3' 3'-ttGCAUGCGCCUUAUGAAGCU-5'	72.9	-0.2
5	5'-CGUACGCGGAAUACUUCGA**U$_a$U**-3' 3'-**U$_a$U**GCAUGCGCCUUAUGAAGCU-5'	74.3	+1.2
6	5'-CGUACGCGGAAUACUUCGAtt-3' 3'-**U$_a$U**GCAUGCGCCUUAUGAAGCU-5'	72.9	-0.2
7	5'-CGUACGCGGAAUACUUCGAtt-3' 3'-ttGCAUGCGCC**U$_a$U**AUGAAGCU-5'	66.0	-7.1
8	5'-CGUACGCGGAAUACUUCGA**U$_a$U**-3' 3'-ttGCAUGCGCC**U$_a$U**AUGAAGCU-5'	66.0	-7.1

Table 3-3 highlights the T_m data for the siRNAs that target pGL2. SiRNA **1** contains an internal U$_a$U modification close to the 3'-end of the sense strand and a thermal decrease of *ca*. 6.5 ºC is observed relative to wild-type. When two internal modifications are present (siRNA **3**), the largest destabilization effect is observed (*ca*. 10 ºC), which is mostly due to a strong structural perturbation occurs at the PNA-RNA junction. On the other hand, modifications introduced at the 3'-overhangs of the duplexes (siRNAs **4-6**) have very little effect on duplex

stability. This is potentially due to the fact that the base stacking of the duplex remains intact when the U_aU modification is placed at the 3'-overhangs. Both siRNA **7** and **8** have internal U_aU modification in the antisense. Although siRNA **8** contains an extra modification on the 3'-overhang of the sense strand which has shown to have little effect on the duplex stability, it has similar thermal stability when compared to siRNA **7**. Same case can be observed when siRNA **1** is compared to siRNA **2** which also has an extra modification on the 3'-overhang of the antisense strand. These T_m changes are consistent with other similar studies involving PNA-DNA hybrids [130]. In general, internal amide-bond modifications display a degree of thermal destabilization; whereas U_aU modifications at the 3'-overhang observe little change in thermal stability.

Table 3-4: Sequences of anti-luciferase siRNAs that target pGL3 and T_m Data

RNA	siRNA duplex	T_m (^{0}C)	ΔT_m (^{0}C)
wt pGL3	5'-CUUACGCUGAGUACUUCGAtt-3' 3'-ttGAAUGCGACUCAUGAAGCU-5'	70.5	--
9	5'-C**U_aU**ACGCUGAGUACUUCGAtt-3' 3'-ttGAAUGCGACUCAUGAAGCU-5'	67.9	-2.6
10	5'-C**U_aU**ACGCUGAGUACUUCGAtt-3' 3'-**U_aU**GAAUGCGACUCAUGAAGCU-5'	63.7	-6.8
11	5'-CUUACGCUGAGUAC**U_aU**CGA**U_aU**-3' 3'-ttGAAUGCGACUCAUGAAGCU-5'	64.8	-5.7
12	5'-CUUACGCUGAGUAC**U_aU**CGA**U_aU**-3' 3'-**U_aU**GAAUGCGACUCAUGAAGCU-5'	61.0	-9.5
13	5'-CUUACGCUGAGUAC**U_aU**CGAtt-3' 3'-ttGAAUGCGACUCAUGAAGCU-5'	64.3	-6.2
14	5'-CUUACGCUGAGUAC**U_aU**CGAtt -3' 3'-**U_aU**GAAUGCGACUCAUGAAGCU -5'	64.5	-6.0
15	5'-CUUACGCUGAGUACUUCGA**U_aU**-3' 3'-ttGAAUGCGACUCAUGAAGCU-5'	69.1	-1.4
16	5'-CUUACGCUGAGUACUUCGA**U_aU**-3' 3'-**U_aU**GAAUGCGACUCAUGAAGCU-5'	70.1	-0.4
17	5'-CUUACGCUGAGUACUUCGAtt-3' 3'-**U_aU**GAAUGCGACUCAUGAAGCU-5'	70.8	+0.3

.

In the next set of experiments, we examined the hybridization affinity of U_aU-modified siRNAs that target pGL3. Including overhangs, there are three potential positions to place a U_aU modification on the sense strand and one position on the antisense strand. **Table 3-4** illustrates

the duplexes studied and their respective T_m. Similar to **Table 3-3**, siRNAs that contain internal U_aU modifications (siRNA **9-14**) display a degree of thermal destabilization with values that are consistent with those obtained for siRNAs that target pGL2. Furthermore, modifications at the 3'-overhangs (siRNA **15-17**) have minimal effect on overall thermal stability.

3.2. Circular Dichroism

3.2.1. Introduction

Changes in the three dimensional structure of RNA can be monitored using CD, which studies the differential absorbance of circularly polarized light [131]. CD can be used to gauge the structure of a double helix because the form of the helix imparts a distinct CD spectra and it has been shown that there is no systematic change in this spectra with base composition [132]. For instance, it is known that RNA duplex in an A-form helix has a shallow trough at approximately 210 nm and a large peak at approximately 262-264 nm and a B-form helix has a trough at 220 nm and a peak at 270 nm with approximately the same magnitude. Z-form duplexes exhibit a collapsed intensity at the 275 maximum compared to the B-form duplexes (**Figure 3-3**) [132].

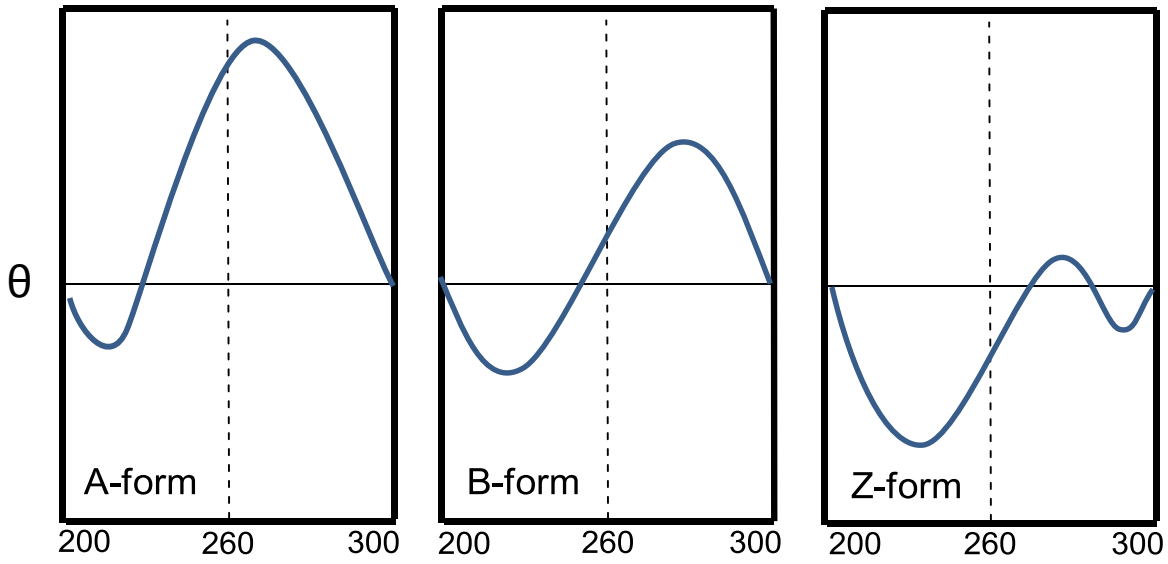

Figure 3-4: Representative CD spectra for three types of helical structures. A-form helices are typical of RNA:RNA duplexes and B-form helices are typical of DNA:DNA duplexes. Figure redrawn from reference [124].

Circular dichroism has been tremendously useful for studying the interactions between chemically modified oligonucleotides with their target sequences. CD is especially useful in the case of backbone-modified oligonucleotides where the chromophore (base) remain unchanged, because any change in the molar ellipticity (θ) can be attributed primarily to a conformational change in the oligonucleotide or complex, revealing valuable information about the secondary structure.

3.2.2. Experimental Procedures

The RNAs used in this section were shown in **Table 3-2, 3-3, and 3-4**. CD spectroscopy was performed on a Jasco J-815 CD equipped with temperature control. Equimolar amounts of each RNA were annealed to their compliment in 500 μL of a sodium phosphate buffer (90 mM

NaCl, 10mM Na_2HPO_4, 1mM EDTA, pH 7) at 90 ºC for 2 minutes and this solution was cooled slowly to room temperature. Four hundred microliters of this solution was transferred to a 0.5 mL quartz cuvette with a one cm path length. CD measurements of each duplex were recorded in quadruplicate from 200 to 310 nm at 20 ºC in the sodium phosphate buffer, with a scanning rate of 50 nm/min and a 0.2 nm data pitch. Three scans were performed for each sample, averaged, and the background was subtracted.

3.2.3. Results and Discussion

To determine whether the internal amide-bond modification in this study alter the overall A-from helical geometry of RNA duplex required for activity [121, 122]. CD was used to assess the global conformation of the modified duplex RNAs. For three uracil 18mer oligonucleotides (**Table 3-2, RNA a, b, and c**), as illustrated in **Figure 3-4**, the samples were compared with the CD spectrum of the unmodified sequence. All four oligonucleotides had negative and positive CD bands observed at approximately 210 and 265 nm, respectively, which corresponds to an A-type duplex. There was a slight difference in crossover point with the chemically modified duplex; however, the overall shapes of the spectra are similar, thus, implying that the global conformation of the duplex RNAs containing a U_aU unit does not alter significantly from wild-type RNA duplex. Furthermore, the overall shape of the CD curves is consistent with other studies involving homopolymeric rA-rU duplex polymers [21].

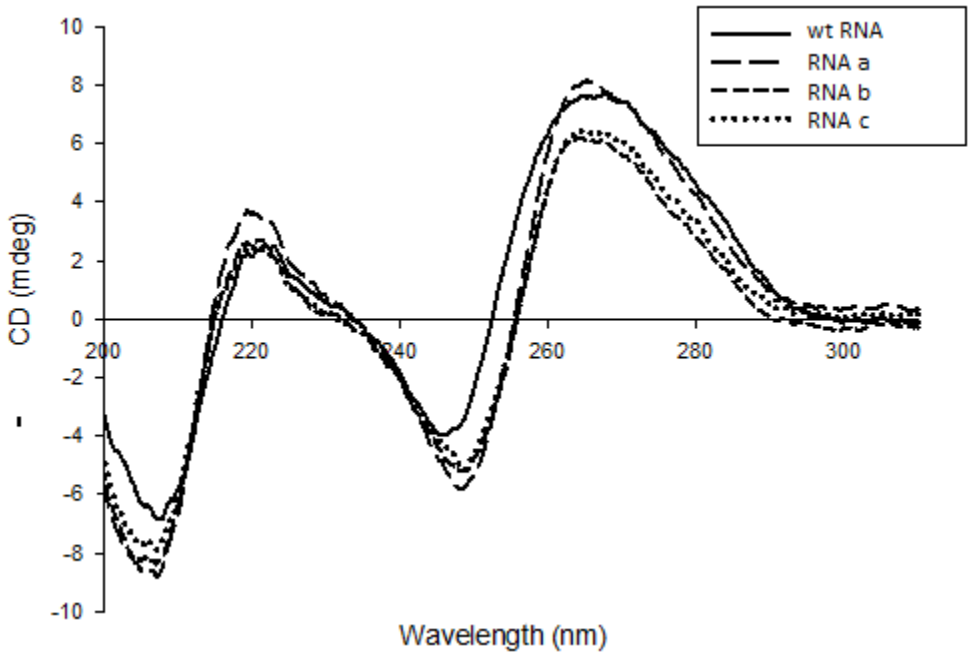

Figure 3-5: CD spectra of RNAs **a-c** complexed with rA_{18} in a sodium phosphate buffer (90 mM NaCl, 10 mM Na_2HPO_4, 1 mM EDTA, pH 7). The solution was scanned from 200 to 310 nm at 20ºC. All scans were performed in quadruplicate and averaged using version 2 of Jasco's Spectra Manager software.

For siRNAs targeting pGL2 and pGL3 vectors, As shown in **Figure 3-5, A** and **B**, negative and positive CD bands at 209 nm and 260 nm, respectively, which were attributable to A-type duplexes, were observed. Although the intensity of the positive and the negative bands of these modified siRNAs containing PNA-RNA dimer unit were slightly smaller than that of unmodified siRNA, a fact that is usually attributed to a reduction in base stacking [133], the shapes of their spectra were similar. These results imply that the global conformation of these modified siRNAs containing PNA-RNA dimer unit are not significantly different from that of the unmodified siRNAs.

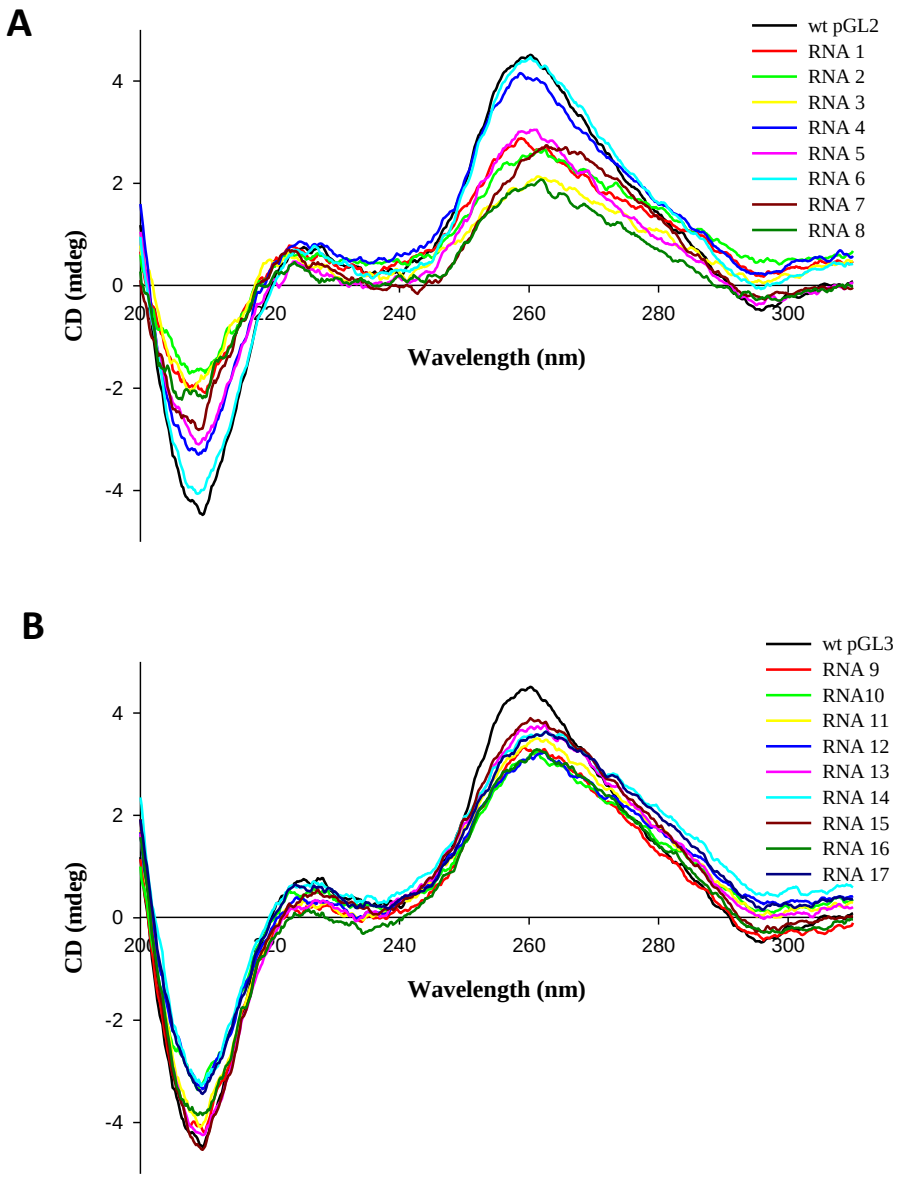

Figure 3-6. RNA duplex conformation of all anti-luciferase siRNAs displayed through circular dichroism spectroscopy. Duplex siRNAs (~1.7 nmol/duplex) were suspended in 400 µL of a sodium phosphate buffer (90 mM NaCl, 10 mM Na_2HPO_4, 1 mM EDTA, pH 7) and the solution was scanned from 200–310 nm at 20 ^{0}C. All scans were performed in quadruplicate and averaged using version 2 of Jasco's Spectra Manager software. (A) Wild-type and modified anti-

luciferase siRNAs **wt pGL2** and **1**–**8**; (B) Wild-type and modified anti-luciferase siRNAs **wt pGL3** and **9**–**17**.

3.3. Chapter Summary

Overall, T_m data support the conclusion that the introduction of one or more U_aU modification at the internal position leads to destabilization, whereas U_aU modifications at the 3'-overhang observe little change in thermal stability. On the other hand, the RNA duplexes that contain the U_aU dimer clearly still retain the overall A-from helical geometry. Although conformational features alone do not decide the interfering activity, an RNA-like A-type conformation is required for effective gene silencing which is required for RNAi activity [122].

Chapter 4: Biological Properties of siRNAs Containing Internal Amide-Bond Linkages

4.1. Investigation of Gene-Silencing Properties of siRNAs Containing Internal Amide-Bond Linkages

4.1.1. Introduction

In this chapter, we focus on the use of synthetic 21-mer siRNA duplex molecules in mammalian cells for transient gene silencing. siRNA molecules are potent effectors of post-transcriptional gene silencing. Using bioluminescent imaging and a mathematical model of siRNA delivery and function, the effects of target-specific siRNA-mediated gene silencing are monitored in cells stably expressing the *firefly* luciferase protein. In a luciferase reporter assay, luciferase genes are placed into mammalian cells through transfection. Expression of the luciferase reporter gene is then measured to quantify the activity of the regulatory proteins in the biological pathway affected by the target element.

Firefly luciferase is widely used as a reporter for studying gene regulation and function, and for pharmaceutical screening [128, 129]. It is a very sensitive genetic reporter due to its high sensitivity dynamic range and its natural absence from mammalian cells. The enzyme catalyzes ATP-dependent D-luciferin oxidation to oxyluciferin, producing light emission centered at 560 nm (**Figure 4-1**). Maximum light output is not achieved until the substrate and co-factors are present in large excess. When assayed under these conditions, light emitted from the reaction is directly proportional to the number of luciferase enzyme molecules.

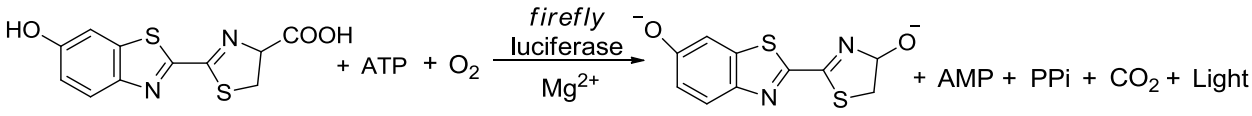

Figure 4-1: Bioluminescent reaction catalyzed by firefly luciferase.

Renilla Luciferase has been widely used in multiplex transcriptional reporter assays or as a normalizing transfection control for *firefly* luciferase assays [134]. *Renilla* luciferase, a monomeric 36,000 Dalton protein, catalyzes coelenterazine oxidation to produce light (**Figure 4-2**) [135].

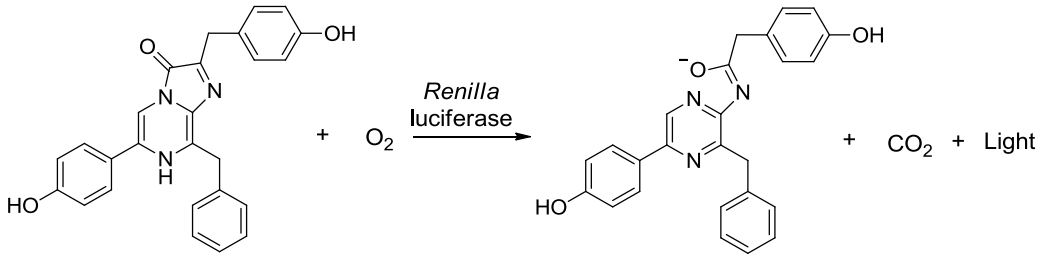

Figure 4-2: Bioluminescent reaction catalyzed by *Renilla* luciferase

In this study, the RNAi-inducing ability of siRNA containing internal amide bond linkages was studied using a dual-luciferase assay. The siRNA sequences were designed to target *firefly* luciferase. HeLa cells were co-transfected with the vector (pGL2 or pGL3 and pRLSV40 luciferase-expressing plasmids) and the indicated the amounts of siRNAs. Both pGL2 and pGL3 are for SV40 promoter driven *firefly* Luciferase expression. pRLSV40 is for thymidine kinase promoter driven *Renilla* Luciferase expression. The signals of *firefly* luciferase were normalized to those of the *Renilla* luciferase. In dual luciferase reporter assays, two luciferase enzymes are simultaneously expressed and detected in a single sample. Dual luciferase reporter assays are ideal for identifying off-target effects due to the sequence homology between *firefly* and *Renilla*

reporter gene and normalizing due to eliminate experimental artifacts. For data normalization experiments, *firefly* reporter gene generally functions as an experimental reporter and the second (*Renilla* reporter gene) as an internal control to account for non-specific experimental variations due to operator error or as a result of non-specific effects of biological manipulations or cell treatments. Additional experimental variations include: differences in cell plating, differences in cell viability or proliferation due to an experimental treatment, edge effects caused by uneven environmental conditions in the cell culture incubator, and non-specific effects of the treatment compound on the function of the reporter itself.

In Messere's work, they showed that the introduction of PNA in the 3'-overhangs in either or both strands of siRNA was well tolerated by the RNAi machinery, because all the modified siRNAs still mediated efficient gene silencing [4]. Similarly, Iwase *et al.* reported that siRNAs containing the amide-linked RNA segments in the 3'-overhangs in both strands effectively inhibited *firefly* luciferase activity comparable to the unmodified siRNA. These results suggest that the amide-linked RNA segments were compatible with the RNAi machinery.

In our study, through solid-phase RNA phosphoramidite chemistry, we were able to control the site-specific location of the PNA monomer by controlling its location within the desired RNA strand. In this chapter, the gene-silencing ability of these end and internally amide-bond modified siRNAs are studied using a dual-luciferase assay. This is the first report that involves amide-bonds as phosphate backbone replacements within the internal regions of siRNAs

4.1.2. Experimental Procedure

Cell Culture

In the present study the human epithelial cervix carcinoma cell line HeLa was used. Cells were routinely maintained in 25 mL DMEM (Dulbecco's modified Eagle's Medium) supplemented with 10% fetal bovine serum (FBS) (Perbio), 1% Penicillin-Streptomycin (Sigma) at 37 °C in a humidified atmosphere containing 5% CO_2. Confluent cells were passaged according to the following protocol: Cells were washed twice with PBS, pH 7.4, (Invitrogen) and incubated with 2 mL of 0.25% Trypsin (SAFC Bioscience) for 2 minutes at 37°C to detach cells from the plastic surfaces. The cell suspension was resuspended in 5 mL of culture medium and counted using a haemocytometer. 1,000,000 cells were seeded into new cell culture flask containing culture medium.

For freezing, the trypsinized cells were supplemented with 5 mL culture medium and centrifuged for 5 minutes at 12,000 rpm in a centrifuge. The cell pellet was resuspended in culture medium. A density of 1,000,000 of cells was transferred to a cryo tube containing 100 µL of dimethylsulfoxide followed by adding 300 µL of FBS, and were slowly cooled down to -80 °C in a polystyrene box. For long-term storage cells were transferred to liquid nitrogen container.

For thawing, frozen cells were dethawed using warm culture medium, transferred to a Falcon tube containing 10 mL of culture medium and centrifuged for 5 minutes at 12,000 rpm to remove residual DMSO followed by resuspension in 1 mL of fresh culture medium to remove residual DMSO. The cell suspension was transferred to a new 25 mL cell culture flask and incubated at 37 °C.

Transfection of HeLa with lipofectamine 2000

Prior to transfection, HeLa cells were seeded on 12-well plates (Greiner Bio-One) at a density of 10,000 cells per well and incubated at 37 ^{0}C with 5 % CO_2 in DMEM containing 10% FBS. After 24 hr, for each well varying concentrations (8, 80 and 800 pM) of all anti-luciferase siRNAs were co-transfected with either 100 ng of pGL2 (Promega) or pGL3 (Promega) and 100 ng of pRLSV40 luciferase-expressing plasmids using 1μL of Lipofectamine 2000 (Invitrogen) in 200 μL of Gibco's Opti-Mem Reduced Serum Medium 1X (Invitrogen) according to the manufacturer's protocol.

Preparation of cells for Luciferase reporter assay

Twenty-four hours after transfection, cell culture media was removed. Cells were washed two times in PBS, lysed for 20 minutes at room temperature in 1xPLB (Passive Lysis Buffer), immediately followed by measurement on a Synergy HT (Bio-Tek) plate luminometer. The cell lysate was loaded onto white and opaque, 96-well plates (Costar) suitable for luminometric measurement. Using the Dual-luciferase Reporter Assay kit (Promega), 30 μL LAR II was first added for firefly luciferases activity measurements followed by adding 30 μL Stop&Glow for *Renilla* Luciferase activity measurements. The observed luminescence was proportional to both *firefly* and *Renilla* luciferase expression, recorded on a luminometer.

Normalization, Interpretation

Three aliquots of each sample were measured to calculate an average value. To determine the efficiency of RNAi constructs, we correlated reporter enzyme activities of transfection of luciferase-expression plasmids with co-transfections of luciferase-expressing plasmids with anti-

luciferase siRNAs. The reporter activity of control transfection (luciferase-expression plasmids) was set to 100%. Different transfections were normalized by *Renilla* luciferase expression and standard deviations were calculated from the differences in RNAi efficiency of repeated transfections.

Transformation of Plasmid DNA into *E. coli* Using the Heat Shock Method

Competent *DH5α E. coli* cells were taken out from -80 ºC freezer (50 µL aliquots) and thawed on ice. 50 ng of circular DNA (Promega) was added into *E.*coli cells followed by 10 min incubation on ice to thaw competent cells. The tube with competent cells and DNA was placed into water bath at 42 °C for 45 seconds (heat shock) and then placed back in ice for 2 minutes to reduce damage to the *E. coli* cells. One mL of LB broth (with no antibiotic added) was added and the transformed cells were incubated at 37 °C for 1 hr with agitation. 100 µL of the resulting culture was spread on warmed agar plates (with Ampicillin added). The cell culture was grown overnight at 37 °C. The single colonies for each DNA plasmids were selected about 12-16 hrs later. The colonies picked were placed in 5 mL LB broth and 50 µL of Ampillicin, and then incubated in the 37 °C shaker overnight.

Mini prep plasmid DNA purification

We purified DNA plasmids from bacterial cultures (Competent *DH5α E. coli*) with the QIAgen QIAprep Spin Mineprep kit Purification System of Promega according to manufacturer's instruction. In brief, 5 mL of an overnight culture were centrifuged 10 minutes at 4,180 rpm (Eppendorf Centrifuge) in order to harvest bacterial cells from culture. The pellet was resuspended in 250 µL of resuspension solution. The addition of 250 µL of cell lysis solution was followed by inverting the tube four times. After addition of 350 µL of neutralization solution

the lysate was again mixed by inverting the tube. After centrifugation at 13000 rpm, the supernatant of the lysate was transferred to the QIAprep spin column. 0.75ml of wash solution was added. The minicolumn was transferred to a microtube and centrifuged for one minutes at full speed (13,000 rpm), to remove residual wash solution. Afterwards the minicolumn was transferred to a new collection tube, 50 μL of EB buffer (10mM Tris-Cl, pH 8.5) was added and after five minute of incubation, the dissolved plasmid DNA was eluted by one minute of centrifugation at 13000 rpm. The purified DNA plasmid was quantified by using a UV spectrometer.

4.1.3. Results and Discussion

The ability of the modified siRNAs to suppress gene expression was studied by a dual-luciferase assay using pGL2/3 and pRLSV40 plasimids which contained *firefly* and *Renilla* luciferase genes, respectively. The siRNA sequences were designed to target *firefly* luciferase. HeLa cells were co-transfected with the luciferase plasmids and the indicated amounts of siRNAs. The control used in this set of experiment is the luciferase activity given by the cells after the 24 hrs transfection with two luciferase plasmids (pGL2/3 and pRLSV40). The signals of *firefly* luciferase were normalized to those of the *Renilla* luciferase. The final relative luciferase signals of each siRNA were normalized to that of the control in each set of experiment.

Both luciferase vectors (pGL2 and pGL3) carry the coding region for *firefly* luciferase [17]. However, there are differences in the coding sequence from each vector which allows us to use two different parent siRNAs. The reason for us to use two different parent siRNA sequences is because the most critical issue in developing the chemically modified siRNA is the placement of the modification in an siRNA duplex. Positional effects of the placement of the modification

have been known to have implications on RNAi activity [54]. In other words, the effect of the modifications on the potency of the siRNA was found to be dependent on the position as well as the type of modification used. By using two different parent siRNAs, we can expand the scope of siRNAs that contain the chemically modified U_aU dimer unit which replaces two adjacent uridine residues in the wild-type parent sequence to examine their function. The sequences of the siRNAs targeting both pGL2 and pGL3 are shown in **Table 3-1**

In chapter 3, based on the results of the thermodynamic study (T_m), we learned that in general, the introduction of this internal amide bond linkage causes destabilization effect, whereas modifications are at the 3'-overhang observe little change in thermal stability. There is a correlation between the thermodynamic and activity based on thermodynamic asymmetry in the siRNA duplex [45, 136]. In thermodynamic asymmetry rule, the siRNA strand containing the thermodynamically less stable 5'-end is preferentially incorporated as the guiding strand of RISC, while the non-guiding sense strand of the siRNA duplex is cleaved by Ago 2 and liberated. It has been shown that siRNA activity is primarily enhanced by favouring the incorporation of the intended antisense strand during RISC complex loading by modulation of siRNA thermodynamic asymmetry. In this chapter, we want to explore how our thermally destabilizing modification (U_aU modification) affects the siRNA potency.

The gene-silencing ability of the chemically-modified siRNAs outlined in Table **2-1** was tested at 8, 80 and 800 pM within HeLa cells. To gauge efficacy, the mammalian cells were co-transfected with pGL2 target *firefly* luciferase plasmid and a non-target *Renilla* luciferase plasmid (pRLSV40). Following transfection, the cells were lysed after 24 hours and luciferase activity was monitored (**Figure 4-3**).

As shown in table **3-3**, both siRNA **1** and **2** contain the U_aU modification near the 3'-end of the sense strand, whereas, siRNA 2 has an additional the U_aU modification at the 3'-overhang of the antisense strand. The potency of both siRNA was relatively limited compared to the wild-type. This suggests that the modification near the 3'-end of the sense strand is not well tolerated. SiRNA **3** contains two internal U_aU-modified siRNAs and exhibits the highest degree of thermal destabilization. There is no appreciable silencing observed with this siRNA. Compared to siRNA **1**, siRNA **3** contains an internal U_aU modification which is place adjacent the Ago 2 cleavage site where target mRNA cleavage occurs on the antisense strand which is a less tolerated modification. There are several explanations for this region's particular sensitivity to modification. First, Because only one strand of RNA remains in the mature RISC, the antisense strand is entirely responsible for silencing activity once the RISC has formed [28]. Thus, it seems reasonable that the antisense strand would have more stringent structural requirements than the sense strand, which serves essentially as a carrier for the antisense strand. As such, modification of the antisense strand had a strong impact on siRNA silencing activity with the most efficient antisense strands being only modestly modified [47]. In addition, target mRNA cleavage occurs opposite the link between the 10th and 11th nucleotides of the antisense RNA, when counting from the 5'-end (in the center of a 21 bp siRNA) [137]. Modifications near this particular area of the antisense strand was found to cause a decrease in RNAi function [52, 138], due to the fact that the phosphate groups from this particular area of the antisense strand are involved in key points of contact with the RISC protein complex [139].

siRNAs **4**–**6** contain the U_aU modification in different combinations at the 3'-overhang. These siRNAs exhibit potency comparable to wild-type. At certain concentrations (800 pM for siRNAs **4** and **6**), some of these siRNAs exhibit increased potency relative to wild-type. These

results indicate that the U_aU modification on 3'-overhangs are well tolerated by RNAi machinery in the sense strand, in the antisense strand and in both strands of the siRNA and can even enhance their potency. This observation is consistent with the several other studies [47, 54, 140]. In a recent study reported by a collaboration amongst various European research groups, they showed destabilizing modification on the 3'-overhang in the sense strand can be utilized to favour antisense strand selection during RISC loading irrespective of the thermodynamic asymmetry of the duplex, thus increase siRNA silencing activity [47].

Finally, for siRNAs **7** and **8**, these RNAs contain the U_aU modification adjacent the Ago 2 cleavage site on the antisense strand. Like siRNA **3**, these siRNAs exhibit reduced silencing compared to wild-type. However, when a U_aU modification is used at the 3'-end of the sense strand in combination with the internally-modified U_aU antisense strand (siRNA **8**), improved potency is observed at 80 and 800 pM when compared to siRNAs **3** and **7**.

This gene-silencing data for pGL2 suggests that internal modifications near the 3'-end of the sense strand are compatible with the RNAi machinery, however at reduced efficacy compared to wild-type. On the other hand, siRNAs functionalized with internal U_aU modifications at the antisense strand (adjacent the Ago 2 cleavage site on the sense strand) are not effective gene-silencing substrates. Furthermore, 3'-U_aU overhang modifications on the sense strand can offer some increase in potency; however, if the U_aU modification is placed on the antisense strand and is used with an siRNA that contains a chemically modified sense strand (siRNAs **2** and **5**), a reduction in potency is observed. This observation of reduced potency with bulky 3'-modifications at the antisense strand has been previously observed by others [141].

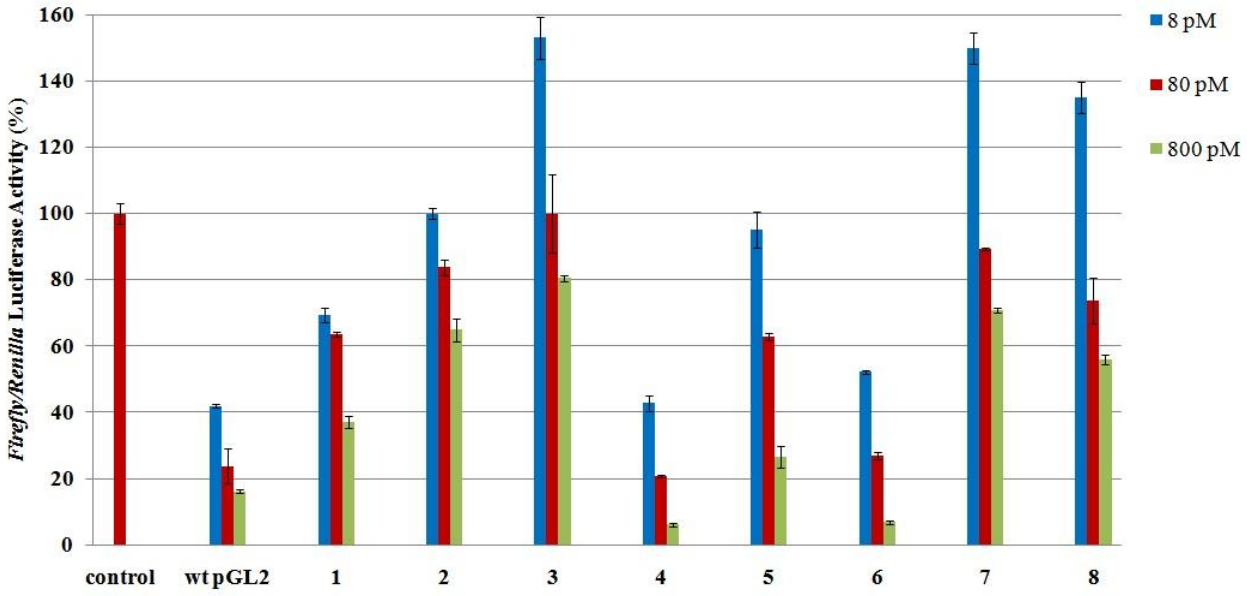

Figure 4-3: Reduction in *firefly* luciferase pGL2 expression related to the potency of amide-bond modified siRNAs using the Dual-luciferase reporter assay. The siRNAs were tested at 8, 80, and 800 pM, with *firefly* luciferase expression normalized to *Renilla* luciferase.

In the next set of experiments (**Figure 4-4**), we examined the efficacy of our siRNAs that target pGL3. **Table 3-4** illustrates the duplexes studied and their respective T_m. In general, all siRNAs silence in a dose-dependent manner. Starting with siRNA **9** and **10**, both of them contain the U_aU modification near the 5'-end of the sense strand. In both cases, it appears that destabilizing the 5'-end of the sense strand led to a decrease in activity at all concentrations tested, This is in good agreement with the selection of sense and antisense strand based on thermal asymmetry in the siRNA duplex [45, 142]. RISC is preferentially loading the antisense strand that has a lower thermostability at the 5'-end. Destabilizing the 5'-end of the sense strand could potentially disfavour the incorporation of the antisense strand into the RISC complex, thus, reducing the siRNA potency. On the other hand, siRNA **10** exhibits a larger degree of thermal destabilization at the 5'-end of the sense strand; its potency is reduced compared to siRNA **9**.

SiRNAs **11–14** contain internal U_aU modifications near the 3'-end of the sense strand. SiRNAs **11** and **13** contain the modification only on the sense strand which is known be more tolerant to chemical modifications. Compared to siRNAs **12** and **14**, siRNA **11** and **13** are more potent. At 80 and 800 pM, siRNA **13** displays potency comparable to wild-type siRNA. SiRNA **12** exhibits the greatest degree of thermal destabilization in this group. It exhibits a great decrease in RNAi function at all concentrations tested. Similarly to the studies with pGL2, the presence of a chemically modified substituent at the 3'-overhang of the antisense strand of the siRNA may impede its activity when used in combination with an internal U_aU modification.

Finally, the group of siRNAs **15 –17** contain U_aU modifications in different combinations at the 3'-overhangs of the sense and antisense strand. As described earlier, placing a destabilizing modification on the 3'-overhang of the sense strand can enhance the siRNA silencing activity which explains why siRNA **15** exhibits silencing comparable to wild-type at 80 and 800 pM. SiRNA **16** has a slight loss in potency compared to siRNA **15**, perhaps due to the effect of modifying the 3'-end of the antisense strand. SiRNA **17** exhibits the lowest potency profile from this group at concentrations of 8 and 80 pM. It contains the U_aU modification at the 3'-end of the antisense strand at which the antisense strand is bound by Ago 2 during RISC loading. Destabilization at this position can potentially affect the potency of siRNA.

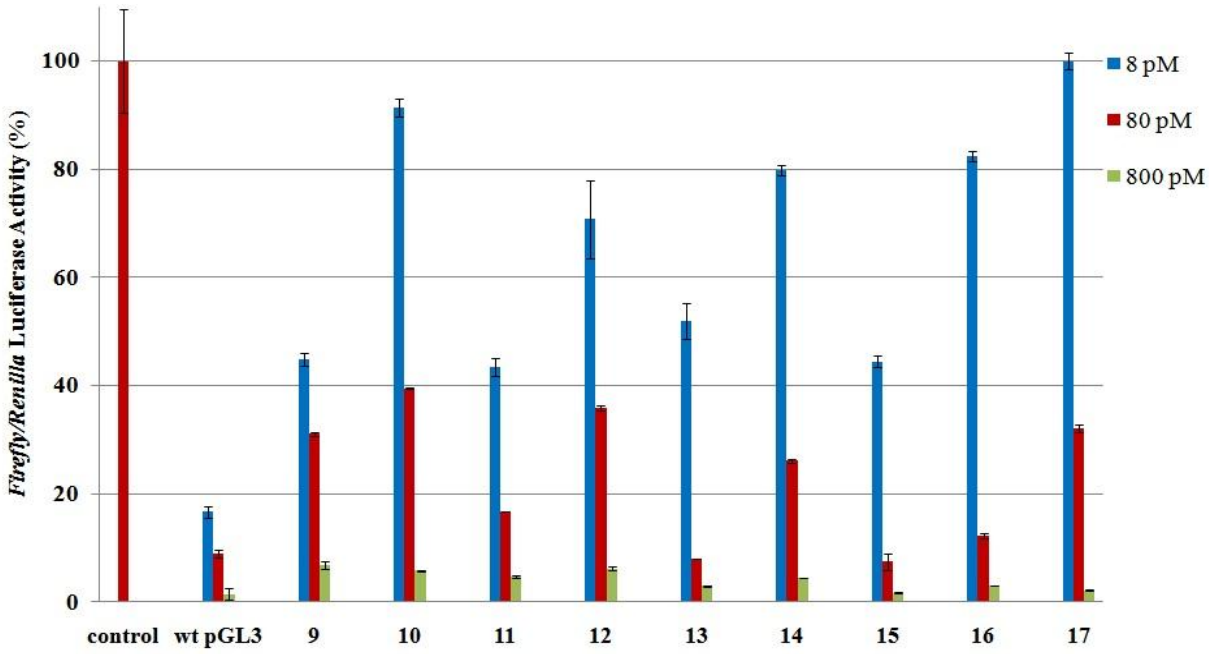

Figure 4-4: Reduction in *firefly* luciferase pGL3 expression related to the potency of amide-bond modified siRNAs using the Dual-luciferase reporter assay. The siRNAs were tested at 8, 80, and 800 pM, with *firefly* luciferase expression normalized to *Renilla* luciferase.

4.2. Enzymatic Stability of siRNAs containing internal amide-bond linkages

4.2.1. Introduction

In order for a cell to protect itself against foreign nucleic acids (i.e. viruses), it produces nucleases to enzymatically degrade foreign DNA and RNA. In order for siRNA to get past the host defense and to have therapeutic benefits, the siRNAs must be able to withstand degradation by exonucleases and endonucleases that catalyze the hydrolysis of phosphodiester bonds. Nature RNA is very quickly degraded in cells. The fact that siRNA is double-stranded provides it with some degree of protection, but not enough for *in vivo* use. Both endo- and exonucleases have

been found to play a key role in degradation of siRNA [143], and expression levels of them inversely correlate with duration of siRNA activity [144]. This and other data suggest that increasing the nuclease resistance of siRNAs can prolong their activity.

Chemical modification is the principal strategy used to improve the nuclease resistance of siRNAs. As demonstrated in chapter one, it has been shown that certain backbone modified oligonucleotides (e.g., phosphorothioate and boranophosphate linkage) show increased enzymatic stability. In the case of the amide-bond backbone modification, Uhlmann and his coworkers have shown that PNA substitutions enhance DNA resistance to serum-derived nucleases [80]. Moreover, in both Messere's and Iwase's study, the introduction of a amide bond modification on only the 3'-overhanging in both or either strands of siRNA leads to significant resistance against serum-derived nucleases [4, 5].

In this section, we examined whether the introduction of PNAs monomer in the 3'-end could lead to a siRNA that is more stable in the extracellular environment. We used fetal bovine serum as models for a 3'-exonuclease and an endonuclease.

4.2.2. Experimental Procedure

Unmodified and modified siRNAs were incubated in 13.5% fetal bovine serum at 37 °C for various times periods. At different time points (0.5, 1.5, 3 and 5 hrs), aliquots of each siRNA were incubated with fetal bovine serum at 37 °C. After 5 hrs, samples were subjected to electrophoresis in 20% polyacrilamide-Tris-Borate-EDTA (TBE) under non-denaturing conditions and visualized by Gel Red (3X) staining.

4.2.3. Results and Discussion

Because of the rapid degradation of unmodified siRNAs in serum, it is clear that some form of protection will be required for systemic delivery. This can be achieved by chemical modification of the siRNA itself. Several studies have shown that chemically modified siRNAs can be highly resistant to nuclease degradation yet still function as effectors of RNA interference [145, 146].

In our study, the stability of siRNAs that have the PNA-RNA dimer on the 3'-overhangs in both or either strands in fetal bovine serum which contains heat-stable nucleases, was examined. Two sets of siRNAs (**4, 5 &6** for pGL2 and **15, 16 &17** for pGL3) (**Table 3-5**) were incubated in water containing 13.5% bovine serum and analyzed by 20% native PAGE under denaturing condition. Nuclease stability can be judged from the relative intensity of the bands at each time point, with degradation indicated by the disappearance of the bands over time. As shown in **Figure 3-5, A**, the unmodified siRNA for pGL2 was completely digested after 1.5 hrs incubation. A similar degradation profile was observed for the unmodified siRNA for pGL3 (**Figure 3-6, A**). On the other hand, siRNA **4, 5**, and **6** were more stable that unmodified siRNA (**Figure 3-5, B, C, and D)**, because after 5 hrs of incubation an electrophoretic band corresponding to the intact duplex was still evident. In the case of pGL3, siRNAs **16** and **17** (**Figure 3-6, C and D)** were gradually digested after 3 hrs. SiRNA **15** (**Figure 3-6, B)** showed a significant improvement in stability, because a band corresponding to the intact duplex was still evident even after 5 hrs of incubation. Overall, these results imply that the introduction of PNA-RNA dimer at the 3'-end of the siRNA where the exonuclease cleaves the terminal nucleotide, increased markedly the resistance to serum-derived nucleases.

Table 3-5: Sequences of anti-luciferase siRNAs that are used in enzymatic stability assays.

RNA	siRNA duplex
wt pGL2	5'-CGUACGCGGAAUACUUCGAtt-3' 3'-ttGCAUGCGCCUUAUGAAGCU-5'
4	5'- CGUACGCGGAAUACUUCGA**U$_a$U**-3' 3'- ttGCAUGCGCCUUAUGAAGCU-5'
5	5'-CGUACGCGGAAUACUUCGA**U$_a$U**-3' 3'-**U$_a$U**GCAUGCGCCUUAUGAAGCU-5'
6	5'-CGUACGCGGAAUACUUCGAtt-3' 3'-**U$_a$U**GCAUGCGCCUUAUGAAGCU-5'
wt pGL3	5'- CUUACGCUGAGUACUUCGAtt-3' 3'- ttGAAUGCGACUCAUGAAGCU-5'
15	5'-CUUACGCUGAGUACUUCGA**U$_a$U**-3' 3'-ttGAAUGCGACUCAUGAAGCU-5'
16	5'-CUUACGCUGAGUACUUCGA**U$_a$U**-3' 3'-**U$_a$U**GAAUGCGACUCAUGAAGCU-5'
17	5'-CUUACGCUGAGUACUUCGAtt-3' 3'-**U$_a$U**GAAUGCGACUCAUGAAGCU-5'

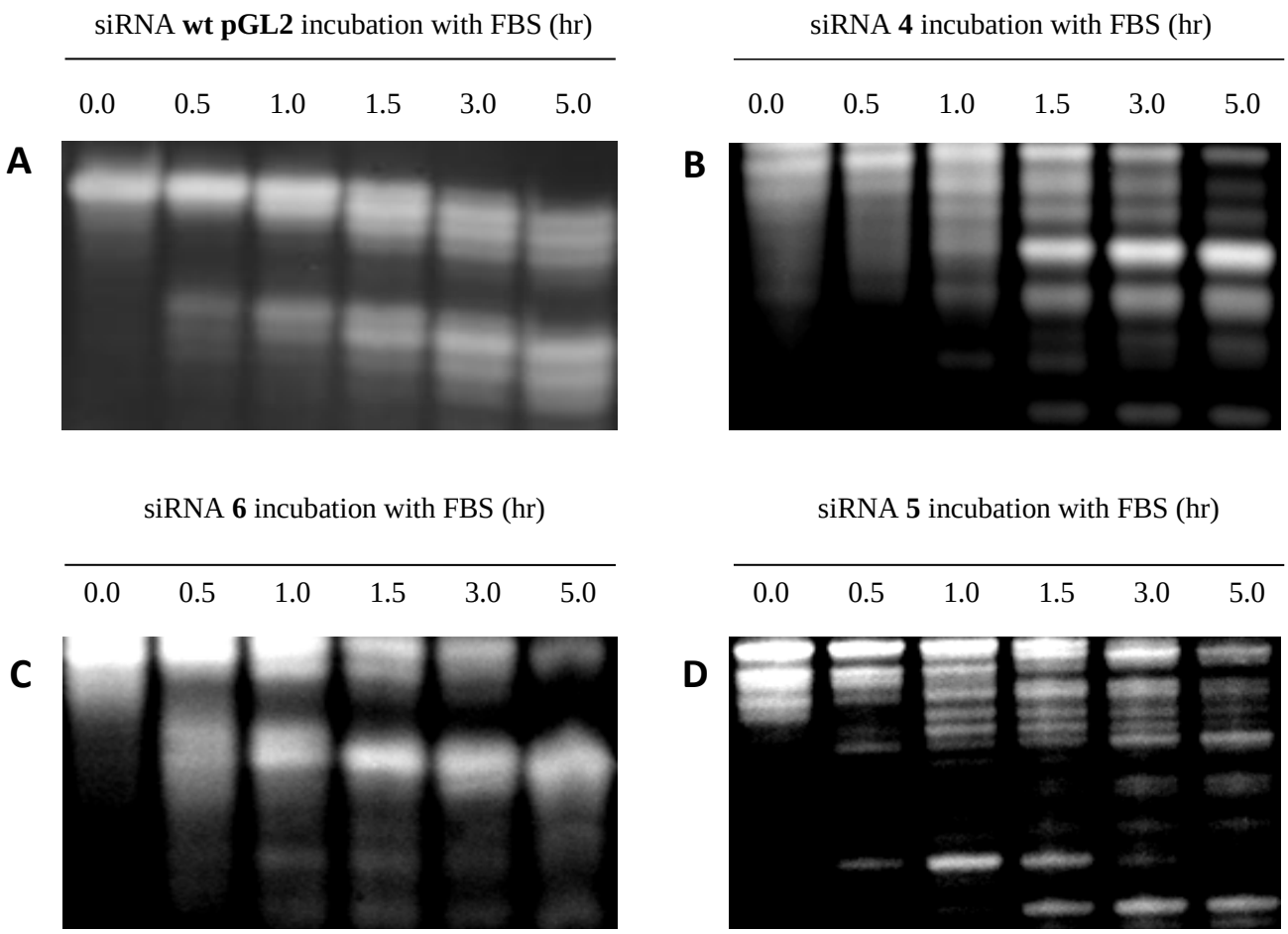

Figure 4-5: Native PAGE gel displaying degradation patterns of 3'-modified pGL2 siRNAs in a time-dependent nuclease stability assay. Samples were incubated at 37 ^{0}C in 13.5% FBS before they were resolved on 20% SDS-PAGE. Bands were stained with Gel Red (3X). (A) Degradation pattern of **wt pGL2** anti-luciferase siRNA; (B) Degradation pattern of siRNA **4**; (C) Degradation pattern of siRNA **6**; (D) Degradation pattern of siRNA **5**.

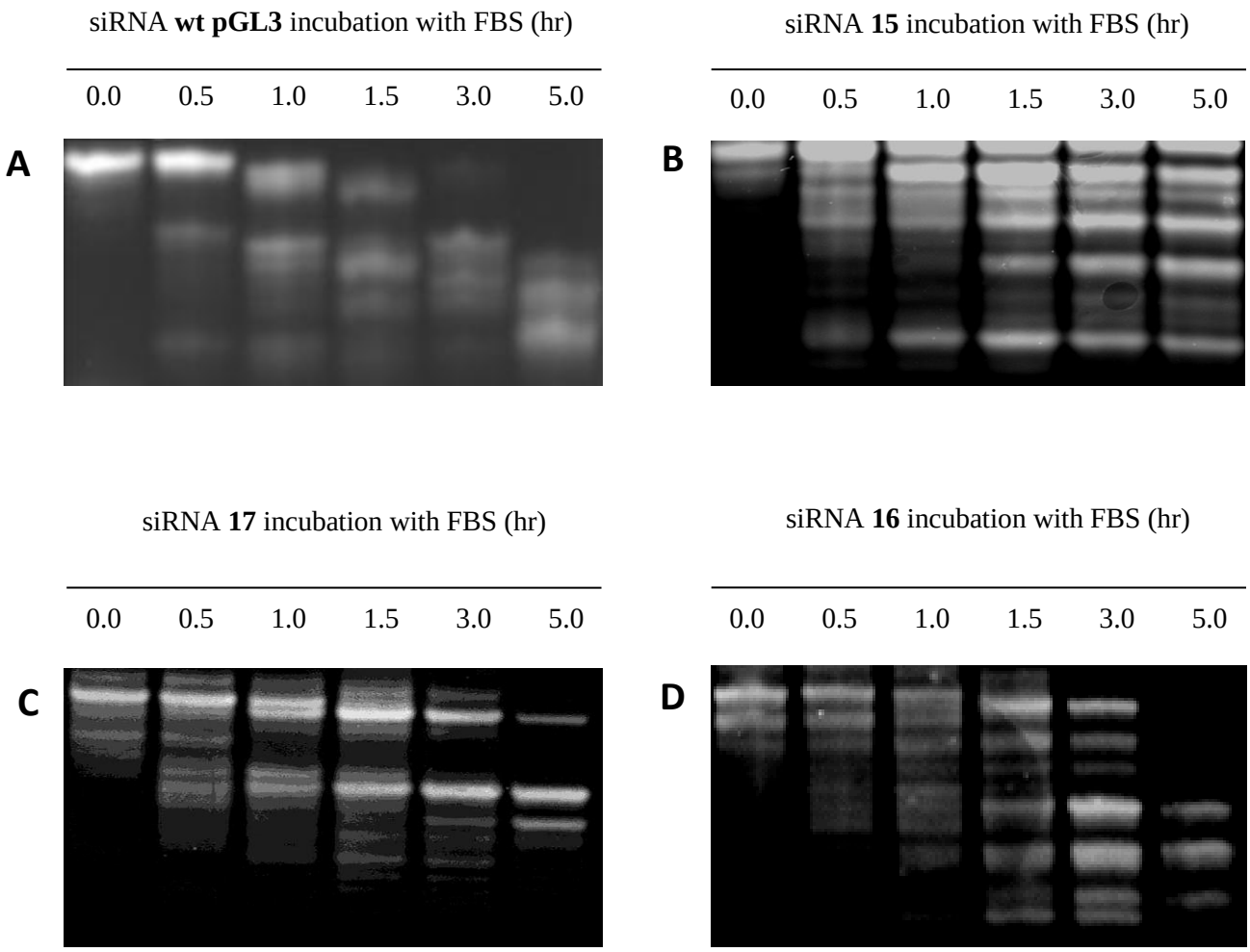

Figure 4-6: Native PAGE gel displaying degradation patterns of 3'-modified pGL3 siRNAs in a time-dependent nuclease stability assay. Samples were incubated at 37 ^{0}C in 13.5% FBS before they were resolved on 20% SDS-PAGE. Bands were stained with Gel Red (3X). (A) Degradation pattern of **wt pGL3** anti-luciferase siRNA; (B) Degradation pattern of siRNA **15**; (C) Degradation pattern of siRNA **17**; (D) Degradation pattern of siRNA **16**.

A question that remains is whether or not nuclease stabilization also affects the kinetics of siRNA-mediated gene silencing. If enhanced nuclease stability allows the siRNAs to remain intact longer inside the cell, it might lead to an increase in the duration of gene inhibition, which

still needs to be proven by further experiment. An ideal modified siRNA design would be expected to enhance both the magnitude and duration of gene silencing. It has been reported that when transfected into cells, modified siRNA was capable of maintaining the knockdown effect for a longer period as compared to unmodified siRNA [53, 122].

Our observations on cell-based luciferase assays indicate that these 3'-end modified siRNAs do not provide considerable advantages *in vitro* with regard to the magnitude of gene silencing. In fact, these modified siRNAs are more costly to produce and frequently show decreased activity relative to unmodified siRNAs of the same sequence. However, the added costs and the potential for decreased activity of nuclease-stabilized siRNAs may be outweighed by other factors for *in vivo* applications. Recent reports have indicated that chemical modifications can modulate the immunostimulatory properties of siRNAs [147]. Moreover, chemical modifications to confer added nuclease stability can increase the bioavailability of an injected siRNA species by protecting it from the rapid nuclease degradation that occurs with unmodified siRNAs. If siRNAs are injected locally, as in intratumoral or intramuscular injection, the added nuclease stability may increase the time during which siRNAs can be internalized by the target cells.

4.3. Chapter summary

In this chapter, we evaluate siRNA that contain internal amide bond linkages to establish novel RNAi substrates for gene-silencing activity in mammalian cells and their nuclease stability. We showed the compatibility of utilizing a neutral amide-bond backbone within siRNAs. Specifically, the internal backbone amide-bond is compatible within the RNAi machinery when placed within the sense strand of the double-stranded siRNA. This is probably due to the better

toleration of sense strand to chemical modification in comparison to the antisense strand that is incorporated into RISC and mediate the binding with target mRNA and mRNA cleavage. In addition, the U_aU unit is compatible as a 3'-overhanging unit. However, when the U_aU unit is place adjacent the Ago 2 cleavage site on the antisense strand, poor efficacy is observed. Nuclease stability assays showed that in general, the siRNAs that contain 3'-U_aU overhangs have increased stability compared to wild-type siRNAs, which can potentially lead to a prolonged duration of RNAi activity *in vivo.*

Chapter 5: Conclusion and Future Work

The end goal of the synthesis and characterization of modified RNA is to extend the biological and pharmacokinetic properties of RNA as a therapeutic tool. The work presented in this dissertation encompasses the synthesis, chemical and biological characterization, and *in vivo* applications of siRNAs that contain internal amide-bond linkages. We were able to use solid phase RNA phosphoramidite chemistry to control the site-specific location of the U_aU modification through the desired RNA strand. The secondary structure of the internal amide-bond modified siRNAs all exhibit the standard A-form helix which is required for their gene-silencing activity [122]. However, it is recommended that these experiments be followed up with NMR of modified siRNA to absolutely determine the configuration. Crystallography may also be helpful in determination of the secondary structure.

The thermodynamic profile tells us that in general, internal amide-bond modifications display a degree of thermal destabilization, whereas U_aU modifications at the 3'-overhang observe little change in thermal stability. Overall, this chemical modification within the backbone of the oligonucleotide causes a small loss in binding affinity.

The ability of to silence a gene using was tested in a human cancer line. We demonstrate that the internal backbone amide-bond is compatible within the RNAi machinery specifically when placed within the sense strand of the double-stranded siRNA. Lastly, based on the results given by the nuclease stability assays, the 3'-end modified siRNA proved to be more stable to hydrolysis by exonucleases.

Our results provide a basis for the further development of synthetic amide-bond linked siRNA molecules with improved properties, including higher resistance to enzymatic degradation, and thus may impact positively on the use of chemically modified siRNAs in RNAi

technology and broaden the vision of translating the technology into a drug platform. Moreover, these molecules represent a further tool for insights into the future studies investigating on RNA recognition by siRNA machinery.

A large amount of work remains to be done on this type of backbone modification within RNAi machinery. Most importantly, we would like to further expand the scope of these internal amide-bond modified siRNAs within the biological system using endogenous gene target, such as house-keeping gene glyceraldehyde-3-phosphate dehydrogenase (GAPDH) or genes involved in disease.

Diseases that are characterized by overexpressed or inappropriate expression of specific genes, or genes that are expressed by invading microorganisms, are candidates for gene-silencing therapies. Malignant diseases such as cancer, in particular, are attractive candidates for this therapeutic approach if no other reason than that conventional cancer therapies are highly toxic. In this section, two potential gene targets will be listed. B-cell lymphoma protein 2 (BCL2) is an important apoptosis inhibitor to regulate programmed cell death in oncology and its overexpression has been implicated in the pathogenesis of some lymphomas [148]. Targeting BCL2 is a promising example of triggering apoptosis in tumour cells. Laboratory studies have shown convincingly that exposing cells to ONDs targeted to BCL2 will specifically decrease the amount of targeted mRNA and protein. For this reason, there is a great deal of interest in targeting BCL2 for therapeutic purpose [149]. Protein kinase C (PKC) comprises a family of biochemically and functionally distinct phospholipid-dependent, cytoplasmic serine/threonine kinases. These proteins have a crucial role in transducing the signals that regulate cell proliferation and differentiation. PKC is overexpressed in several tumours, and antisense inhibitors of these enzymes have shown some antitumor activity *in vitro* [150, 151]. Results of

two studies that used identical 20-mer phosphorothioate ODN against PKC have been published [150, 152]. The ODN was well tolerated. As a part of future direction, we would like to look into whether our internal amide bond modified siRNAs will have the same gene silencing ability as illustrated in other studies when used to target BCL2 and PKC.

Secondly, we would like to examine the nuclease stability against endonucleases using siRNAs that contain the U_aU modification in the internal Watson-Crick region. In addition, we would like to know whether increased stability seen with modified siRNAs can prolonged the duration of RNAi *in vivo* because the duration of gene inhibition by siRNA is a primary factor in determining the dosing schedules required to achieve therapeutic effects. We could transfect HeLa cells with unmodified and modified siRNAs and the luciferase activity of the cells will be monitored over time through live-cell bioluminescent imaging. This will reveal the impact of modified siRNA nuclease stability on the kinetics of siRNA-mediated gene silencing.

Lastly, due to the fact that the ability of the siRNA to silence gene expression is predicated on its capacity to cross the cell membrane and gain access to the RISC machinery in the cytoplasm, we would also like to determine the lipophilicity of modified siRNAs to facilitate cellular delivery through passive transport across the cell membrane. An efficient method involves utilizing radiolabeled oligonucleotides to measure the partitioning between 1-octanol and aqueous phases[153].

In conclusion, this is the first report that involves amide-bonds as phosphate backbone replacements within the internal regions of siRNAs and thus opens the future possibility for examining and utilizing this modification in studying new structure-function relationships.

References

1. IARC. *Globocan 2008*. 2010.
2. Tekade, R.K., P.V. Kumar, and N.K. Jain, Dendrimers in Oncology: An Expanding Horizon. *Chem Revi*, **2009**. *109*: p. 49-87.
3. Yang, W., Nucleases: diversity of structure, function and mechanism. *Q Rev of Biophys*, **2011**. *44*: p. 1-93.
4. Potenza, N., L. Moggio, G. Milano, V. Salvatore, B. Di Blasio, A. Russo, and A. Messere, RNA interference in Mammalia cells by RNA-3'-PNA chimeras. *Int J Mol Sci*, **2008**. *9*: p. 299-315.
5. Iwase, R., T. Toyama, and K. Nishimori, Solid-phase synthesis of modified RNAs containing amide-linked oligoribonucleosides at their 3 '-end and their application to siRNA. *Nucleosides Nucleotides & Nucleic Acids*, **2007**. *26*: p. 1451-1454.
6. Caruthers, M.H., Gene synthesis machines-DNA chemistry and its uses. *Science*, **1985**. *230*: p. 281-285.
7. Gong, W. and J.-P. Desaulniers, Synthesis and properties of RNAs that contain a PNA-RNA dimer. *Nucleos Ncleot Nucl*, **2012**. *31*: p. 389-400.
8. Stephenson, M.L. and P.C. Zamecnik, Inhibition of Rous-Sarcoma viral-RNA transplation by a specific oligodeoxyribonucleotide. *P Natl Acad Sci USA*, **1978**. *75*: p. 285-288.
9. Opalinska, J.B. and A.M. Gewirtz, Nucleic-acid therapeutics: Basic principles and recent applications. *Nat Rev Drug Discov*, **2002**. *1*: p. 503-514.
10. Juliano, R., M.R. Alam, V. Dixit, and H. Kang, Mechanisms and strategies for effective delivery of antisense and siRNA oligonucleotides. *Nucleic Acids Res.*, **2008**. *36*: p. 4158-4171.
11. Praseuth, D., A.L. Guieysse, and C. Helene, Triple helix formation and the antigene strategy for sequence-specific control of gene expression. *BBA-Gene Struct Expr*, **1999**. *1489*: p. 181-206.
12. Dorsett, Y. and T. Tuschl, siRNAs: Applications in functional genomics and potential as therapeutics. *Nat Rev Drug Discov*, **2004**. *3*: p. 318-329.
13. Sen, G.L. and H.M. Blau, A brief history of RNAi: the silence of the genes. *FASEB J.*, **2006**. *20*: p. 1293-1299.
14. Romano, N. and G. Macino, Quelling-transient inactivation of gene-expression in neurospora-crassa by transformation with homologous sequences. *Mol. Microbiol.*, **1992**. *6*: p. 3343-3353.
15. Guo, S. and K.J. Kemphues, Par-1, A gene required for establishing polarity in C elegans embryos, encodes a putative ser/thr kinase that is asymmetrically distributed. *Cell*, **1995**. *81*: p. 611-620.
16. Fire, A., S.Q. Xu, M.K. Montgomery, S.A. Kostas, S.E. Driver, and C.C. Mello, Potent and specific genetic interference by double-stranded RNA in Caenorhabditis elegans. *Nature*, **1998**. *391*: p. 806-811.
17. Elbashir, S.M., J. Harborth, W. Lendeckel, A. Yalcin, K. Weber, and T. Tuschl, Duplexes of 21-nucleotide RNAs mediate RNA interference in cultured mammalian cells. *Nature*, **2001**. *411*: p. 494-498.
18. de Fougerolles, A., H.-P. Vornlocher, J. Maraganore, and J. Lieberman, Interfering with disease: a progress report on siRNA-based therapeutics. *Nat Rev Drug Discov*, **2007**. *6*: p. 443-453.
19. Hamilton, A., O. Voinnet, L. Chappell, and D. Baulcombe, Two classes of short interfering RNA in RNA silencing. *EMBO J.*, **2002**. *21*: p. 4671-4679.
20. Samuel-Abraham, S. and J.N. Leonard, Staying on message: design principles for controlling nonspecific responses to siRNA. *FEBS J.*, **2010**. *277*: p. 4828-4836.
21. Matranga, C., Tomari, Y., Shin, C., Bartel, D. P. & Zamore, P. D. , Passenger-strand cleavage facilitates assembly of siRNA into Ago2-containing RNAi enzyme complexes. *Cell*, **2005**. *123*: p. 607-620.

22. Rand, T.A., Petersen, S., Du, F. & Wang, X., Argonaute2 cleaves the anti-guide strand of siRNA during RISC activation. *Cell*, **2005**. *123*: p. 621-629.
23. Zamore, P.D., T. Tuschl, P.A. Sharp, and D.P. Bartel, RNAi: Double-stranded RNA directs the ATP-dependent cleavage of mRNA at 21 to 23 nucleotide intervals. *Cell*, **2000**. *101*: p. 25-33.
24. Yi, R., Y. Qin, I.G. Macara, and B.R. Cullen, Exportin-5 mediates the nuclear export of pre-microRNAs and short hairpin RNAs. *Gene Dev*, **2003**. *17*: p. 3011-3016.
25. Hammond, S.M., E. Bernstein, D. Beach, and G.J. Hannon, An RNA-directed nuclease mediates post-transcriptional gene silencing in Drosophila cells. *Nature*, **2000**. *404*: p. 293-296.
26. Lingel, A. and M. Sattler, Novel modes of protein-RNA recognition in the RNAi pathway. *Curr Opin Struc Biol*, **2005**. *15*: p. 107-115.
27. Carmell, M.A., Z.Y. Xuan, M.Q. Zhang, and G.J. Hannon, The Argonaute family: tentacles that reach into RNAi, developmental control, stem cell maintenance, and tumorigenesis. *Genes Dev.*, **2002**. *16*: p. 2733-2742.
28. Martinez, J., A. Patkaniowska, H. Urlaub, R. Luhrmann, and T. Tuschl, Single-stranded antisense siRNAs guide target RNA cleavage in RNAi. *Cell*, **2002**. *110*: p. 563-574.
29. Song, J.J., S.K. Smith, G.J. Hannon, and L. Joshua-Tor, Crystal structure of argonaute and its implications for RISC slicer activity. *Science*, **2004**. *305*: p. 1434-1437.
30. Robb, G.B. and T.M. Rana, RNA helicase A interacts with RISC in human cells and functions in RISC loading. *Mol. Cell*, **2007**. *26*: p. 523-537.
31. Tomari, Y., C. Matranga, B. Haley, N. Martinez, and P.D. Zamore, A protein sensor for siRNA asymmetry. *Science*, **2004**. *306*: p. 1377-1380.
32. Valencia-Sanchez, M.A., J.D. Liu, G.J. Hannon, and R. Parker, Control of translation and mRNA degradation by miRNAs and siRNAs. *Gene Dev*, **2006**. *20*: p. 515-524.
33. Manoharan, M., RNA interference and chemically modified small interfering RNAs. *Curr. Opin. Chem. Biol.*, **2004**. *8*: p. 570-579.
34. Reynolds, A., D. Leake, Q. Boese, S. Scaringe, W.S. Marshall, and A. Khvorova, Rational siRNA design for RNA interference. *Nat Biotechno*, **2004**. *22*: p. 326-330.
35. Lewis, B.P., I.H. Shih, M.W. Jones-Rhoades, D.P. Bartel, and C.B. Burge, Prediction of mammalian microRNA targets. *Cell*, **2003**. *115*: p. 787-798.
36. Ma, J.B., Y.R. Yuan, G. Meister, Y. Pei, T. Tuschl, and D.J. Patel, Structural basis for 5 '-end-specific recognition of guide RNA by the A-fulgidus Piwi protein. *Nature*, **2005**. *434*: p. 666-670.
37. Gregory, R.I., T.P. Chendrimada, N. Cooch, and R. Shiekhattar, Human RISC couples microRNA biogenesis and posttranscriptional gene silencing. *Cell*, **2005**. *123*: p. 631-640.
38. Gray, N.S., Drug discovery through industry-academic partnerships. *Nat. Chem. Biol.*, **2006**. *2*: p. 649-653.
39. Zentilin, L. and M. Giacca, In vivo transfer and expression of genes coding for short interfering RNAs. *Curr Pharm Biotechno*, **2004**. *5*: p. 341-347.
40. Clayton, J., Rnai options. *Nature*, **2004**. *431*: p. 599-599.
41. Perron, M.P. and P. Provost, *Protein Components of the microRNA Pathway and Human Diseases*, in *Met Mol Biol*, M. Sioud, Editor. 2009. p. 369-385.
42. Pellino, J.L., L. Jaskiewicz, W. Filipowicz, and E.J. Sontheimer, ATP modulates siRNA interactions with an endogenous human Dicer complex. *RNA*, **2005**. *11*: p. 1719-1724.
43. Kini, H.K. and S.P. Walton, In vitro binding of single-stranded RNA by human Dicer. *FEBS Lett.*, **2007**. *581*: p. 5611-5616.
44. Chen, P.Y., L. Weinmann, D. Gaidatzis, Y. Pei, M. Zavolan, T. Tuschl, and G. Meister, Strand-specific 5 -*O*-methylation of siRNA duplexes controls guide strand selection and targeting specificity. *RNA*, **2008**. *14*: p. 263-274.
45. Schwarz, D.S., G. Hutvagner, T. Du, Z.S. Xu, N. Aronin, and P.D. Zamore, Asymmetry in the assembly of the RNAi enzyme complex. *Cell*, **2003**. *115*: p. 199-208.

46. Tafer, H., S.L. Ameres, G. Obernosterer, C.A. Gebeshuber, R. Schroeder, J. Martinez, and I.L. Hofacker, The impact of target site accessibility on the design of effective siRNAs. *Nat. Biotechnol.*, **2008**. *26*: p. 578-583.
47. Bramsen, J.B., M.B. Laursen, A.F. Nielsen, T.B. Hansen, C. Bus, N. Langkjaer, B.R. Babu, T. Hojland, M. Abramov, A. Van Aerschot, D. Odadzic, R. Smicius, J. Haas, C. Andree, J. Barman, M. Wenska, P. Srivastava, C. Zhou, D. Honcharenko, S. Hess, E. Mueller, G.V. Bobkov, S.N. Mikhailov, E. Fava, T.F. Meyer, J. Chattopadhyaya, M. Zerial, J.W. Engels, P. Herdewijn, J. Wengel, and J. Kjems, A large-scale chemical modification screen identifies design rules to generate siRNAs with high activity, high stability and low toxicity. *Nucleic Acids Res.*, **2009**. *37*: p. 2867-2881.
48. Zacharias, M. and J.W. Engels, Influence of a fluorobenzene nucleobase analogue on the conformational flexibility of RNA studied by molecular dynamics simulations. *Nucleic Acids Res.*, **2004**. *32*: p. 6304-6311.
49. Eckstein, F., Developments in RNA chemistry, a personal view. *Biochimie*, **2002**. *84*: p. 841-848.
50. Harborth, J., S.M. Elbashir, K. Vandenburgh, H. Manninga, S.A. Scaringe, K. Weber, and T. Tuschl, Sequence, chemical, and structural variation of small interfering RNAs and short hairpin RNAs and the effect on mammalian gene silencing. *Antisense Nucleic A*, **2003**. *13*: p. 83-105.
51. Krieg, A.M. and C.A. Stein, Phosphorothioate oligodeoxynucleotides-antisense or anti-protein. *Antisense Res Dev*, **1995**. *5*: p. 241-241.
52. Hall, A.H.S., J. Wan, E.E. Shaughnessy, B.R. Shaw, and K.A. Alexander, RNA interference using boranophosphate siRNAs: structure-activity relationships. *Nucleic Acids Res.*, **2004**. *32*: p. 5991-6000.
53. Czauderna, F., M. Fechtner, S. Dames, H. Aygun, A. Klippel, G.J. Pronk, K. Giese, and J. Kaufmann, Structural variations and stabilising modifications of synthetic siRNAs in mammalian cells. *Nucleic Acids Res.*, **2003**. *31*: p. 2705-2716.
54. Prakash, T.P., C.R. Allerson, P. Dande, T.A. Vickers, N. Sioufi, R. Jarres, B.F. Baker, E.E. Swayze, R.H. Griffey, and B. Bhat, Positional effect of chemical modifications on short interference RNA activity in mammalian cells. *J. Med. Chem.*, **2005**. *48*: p. 4247-4253.
55. Dowler, T., D. Bergeron, A.L. Tedeschi, L. Paquet, N. Ferrari, and M.J. Damha, Improvements in siRNA properties mediated by 2 '-deoxy-2 '-fluoro-beta-D-arabinonucleic acid (FANA). *Nucleic Acids Res.*, **2006**. *34*: p. 1669-1675.
56. Obika, S., D. Nanbu, Y. Hari, K. Morio, Y. In, T. Ishida, and T. Imanishi, Synthesis of 2'-O,4'-C-methyleneuridine and -cytidine. Novel bicyclic nucleosides having a fixed C-3'-endo sugar puckering. *Tetrahedron Lett.*, **1997**. *38*: p. 8735-8738.
57. Koshkin, A.A., S.K. Singh, P. Nielsen, V.K. Rajwanshi, R. Kumar, M. Meldgaard, C.E. Olsen, and J. Wengel, LNA (Locked Nucleic Acids): Synthesis of the adenine, cytosine, guanine, 5-methylcytosine, thymine and uracil bicyclonucleoside monomers, oligomerisation, and unprecedented nucleic acid recognition. *Tetrahedron*, **1998**. *54*: p. 3607-3630.
58. Braasch, D.A., S. Jensen, Y.H. Liu, K. Kaur, K. Arar, M.A. White, and D.R. Corey, RNA interference in mammalian cells by chemically-modified RNA. *Biochemistry*, **2003**. *42*: p. 7967-7975.
59. Elmen, J., H. Thonberg, K. Ljungberg, M. Frieden, M. Westergaard, Y.H. Xu, B. Wahren, Z.C. Liang, H. Urum, T. Koch, and C. Wahlestedt, Locked nucleic acid (LNA) mediated improvements in siRNA stability and functionality. *Nucleic Acids Res.*, **2005**. *33*: p. 439-447.
60. Behlke, M.A., Chemical Modification of siRNAs for In Vivo Use. *Oligonucleotides*, **2008**. *18*: p. 305-319.
61. Singh, S.K. and P.B. Hajeri, siRNAs: their potential as therapeutic agents - Part II. Methods of delivery. *Drug Discov. Today*, **2009**. *14*: p. 859-865.
62. Whitehead, K.A., R. Langer, and D.G. Anderson, Knocking down barriers: advances in siRNA delivery. *Nat Rev Drug Discov*, **2009**. *8*: p. 129-138.

63. Thakker, D.R., F. Natt, D. Husken, H. van der Putten, R. Maier, D. Hoyer, and J.F. Cryan, siRNA-mediated knockdown of the serotonin transporter in the adult mouse brain. *Mol. Psychiatry*, **2005**. *10*: p. 782-789.
64. Dorn, G., S. Patel, G. Wotherspoon, M. Hemmings-Mieszczak, J. Barclay, F.J.C. Natt, P. Martin, S. Bevan, A. Fox, P. Ganju, W. Wishart, and J. Hall, siRNA relieves chronic neuropathic pain. *Nucleic Acids Res.*, **2004**. *32*.
65. Zhang, X.C., P.Y. Shan, D.H. Jiang, P.W. Noble, N.G. Abraham, A. Kappas, and P.J. Lee, Small interfering RNA targeting heme oxygenase-1 enhances ischemia-reperfusion-induced lung apoptosis. *J. Biol. Chem.*, **2004**. *279*: p. 10677-10684.
66. Shen, J., R. Samul, R.L. Silva, H. Akiyama, H. Liu, Y. Saishin, S.F. Hackett, S. Zinnen, K. Kossen, K. Fosnaugh, C. Vargeese, A. Gomez, K. Bouhana, R. Aitchison, P. Pavco, and P.A. Campochiaro, Suppression of ocular neovascularization with siRNA targeting VEGF receptor 1. *Gene Ther.*, **2006**. *13*: p. 225-234.
67. Soutschek, J., A. Akinc, B. Bramlage, K. Charisse, R. Constien, M. Donoghue, S. Elbashir, A. Geick, P. Hadwiger, J. Harborth, M. John, V. Kesavan, G. Lavine, R.K. Pandey, T. Racie, K.G. Rajeev, I. Rohl, I. Toudjarska, G. Wang, S. Wuschko, D. Bumcrot, V. Koteliansky, S. Limmer, M. Manoharan, and H.P. Vornlocher, Therapeutic silencing of an endogenous gene by systemic administration of modified siRNAs. *Nature*, **2004**. *432*: p. 173-178.
68. McNamara, J.O., E.R. Andrechek, Y. Wang, K. D Viles, R.E. Rempel, E. Gilboa, B.A. Sullenger, and P.H. Giangrande, Cell type-specific delivery of siRNAs with aptamer-siRNA chimeras. *Nat. Biotechnol.*, **2006**. *24*: p. 1005-1015.
69. Mok, H., J.W. Park, and T.G. Park, Antisense oligodeoxylutudeotide-conjugated hyaluronic Acid/Protamine nanocomplexes for intracellular gene inhibition. *Bioconj. Chem.*, **2007**. *18*: p. 1483-1489.
70. Nielsen, P.E., M. Egholm, R.H. Berg, and O. Buchardt, Sequence-selective recognition of DNA by strand displacement with a thymine-substituted polyamide. *Science*, **1991**. *254*: p. 1497-1500.
71. Porcheddu, A. and G. Giacomelli, Peptide nucleic acids (PNAs), a chemical overview. *Curr. Med. Chem.*, **2005**. *12*: p. 2561-2599.
72. Demidov, V.V., V.N. Potaman, M.D. Frankkamenetskii, M. Egholm, O. Buchard, S.H. Sonnichsen, and P.E. Nielsen, Stability of peptide nucleic acids in human serum and cellular-extracts. *Biochem. Pharmacol.*, **1994**. *48*: p. 1310-1313.
73. Egholm, M., O. Buchardt, L. Christensen, C. Behrens, S.M. Freier, D.A. Driver, R.H. Berg, S.K. Kim, B. Norden, and P.E. Nielsen, PNA hybridizes to complementary oligonucleotides obeying the watson-crick hydrogen-bonding rules. *Nature*, **1993**. *365*: p. 566-568.
74. Egholm, M., P.E. Nielsen, O. Buchardt, and R.H. Berg, Recognition of guanine and adenine in DNA by cytosine and thymine cotaining peptide nucleic acids (PNA). *J Amer Chem Soc*, **1992**. *114*: p. 9677-9678.
75. Phylactou, L.A., Ribozyme and peptide-nucleic acid-based gene therapy. *Adv Drug Deliver Rev*, **2000**. *44*: p. 97-108.
76. Armitage, B.A., The impact of nucleic acid secondary structure on PNA hybridization. *Drug Discov. Today*, **2003**. *8*: p. 222-228.
77. Nielsen, P.E., Structural and biological properties of peptide nucleic acid (PNA). *Pure Appl Chem*, **1998**. *70*: p. 105-110.
78. Hyrup, B. and P.E. Nielsen, Peptide nucleic acids (PNA): Synthesis, properties and potential applications. *Bioorg. Med. Chem.*, **1996**. *4*: p. 5-23.
79. Egholm, M., O. Buchardt, P.E. Nielsen, and R.H. Berg, Peptide nucleic acids (PNA) - oligonucleotide analoge with an achiral peptide backbone. *J. Am. Chem. Soc.*, **1992**. *114*: p. 1895-1897.
80. Uhlmann, E., Peptide nucleic acids (PNA) and PNA-DNA chimeras: From high binding affinity towards biological function. *Biol. Chem.*, **1998**. *379*: p. 1045-1052.

81. Shakeel, S., S. Karim, and A. Ali, Peptide nucleic acid (PNA) - a review. *J Chem Techno Biotechno*, **2006**. *81*: p. 892-899.
82. Tomac, S., M. Sarkar, T. Ratilainen, P. Wittung, P.E. Nielsen, B. Norden, and A. Graslund, Ionic effects on the stability and conformation of peptide nucleic acid complexes. *J Amer Chem Soc*, **1996**. *118*: p. 5544-5552.
83. Bonham, M.A., S. Brown, A.L. Boyd, P.H. Brown, D.A. Bruckenstein, J.C. Hanvey, S.A. Thomson, A. Pipe, F. Hassman, J.E. Bisi, B.C. Froehler, M.D. Matteucci, R.W. Wagner, S.A. Noble, and L.E. Babiss, An assessment of the antisense properties of RNAse H-competent and steric-blocking oligomers. *Nucleic Acids Res.*, **1995**. *23*: p. 1197-1203.
84. Wittung, P., J. Kajanus, K. Edwards, G. Haaima, P.E. Nielsen, B. Norden, and B.G. Malmstrom, Phospholipid membrane permeability of peptide nucleic acid. *FEBS Lett.*, **1995**. *375*: p. 27-9.
85. Uhlmann, E., D.W. Will, G. Breipohl, D. Langner, and A. Ryte, Synthesis and properties of PNA/DNA chimeras. *Angew Chem Int Edit*, **1996**. *35*: p. 2632-2635.
86. Ray, A. and B. Norden, Peptide nucleic acid (PNA): its medical and biotechnical applications and promise for the future. *FASEB J.*, **2000**. *14*: p. 1041-1060.
87. Sharma, S., U.B. Sonavane, and R.R. Joshi, Quantum Chemical Studies of Peptide Nucleic Acid Monomers and Role of Cyclohexyl Modification on Backbone Flexibility. *Int J Quant Chem*, **2009**. *109*: p. 890-896.
88. Demidov, V., M.D. Frankkamenetskii, M. Egholm, O. Buchardt, and P.E. Nielsen, Sequence selective double-strand DNA cleavage by peptide nucleic acid (PNA) targeting using nuclease S1. *Nucleic Acids Res.*, **1993**. *21*: p. 2103-2107.
89. Demers, D.B., E.T. Curry, M. Egholm, and A.C. Sozer, Enhanced PCR amplification of vntr locus D1S80 using peptide nucleic acid (PNA). *Nucleic Acids Res.*, **1995**. *23*: p. 3050-3055.
90. Orum, H., P.E. Nielsen, M. Jorgensen, C. Larsson, C. Stanley, and T. Koch, Sequence-specific purification of nucleic-acids by PNA-controlled hybrid selection. *BioTechniques*, **1995**. *19*: p. 472-480.
91. PerryOkeefe, H., X.W. Yao, J.M. Coull, M. Fuchs, and M. Egholm, Peptide nucleic acid pre-gel hybridization: An alternative to Southern hybridization. *PNAS*, **1996**. *93*: p. 14670-14675.
92. Veselkov, A.G., V.V. Demidov, P.E. Nielsen, and M.D. FrankKamenetskii, A new class of genome rare cutters. *Nucleic Acids Res.*, **1996**. *24*: p. 2483-2487.
93. Hanvey, J.C., N.J. Peffer, J.E. Bisi, S.A. Thomson, R. Cadilla, J.A. Josey, D.J. Ricca, C.F. Hassman, M.A. Bonham, K.G. Au, S.G. Carter, D.A. Bruckenstein, A.L. Boyd, S.A. Noble, and L.E. Babiss, Antisense and antigene properties of peptide nucleic acids. *Science*, **1992**. *258*: p. 1481-1485.
94. Boffa, L.C., P.L. Morris, E.M. Carpaneto, M. Louissaint, and V.G. Allfrey, Invasion of the CAG triplet repeats by a complementary peptide nucleic acid inhibits transcription of the androgen receptor and TATA-binding protein genes and correlates with refolding of an active nucleosome containing a unique AR gene sequence. *J. Biol. Chem.*, **1996**. *271*: p. 13228-13233.
95. Orum, H., P.E. Nielsen, M. Egholm, R.H. Berg, O. Buchardt, and C. Stanley, Single-base pair mutation analysis by PNA directed PCR clamping. *Nucleic Acids Res.*, **1993**. *21*: p. 5332-5336.
96. Carlsson, C., M. Jonsson, B. Norden, M.T. Dulay, R.N. Zare, J. Noolandi, P.E. Nielsen, L.C. Tsui, and J. Zielenski, Screening for genetic mutations. *Nature*, **1996**. *380*: p. 207-207.
97. Thiede, C., E. Bayerdorffer, R. Blasczyk, B. Wittig, and A. Neubauer, Simple and sensitive detection of mutations in the ras proto-oncogenes using PNA-mediated PCR clamping. *Nucleic Acids Res.*, **1996**. *24*: p. 983-984.
98. Wang, J., E. Palecek, P.E. Nielsen, G. Rivas, X.H. Cai, H. Shiraishi, N. Dontha, D.B. Luo, and P.A.M. Farias, Peptide nucleic acid probes for sequence-specific DNA biosensors. *J Amer Chem Soc*, **1996**. *118*: p. 7667-7670.
99. Corey, D.R., Peptide nucleic acids: Expanding the scope of nucleic acid recognition. *Trends Biotechnol.*, **1997**. *15*: p. 224-229.

100. Eriksson, M. and P.E. Nielsen, PNA nucleic acid complexes. Structure, stability and dynamics. *Q Rev of Biophys*, **1996**. *29*: p. 369-394.
101. Pooga, M., U. Soomets, M. Hallbrink, A. Valkna, K. Saar, K. Rezaei, U. Kahl, J.X. Hao, X.J. Xu, Z. Wiesenfeld-Hallin, T. Hokfelt, T. Bartfai, and U. Langel, Cell penetrating PNA constructs regulate galanin receptor levels and modify pain transmission in vivo. *Nat. Biotechnol.*, **1998**. *16*: p. 857-861.
102. Hamilton, S.E., C.G. Simmons, I.S. Kathiriya, and D.R. Corey, Cellular delivery of peptide nucleic acids and inhibition of human telomerase. *Chem & Biol*, **1999**. *6*: p. 343-351.
103. Fraser, G.L., J. Holmgren, P.B.S. Clarke, and C. Wahlestedt, Antisense inhibition of delta-opioid receptor gene function in vivo by peptide nucleic acids. *Mol. Pharmacol.*, **2000**. *57*: p. 725-731.
104. Ganesh, K.N. and P.E. Nielsen, Peptide nucleic acids: Analogs and derivatives. *Curr Org Chem*, **2000**. *4*: p. 931-943.
105. Finn, P.J., N.J. Gibson, R. Fallon, A. Hamilton, and T. Brown, Synthesis and properties of DNA-PNA chimeric oligomers. *Nucleic Acids Res.*, **1996**. *24*: p. 3357-3363.
106. Moggio, L., A. Romanelli, R. Gambari, N. Bianchi, M. Borgatti, E. Fabbri, I. Mancini, B. di Blasio, C. Pedone, and A. Messere, Alternate PNA-DNA Chimeras (PNA-DNA)(n): Synthesis, binding properties and biological activity. *Biopolymers*, **2007**. *88*: p. 815-822.
107. Hall, A.H.S., J. Wan, A. Spesock, Z. Sergueeva, B.R. Shaw, and K.A. Alexander, High potency silencing by single-stranded boranophosphate siRNA. *Nucleic Acids Res.*, **2006**. *34*: p. 2773-2781.
108. Xu, Q., D. Katkevica, and E. Rozners, Toward amide-modified RNA: Synthesis of 3 '-aminomethyl-5 '-carboxy-3 ',5 '-dideoxy nucleosides. *J Org Chem*, **2006**. *71*: p. 5906-5913.
109. Efthymiou, T.C., B. Peel, V. Huynh, and J.-P. Desaulniers, Evaluation of siRNAs that contain internal variable-length spacer linkages. *Bioorg. Med. Chem. Lett.*, **2012**. *22*: p. 5590-4.
110. Moffatt, J.G. and H.G. Khorana, Nucleoside polyphosphates. 10. synthesis and some reactions of nucleoside-5' phosphoromorpholidates and related compounds-improved methods for preparation of nucleoside-5' polyphoshpates. *J Amer Chem Soc*, **1961**. *83*: p. 649-&.
111. Dorper, T. and E.L. Winnacker, Improvements in the phosphoramidite procedure for the synthesis of oligodeoxyribonucleotides. *Nucleic Acids Res.*, **1983**. *11*: p. 2575-2584.
112. Merrifield, R.B., Peptides synthesis on a solid polymer. *Fed Proc*, **1962**. *21*: p. 412-&.
113. Still, W.C., M. Kahn, and A. Mitra, Rapid chromatographic technique for preparative separations with moderate resolution. *J Org Chem*, **1978**. *43*: p. 2923-2925.
114. Thansandote, P., C. Gouliaras, M.O. Turcotte-Savard, and M. Lautens, A Rapid Approach to the Synthesis of Highly Functionalized Tetrahydroisoquinolines. *Journal of Organic Chemistry*, **2009**. *74*: p. 1791-1793.
115. Kryatova, O.P., W.H. Connors, C.F. Bleczinski, A.A. Mokhir, and C. Richert, A 2 '-acylamido cap that increases the stability of oligonucleotide duplexes. *Organic Letters*, **2001**. *3*: p. 987-990.
116. Winans, K.A. and C.R. Bertozzi, An inhibitor of the human UDP-GlcNAc 4-epimerase identified from a uridine-based library: A strategy to inhibit O-linked glycosylation. *Chemistry & Biology*, **2002**. *9*: p. 113-129.
117. Valeur, E. and M. Bradley, Amide bond formation: beyond the myth of coupling reagents. *Chemical Society Reviews*, **2009**. *38*: p. 606-631.
118. Vaultier, M., N. Knouzi, and R. Carrie, Reducation of azides into primary amines by a general-method using the staudinger reaction. *Tetrahedron Lett.*, **1983**. *24*: p. 763-764.
119. Rana, T.M., Illuminating the silence: understanding the structure and function of small RNAs. *Nature Reviews Molecular Cell Biology*, **2007**. *8*: p. 23-36.
120. Preall, J.B. and E.J. Sontheimer, RNAi: RISC gets loaded. *Cell*, **2005**. *123*: p. 543-545.
121. Chiu, Y.L. and T.M. Rana, RNAi in human cells: Basic structural and functional features of small interfering RNA. *Mol. Cell*, **2002**. *10*: p. 549-561.
122. Chiu, Y.L. and T.M. Rana, siRNA function in RNAi: A chemical modification analysis. *RNA*, **2003**. *9*: p. 1034-1048.

123. Heale, B.S.E., H.S. Soifer, C. Bowers, and J.J. Rossi, siRNA target site secondary structure predictions using local stable substructures. *Nucleic Acids Research*, **2005**. *33*.
124. Saenger, W., Principles of nucleic acid structure, in *Springer-Verlag, New York*1984.
125. Ponnuswamy, P.K. and M.M. Gromiha, On the conformational stability of oligonucleotide duplexes and transfer-RNA molecules. *J of Theo Biol*, **1994**. *169*: p. 419-432.
126. Manoharan, M., 2 '-Carbohydrate modifications in antisense oligonucleotide therapy: importance of conformation, configuration and conjugation. *Biochimica Et Biophysica Acta-Gene Structure and Expression*, **1999**. *1489*: p. 117-130.
127. McDowell, J.A. and D.H. Turner, Investigation of the structural basis for thermodynamic stabilities of tandem GU mismatches: Solution structure of (rGAGGUCUC)(2) by two-dimensional NMR and simulated annealing. *Biochemistry*, **1996**. *35*: p. 14077-14089.
128. Alam, J. and J.L. Cook, Reporter genes-application of the study of mammalian gene-transcription. *Anal. Biochem.*, **1990**. *188*: p. 245-254.
129. Bronstein, I., J. Fortin, P.E. Stanley, G. Stewart, and L.J. Kricka, CHEMILUMINESCENT AND BIOLUMINESCENT REPORTER GENE ASSAYS. *Analytical Biochemistry*, **1994**. *219*: p. 169-181.
130. Bajor, Z., G. Sagi, Z. Tegyey, and F. Kraicsovits, PNA-DNA chimeras containing 5-alkynyl-pyrimidine PNA units. Synthesis, binding properties, and enzymatic stability. *Nucleosides Nucleotides & Nucleic Acids*, **2003**. *22*: p. 1963-1983.
131. Wold, F., *Foundations of modern biochemistry series macro molecules structure and function*. Foundations of Modern Biochemistry Series Macro Molecules Structure and Function. 1971. 305-305.
132. Gratzer, W.B. and E.G. Richards, Evaluation of RNA conformation from circular dichroism and optical rotatory dispersion data. *Biopolymers*, **1971**. *10*: p. 2607-&.
133. Pescitelli, G., L. Di Bari, and N. Berova, Conformational aspects in the studies of organic compounds by electronic circular dichroism. *Chem Soc Rev*, **2011**. *40*: p. 4603-4625.
134. Nieuwenhuijsen, B.W., Y.P. Huang, Y.R. Wang, F. Ramirez, G. Kalgaonkar, and K.H. Young, A dual luciferase multiplexed high-throughput screening platform for protein-protein interactions. *J. Biomol. Screen.*, **2003**. *8*: p. 676-684.
135. Matthews, J.C., K. Hori, and M.J. Cormier, Purification and properties of Renilla-reniformis luciferase. *Biochemistry*, **1977**. *16*: p. 85-91.
136. Khvorova, A., A. Reynolds, and S.D. Jayasena, Functional siRNAs and rniRNAs exhibit strand bias. *Cell*, **2003**. *115*: p. 209-216.
137. Elbashir, S.M., J. Martinez, A. Patkaniowska, W. Lendeckel, and T. Tuschl, Functional anatomy of siRNAs for mediating efficient RNAi in Drosophila melanogaster embryo lysate. *EMBO J.*, **2001**. *20*: p. 6877-6888.
138. Carrel, A., Results of the transplantation of blood vessels, organs and limbs. *J Amer Med Asso*, **1908**. *51*: p. 1662-1667.
139. Wang, Y., S. Juranek, H. Li, G. Sheng, T. Tuschl, and D.J. Patel, Structure of an argonaute silencing complex with a seed-containing guide DNA and target RNA duplex. *Nature*, **2008**. *456*: p. 921-U72.
140. Addepalli, H., Meena, C.G. Peng, G. Wang, Y. Fan, K. Charisse, K.N. Jayaprakash, K.G. Rajeev, R.K. Pandey, G. Lavine, L. Zhang, K. Jahn-Hofmann, P. Hadwiger, M. Manoharan, and M.A. Maier, Modulation of thermal stability can enhance the potency of siRNA. *Nucleic Acids Res.*, **2010**. *38*: p. 7320-7331.
141. Somoza, A., M. Terrazas, and R. Eritja, Modified siRNAs for the study of the PAZ domain. *Chem Comm*, **2010**. *46*: p. 4270-4272.
142. NL, T., *Transplant: From Myth to Reality*, *New Haven*. 2003: Yale University Press.
143. Kennedy, S., D. Wang, and G. Ruvkun, A conserved siRNA-degrading RNase negatively regulates RNA interference in C-elegans. *Nature*, **2004**. *427*: p. 645-649.

144. Takabatake, Y., Y. Isaka, M. Mizui, H. Kawachi, S. Takahara, and E. Imai, Chemically modified siRNA prolonged RNA interference in renal disease. *Biochem and Biophys Res Comm*, **2007**. *363*: p. 432-437.
145. Layzer, J.M., A.P. McCaffrey, A.K. Tanner, Z. Huang, M.A. Kay, and B.A. Sullenger, In vivo activity of nuclease-resistant siRNAs. *RNA*, **2004**. *10*: p. 766-771.
146. Choung, S., Y.J. Kim, S. Kim, H.O. Park, and Y.C. Choi, Chemical modification of siRNAs to improve serum stability without loss of efficacy. *Biochem. Biophys. Res. Commun.*, **2006**. *342*: p. 919-927.
147. Judge, A.D., G. Bola, A.C.H. Lee, and I. MacLachlan, Design of noninflammatory synthetic siRNA mediating potent gene silencing in vivo. *Mol. Ther.*, **2006**. *13*: p. 494-505.
148. Yang, E. and S.J. Korsmeyer, Molecular thanatopsis: A discourse on the BCL2 family and cell death. *Blood*, **1996**. *88*: p. 386-401.
149. Reed, J.C., C. Stein, C. Subasinghe, S. Haldar, C.M. Croce, S. Yum, and J. Cohen, Antisense-mediated inhibition of BCL2 protooncogene expression and leukemic-cell growth and survival comparisons of phosphodiester and phosphorothioate oligonucleoxynucleotides. *Cancer Res.*, **1990**. *50*: p. 6565-6570.
150. Nemunaitis, J., J.T. Holmlund, M. Kraynak, D. Richards, J. Bruce, N. Ognoskie, T.J. Kwoh, R. Geary, A. Dorr, D. Von Hoff, and S.G. Eckhard, Phase I evaluation of ISIS 3521, an antisense oligodeoxynucleotide to protein kinase C-alpha, in patients with advanced cancer. *J Clin Oncol*, **1999**. *17*: p. 3586-3595.
151. Dean, N.M., R. McKay, L. Miraglia, T. Geiger, M. Muller, D. Fabbro, and C.F. Bennett, Antisense oligonucleotides as inhibitors of signal transduction: Development from research tools to therapeutic agents. *Biochem. Soc. Trans.*, **1996**. *24*: p. 623-629.
152. Yuen, A.R., J. Halsey, G.A. Fisher, J.T. Holmlund, R.S. Geary, T.J. Kwoh, A. Dorr, and B.I. Sikic, Phase I study of an antisense oligonucleotide to protein kinase C-alpha (ISIS 3521/CGP 64128A) in patients with cancer. *Clin. Cancer. Res.*, **1999**. *5*: p. 3357-3363.
153. Dagle, J.M., M.E. Andracki, R.J. Devine, and J.A. Walder, Physical-properties of oligonucleotides containing phosphoramidite-modified internucleoside linkages. *Nucleic Acids Res.*, **1991**. *19*: p. 1805-1810.

Appendix

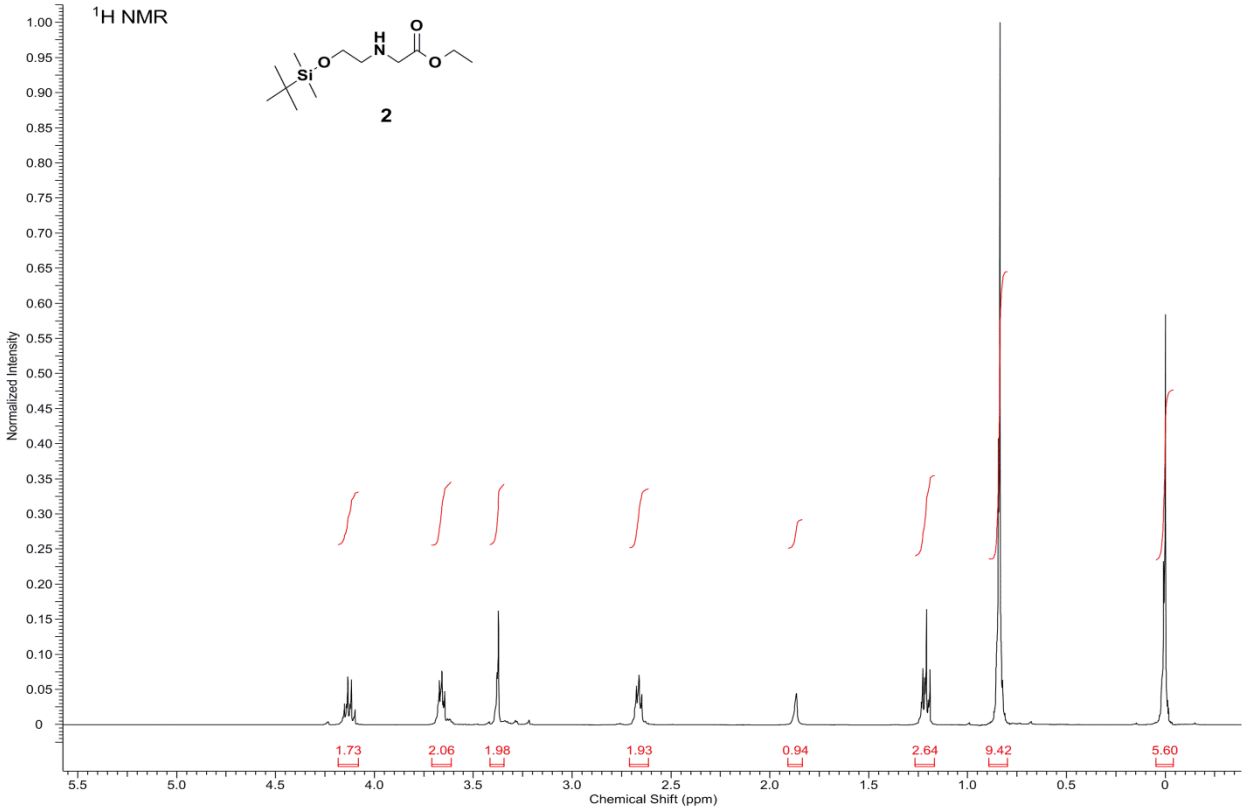
^{1}H NMR
2
Normalized Intensity
Chemical Shift (ppm)
1.73
2.06
1.98
1.93
0.94
2.64
9.42
5.60

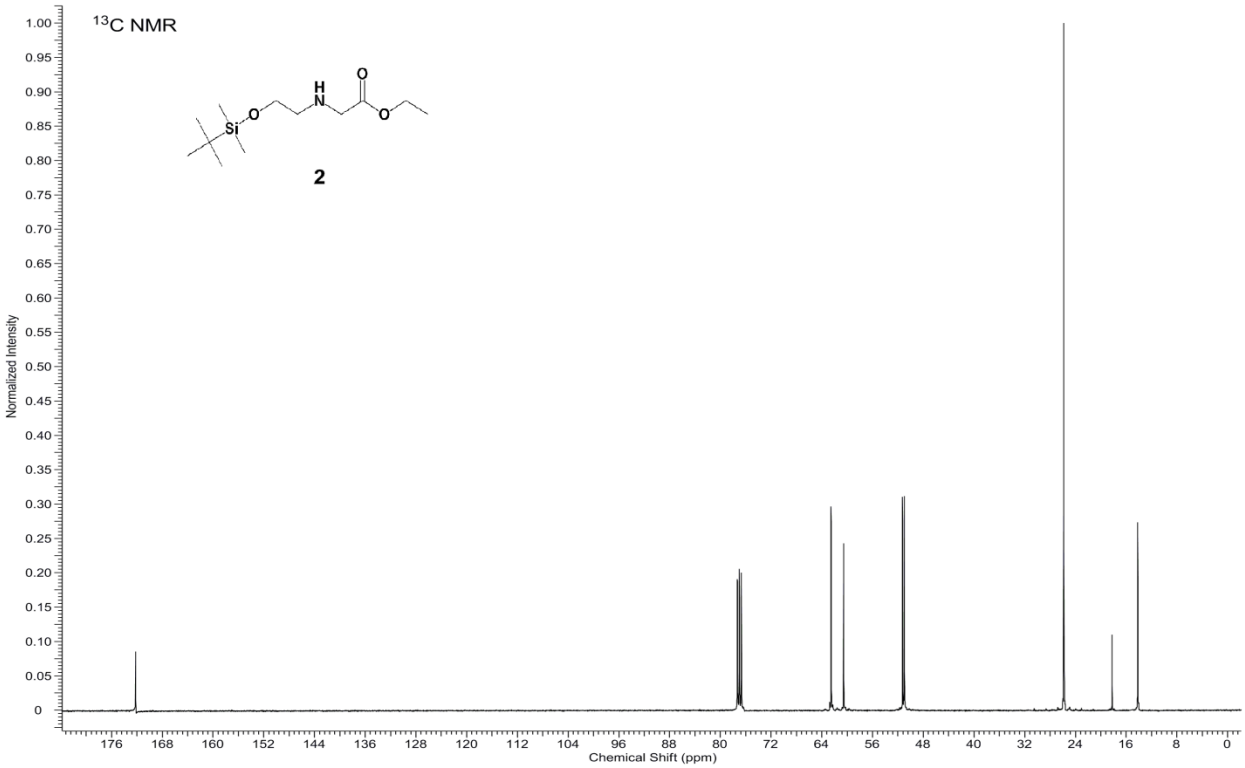
^{13}C NMR
2
Normalized Intensity
Chemical Shift (ppm)

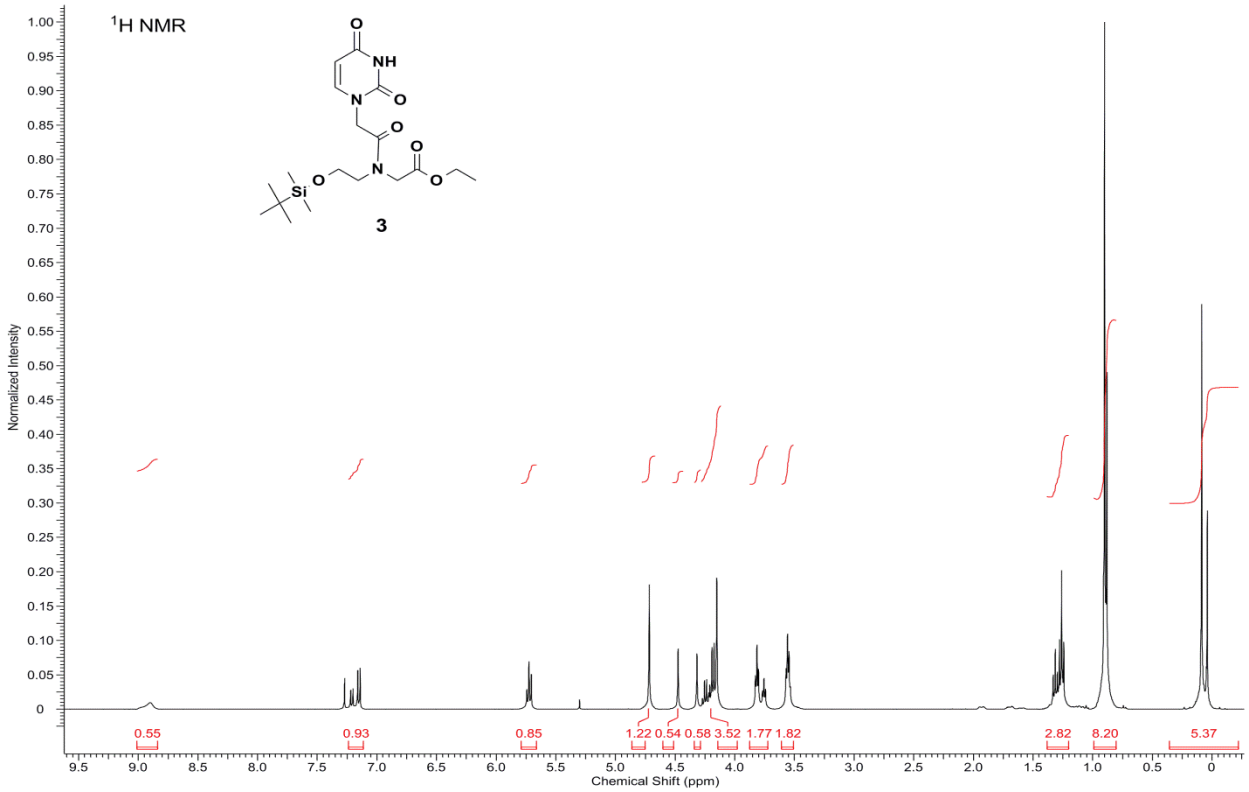
^{1}H NMR
3
Normalized Intensity
Chemical Shift (ppm)
0.55
0.93
0.85
1.22
0.54
0.58
3.52
1.77
1.82
2.82
8.20
5.37

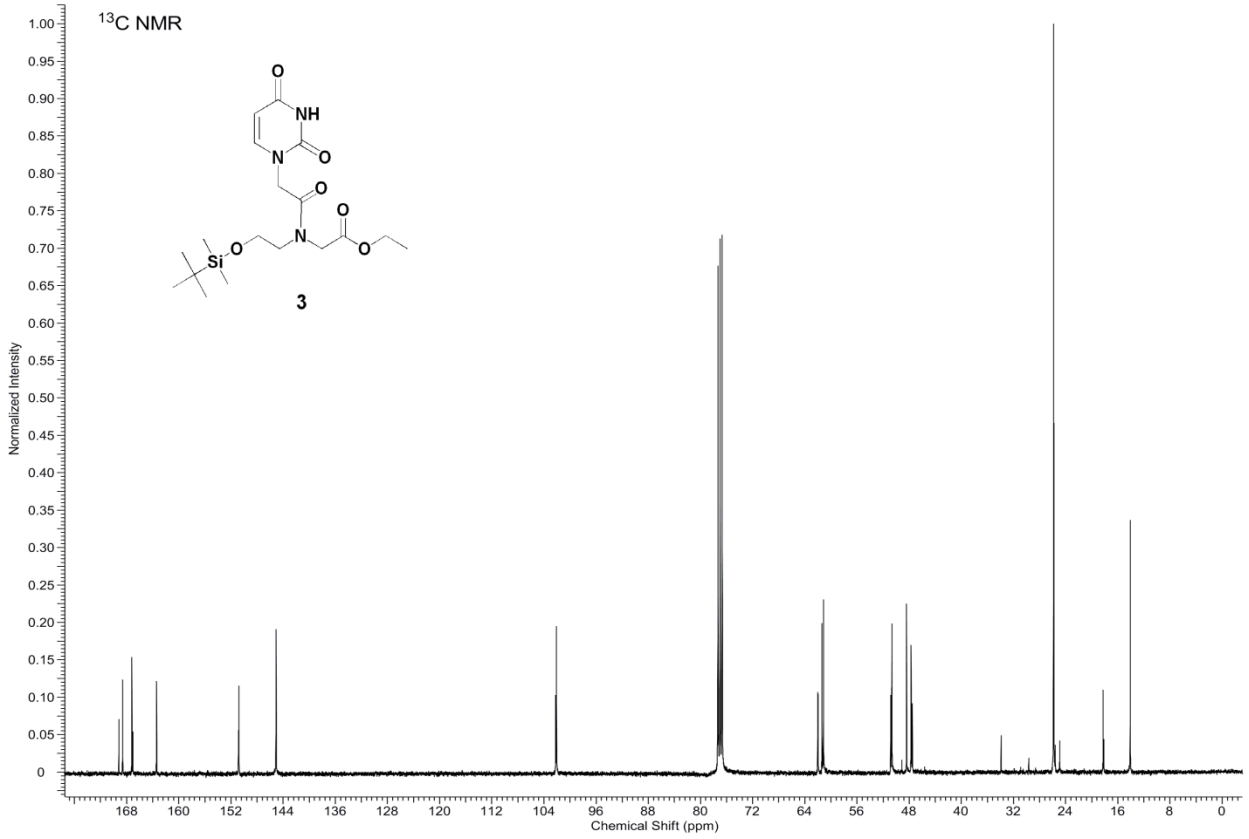
^{13}C NMR
3
Normalized Intensity
Chemical Shift (ppm)

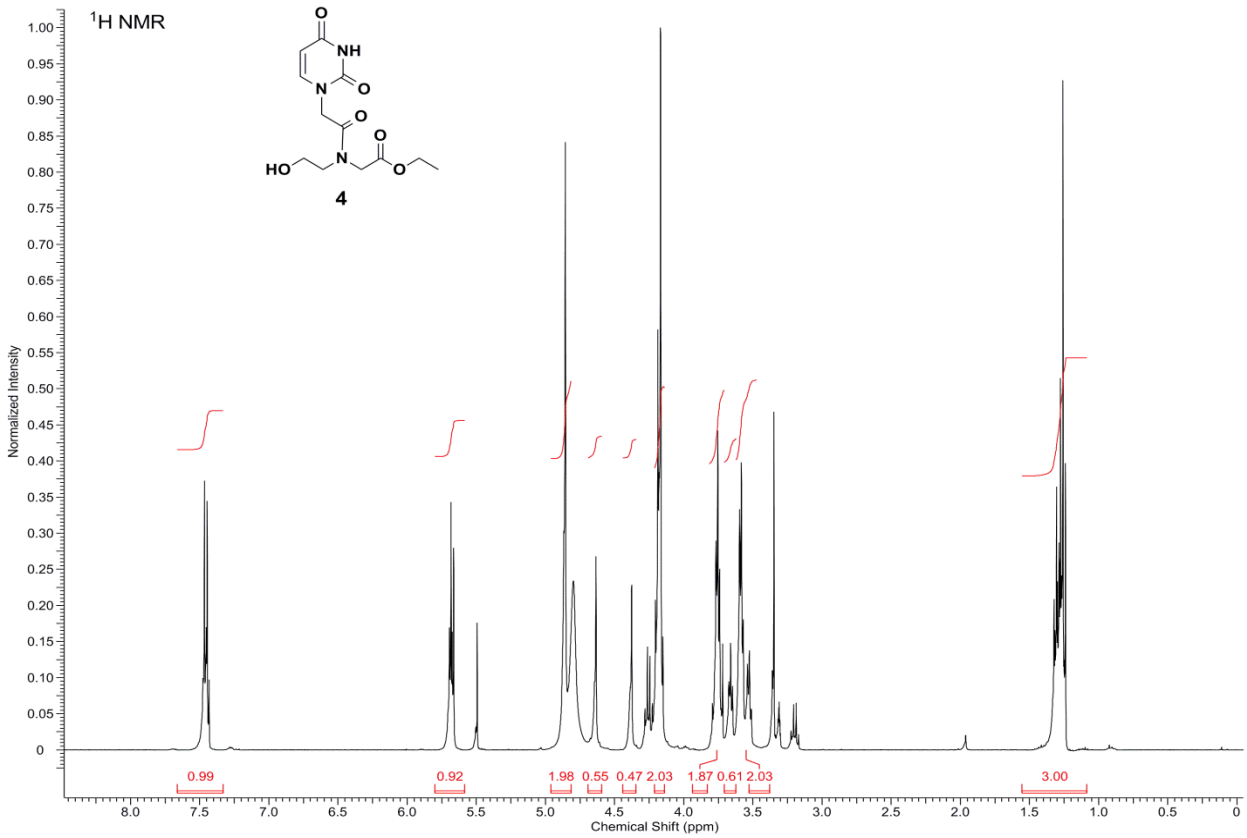
^{1}H NMR
4
Normalized Intensity
Chemical Shift (ppm)
0.99
0.92
1.98
0.55
0.47
2.03
1.87
0.61
2.03
3.00

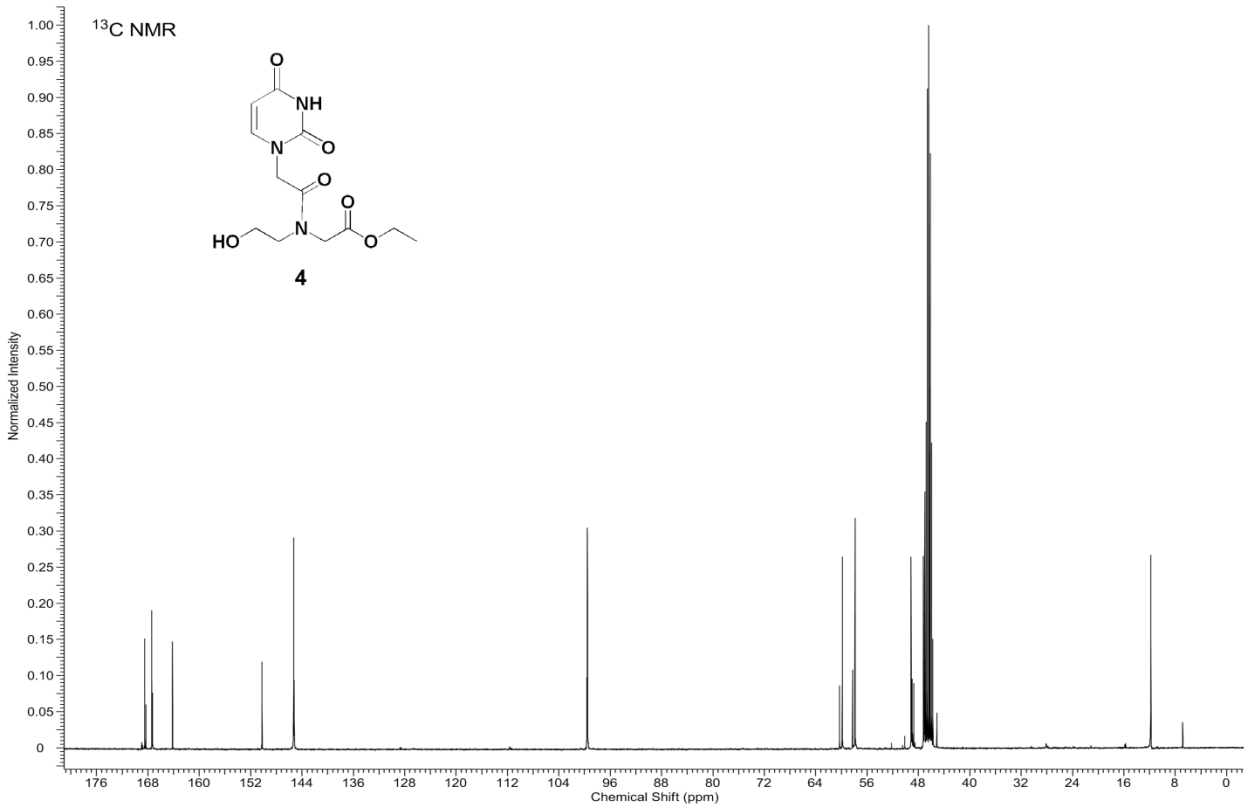
^{13}C NMR
4
Normalized Intensity
Chemical Shift (ppm)

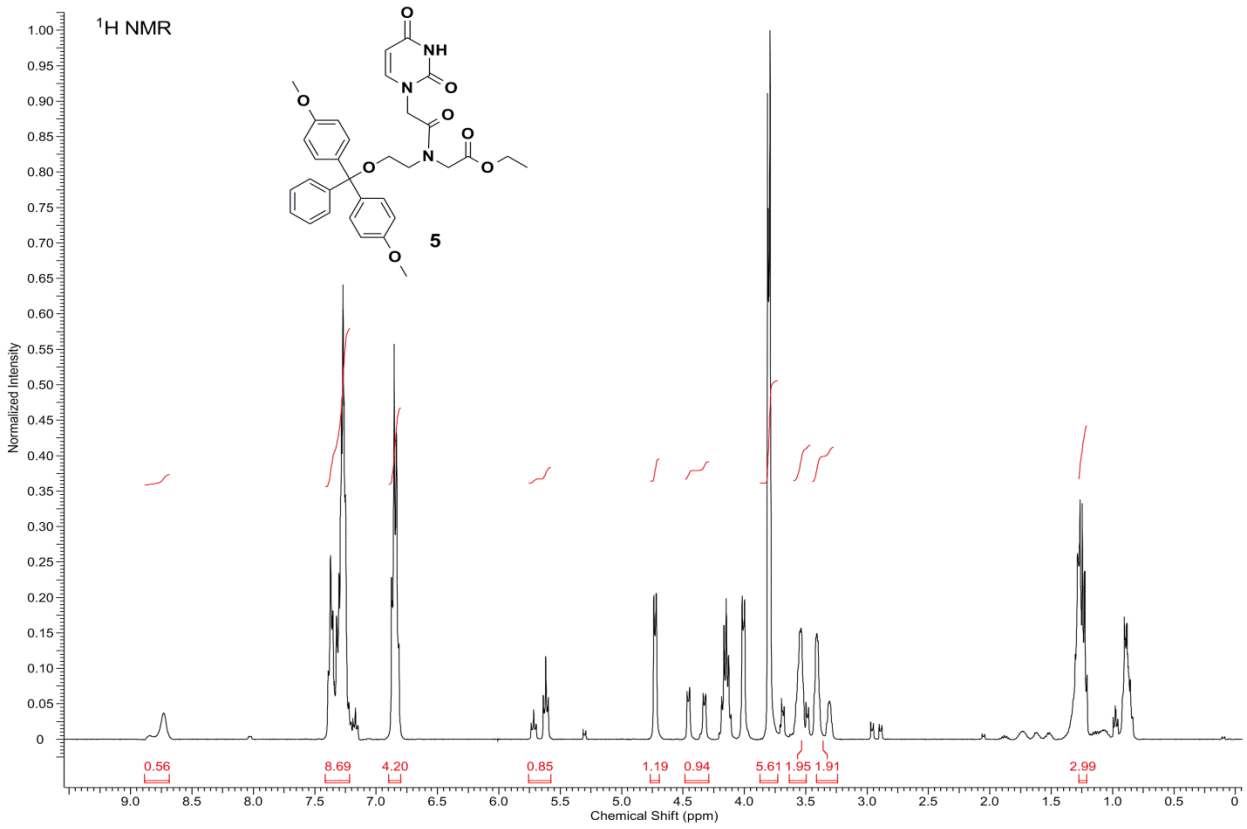
^{1}H NMR
5
Normalized Intensity
Chemical Shift (ppm)
0.56
8.69
4.20
0.85
1.19
0.94
5.61
1.95
1.91
2.99

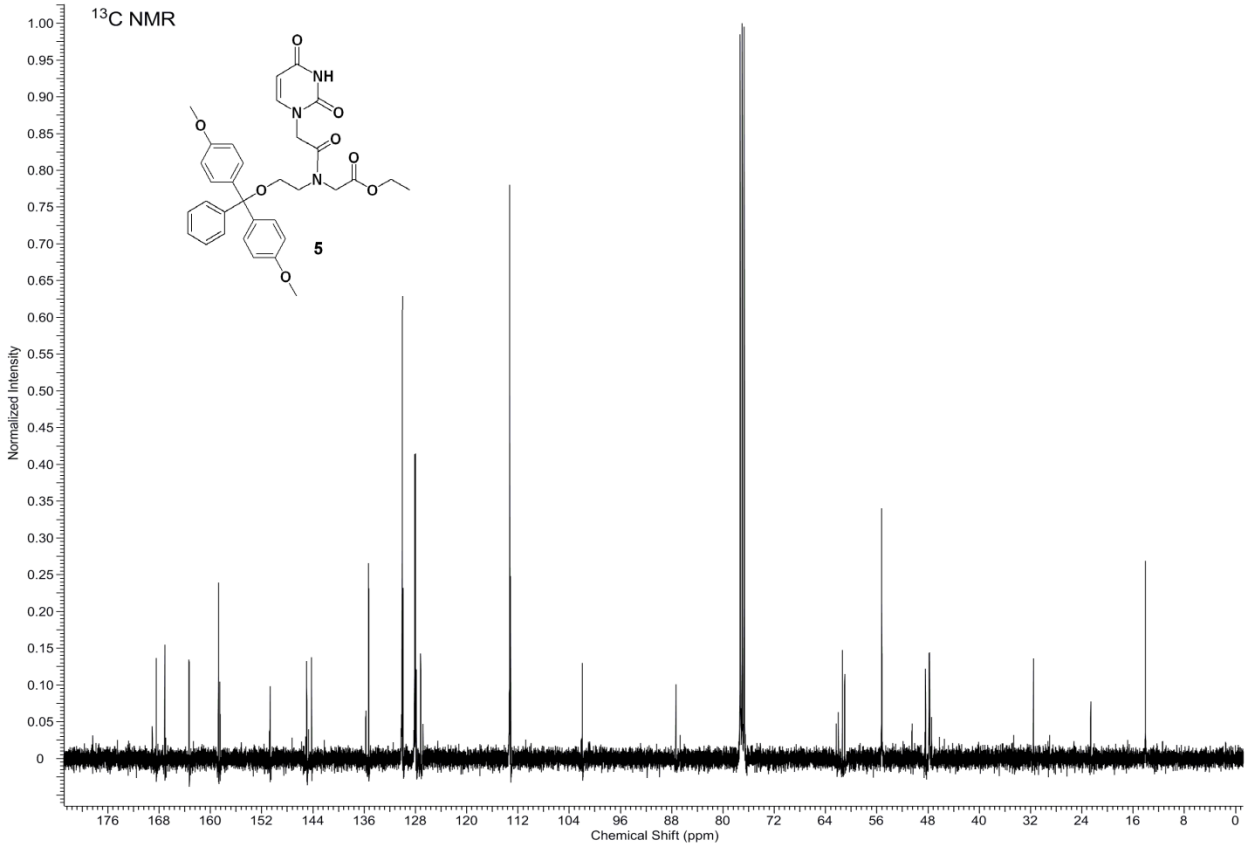
^{13}C NMR
5
Normalized Intensity
Chemical Shift (ppm)

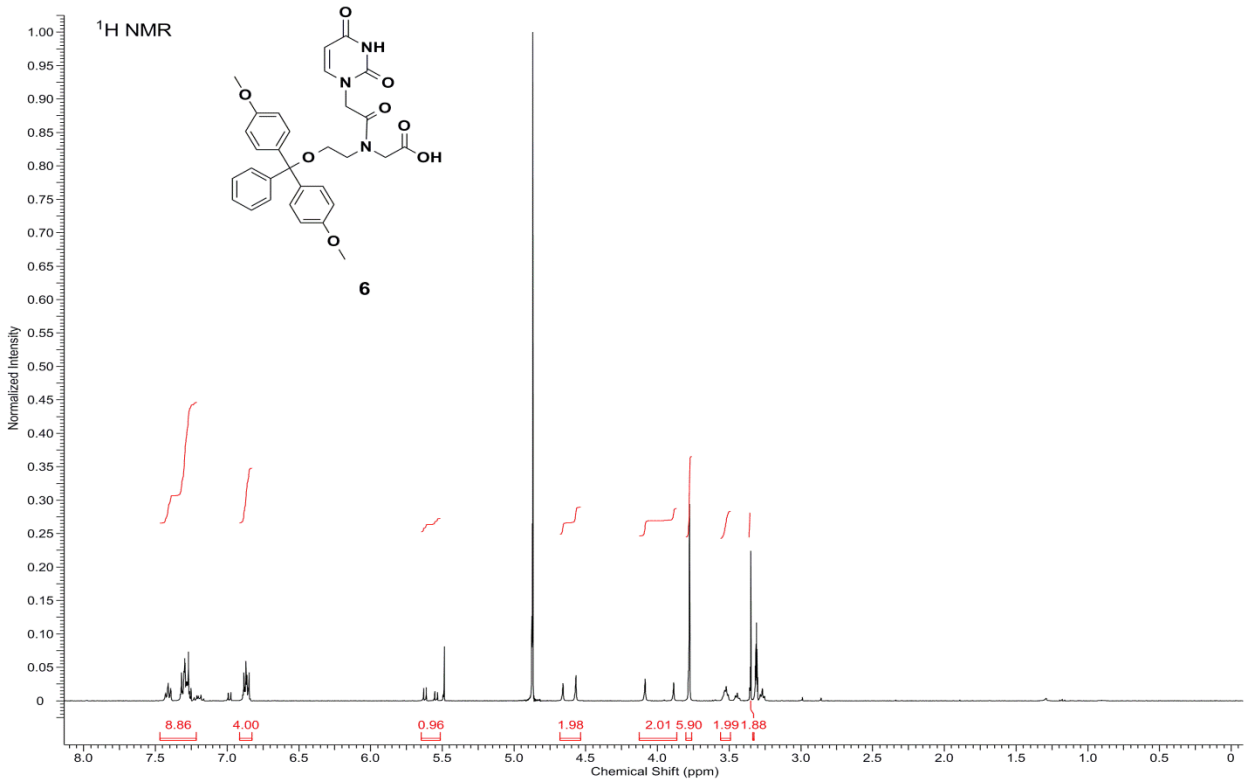
^{1}H NMR
6
Normalized Intensity
Chemical Shift (ppm)
8.86
4.00
0.96
1.98
2.01
5.90
1.99
1.88

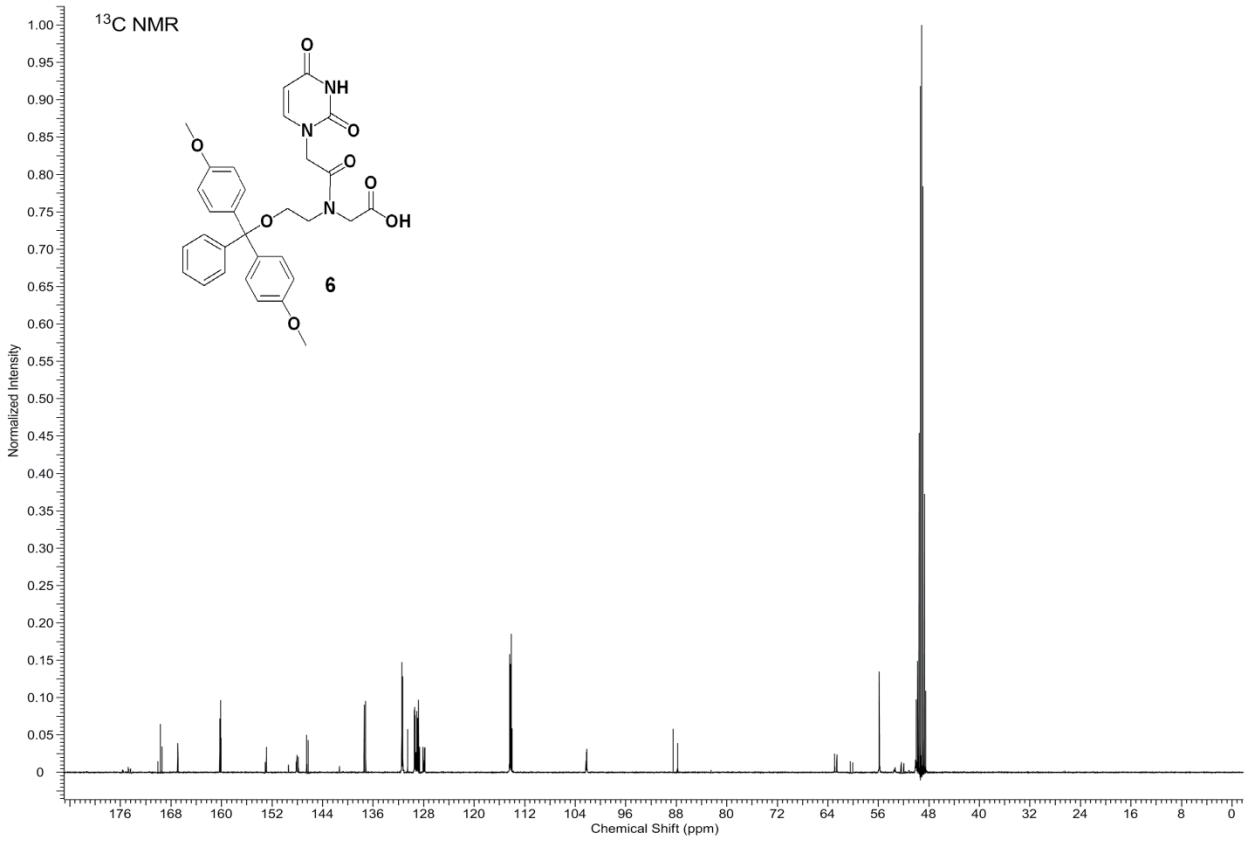
^{13}C NMR
6
Normalized Intensity
Chemical Shift (ppm)

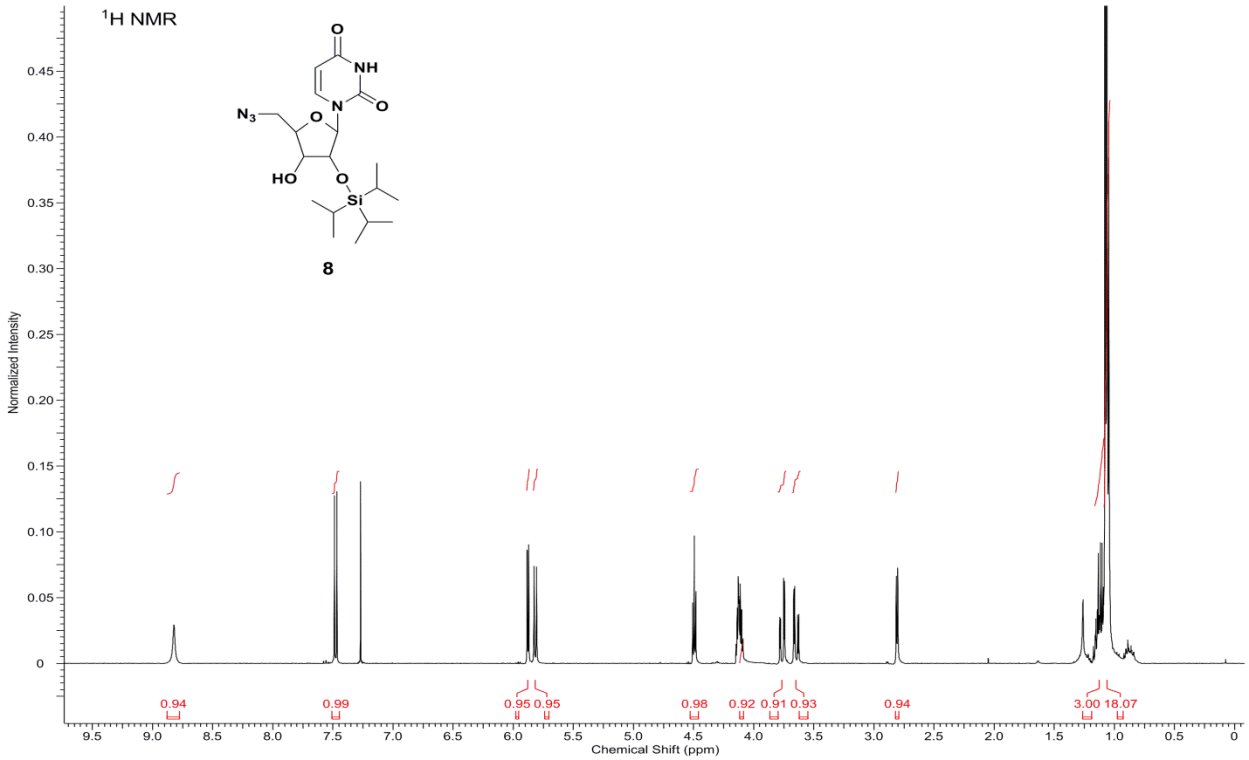
^{1}H NMR
8
Normalized Intensity
Chemical Shift (ppm)
0.94
0.99
0.95 0.95
0.98
0.92 0.91 0.93
0.94
3.00 18.07

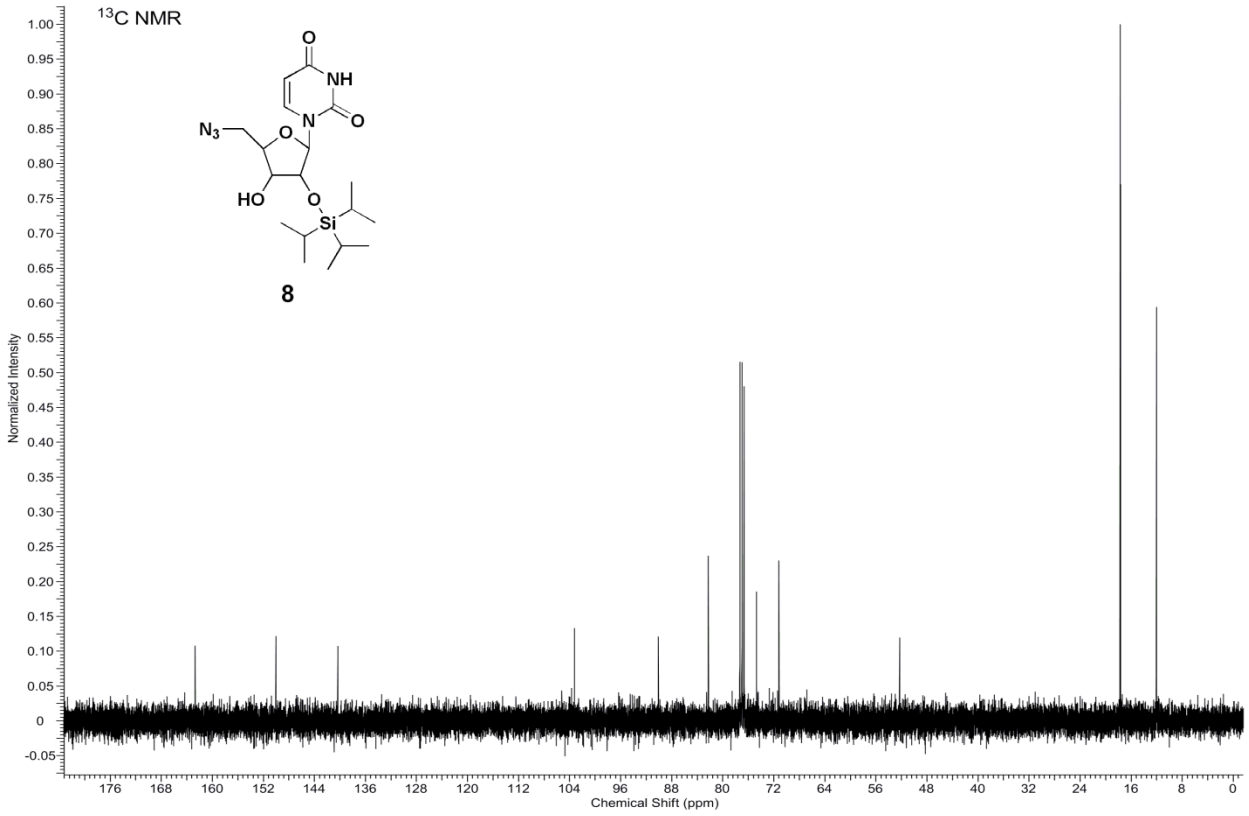
^{13}C NMR
8
Normalized Intensity
Chemical Shift (ppm)

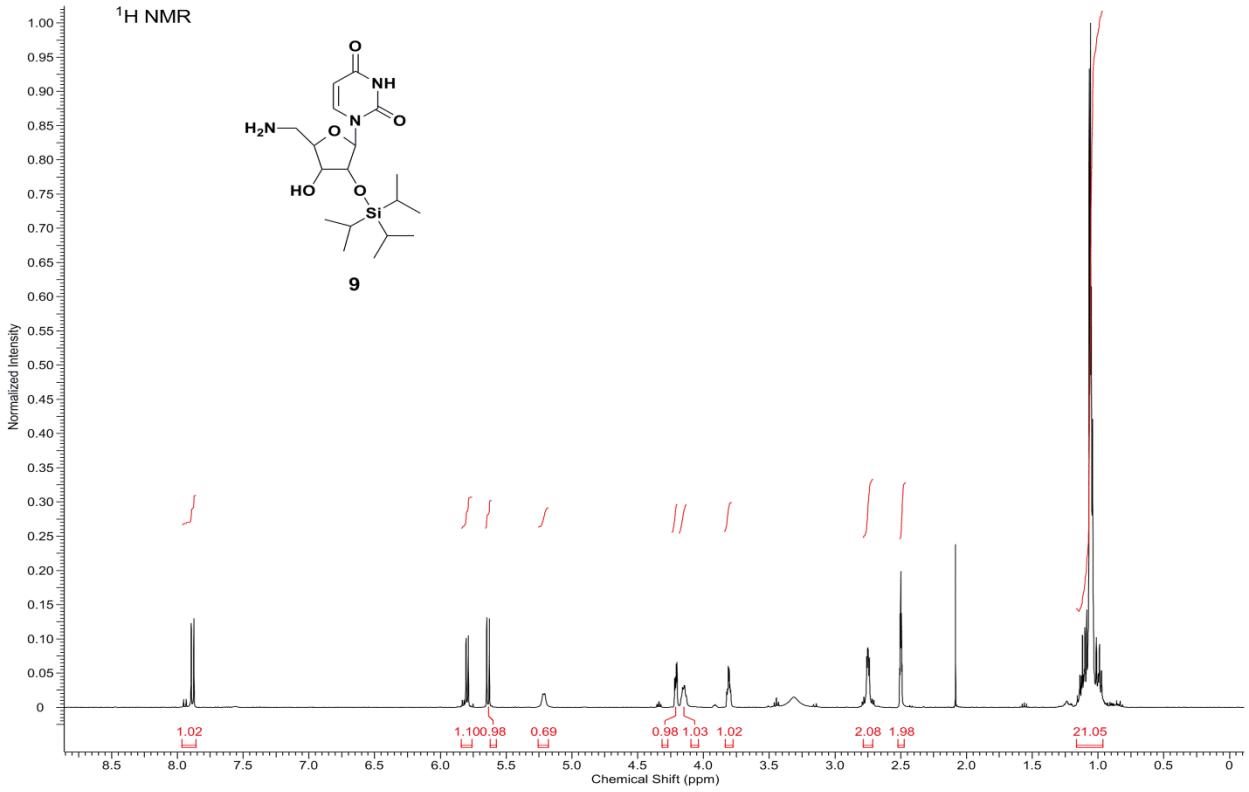
^{1}H NMR
9
Normalized Intensity
Chemical Shift (ppm)
1.02
1.10
0.98
0.69
0.98
1.03
1.02
2.08
1.98
21.05

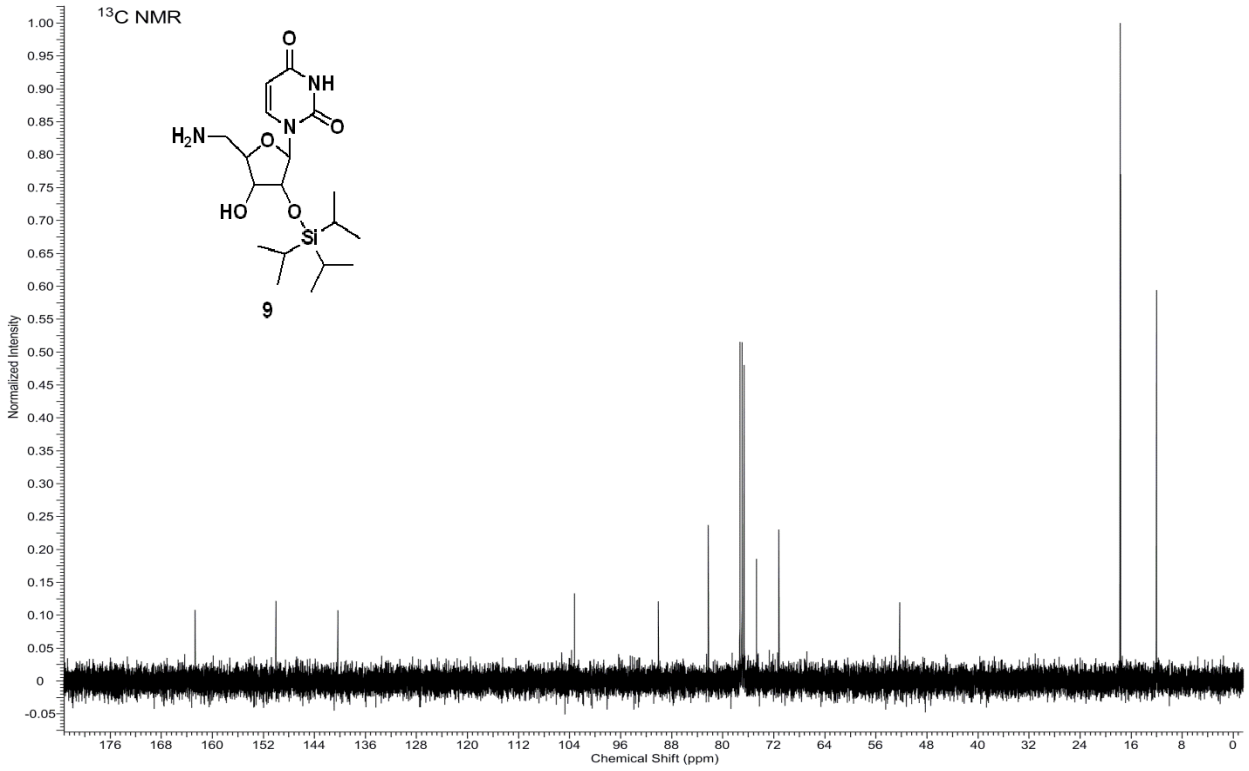
^{13}C NMR
9
Normalized Intensity
Chemical Shift (ppm)

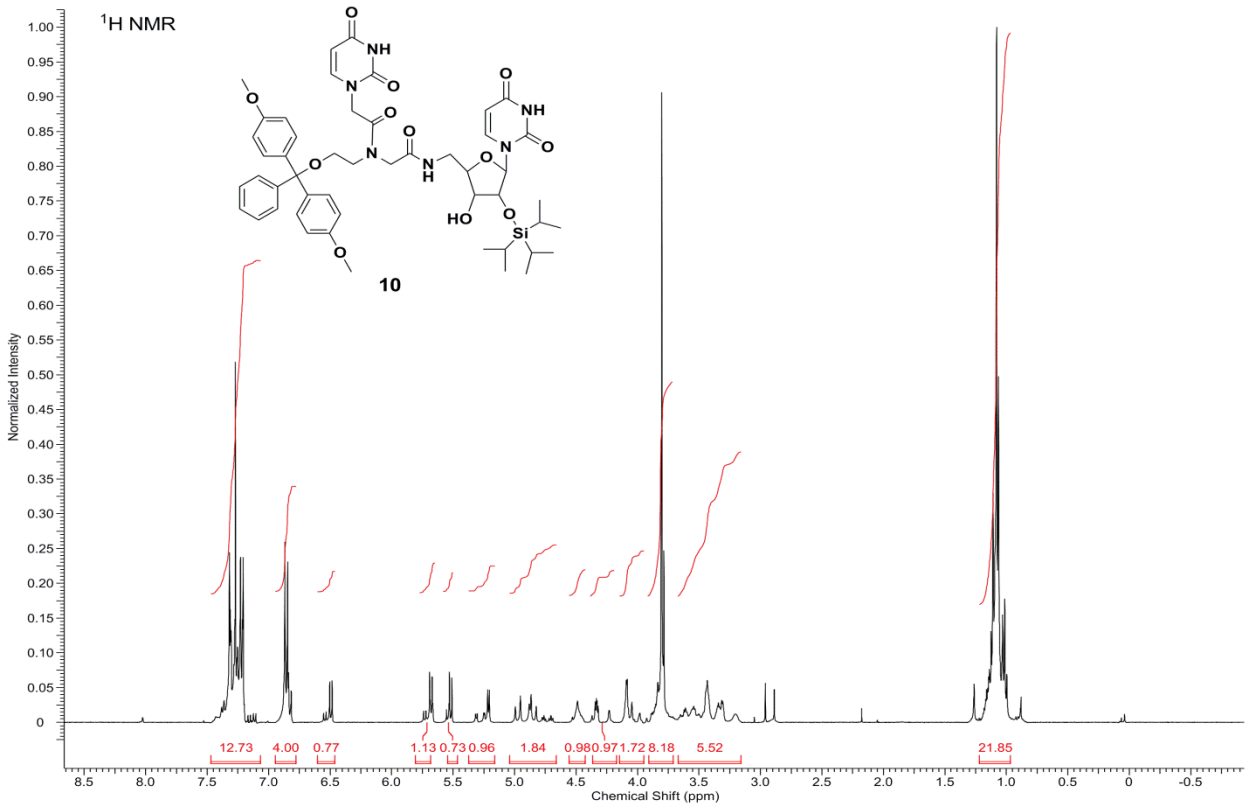
^{1}H NMR
10
Normalized Intensity
Chemical Shift (ppm)
12.73
4.00
0.77
1.13
0.73
0.96
1.84
0.98
0.97
1.72
8.18
5.52
21.85

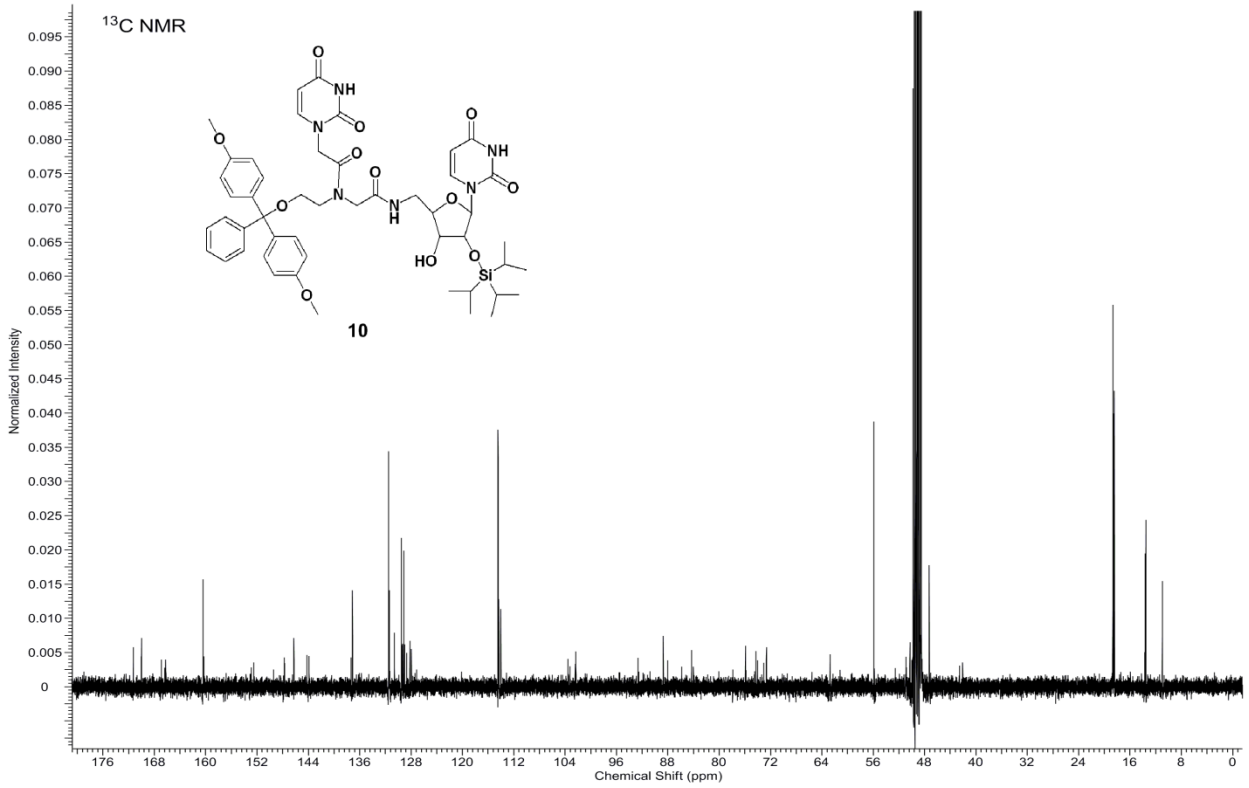
^{13}C NMR
10
Normalized Intensity
Chemical Shift (ppm)

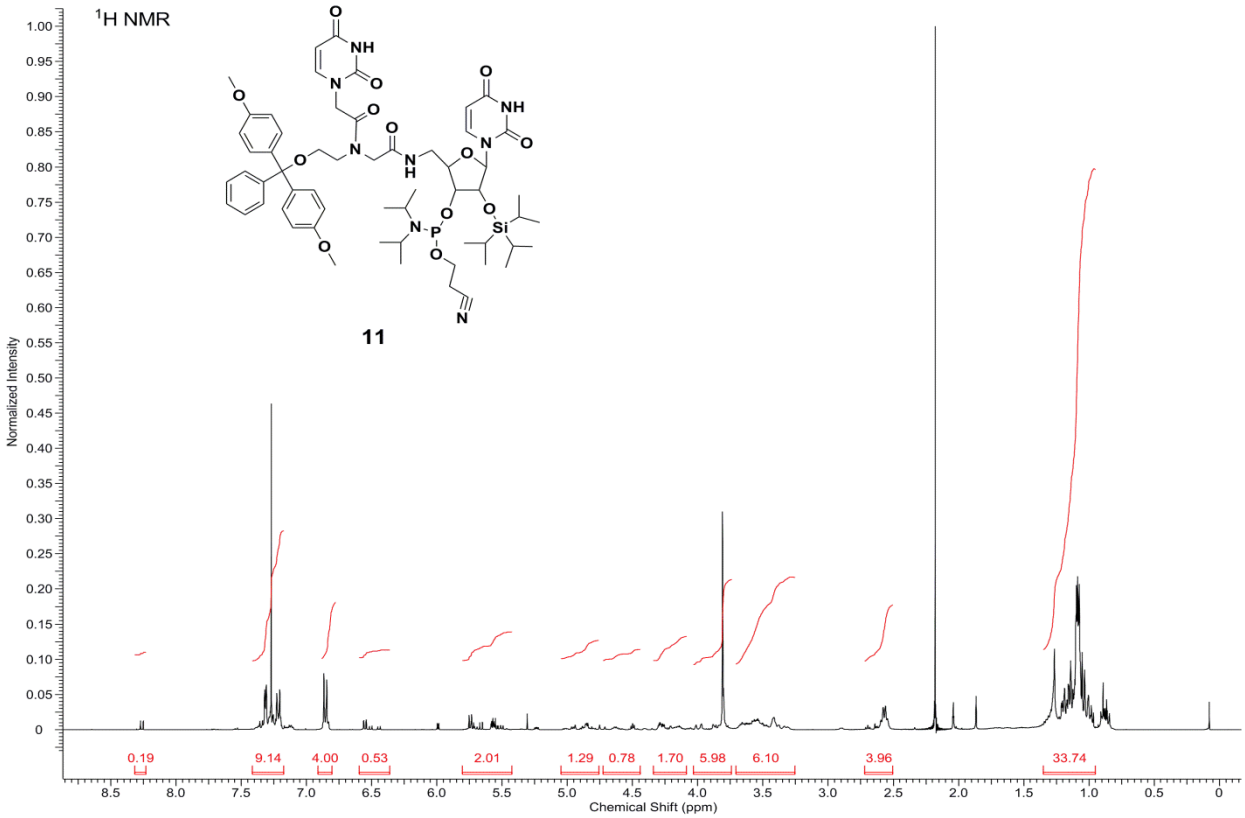
^{1}H NMR
11
Normalized Intensity
Chemical Shift (ppm)
0.19
9.14
4.00
0.53
2.01
1.29
0.78
1.70
5.98
6.10
3.96
33.74

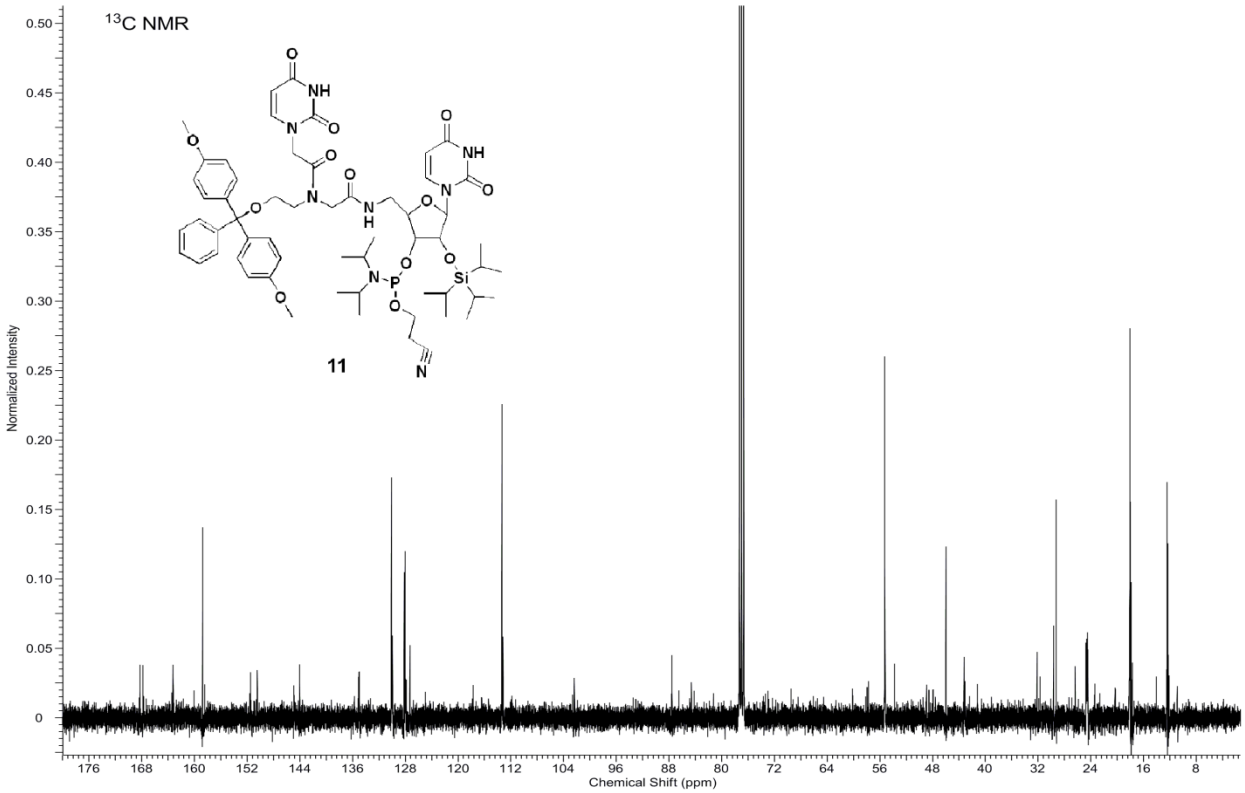
^{13}C NMR
11
Normalized Intensity
Chemical Shift (ppm)